

# Studies on daylight responsive smart wireless driver for white LED modules

Thesis submitted by

**Vishwanath Gupta**

Doctor of Philosophy (Engineering)

Electrical Engineering Department

Faculty Council of Engineering & Technology

Jadavpur University

Kolkata, India

**2023**



**1. Title of the thesis:** Studies on daylight responsive smart wireless driver for white LED modules

**2. Name, Designation & Institution of the Supervisors:**

1) Dr. Biswanath Roy, Professor, Electrical Engineering Department, Jadavpur University

2) Dr. Biswarup Basak, Former Professor, Department of Electrical Engineering, Indian Institute of Engineering Science and Technology, Shibpur



### 3. List of Publications:

#### A. Journal Publications: 3

**A1. Vishwanath Gupta**, Biswarup Basak, Kamalika Ghosh & Biswanath Roy. **2020**. Universal control algorithm for automatic current regulated LED driver. **International Journal of Power Electronics**. **12(2):169-180**, doi: 10.1504/IJPELEC.2020.10029994.

**A2. Vishwanath Gupta**, Biswarup Basak, & Biswanath Roy. **2022**. Design and performance evaluation of an automatic dimmable fault-adaptive LED driver circuit. **Light and Engineering**. **31(4):40-49**, doi: <https://doi.org/10.33383/2022-062>.

**A3. Vishwanath Gupta**, Purnima Mandal, Biswarup Basak, & Biswanath Roy. **2023**. A Real-time Wireless Light Controller for Tunable-White LED based Indoor Lighting System. **LEUKOS**. (manuscript communicated on 27th July, 2023)

#### B. Conference Publications: 5

**B1. Vishwanath Gupta**, Kamalika Ghosh & Biswanath Roy. **2017**. Design topology based comparative study on electric and photometric parameters of commercially available LED lamp systems. **2nd International Conference for Convergence in Technology (I2CT)**, Mumbai, India, **2017**, pp. **116-123**, doi: 10.1109/I2CT.2017.8226105.



**B2. Vishwanath Gupta, Biswarup Basak, Kamalika Ghosh & Biswanath Roy. 2017. Stability analysis of a universal LED driver. IEEE Calcutta Conference (CALCON), Kolkata, India, 2017, pp. 279-283, doi: 10.1109/CALCON.2017.8280739.**

**B3. Vishwanath Gupta, Biswarup Basak & Biswanath Roy. 2020. A Fault-Detecting and Motion-Sensing Wireless Light Controller for LED Lighting System. 2020 IEEE Calcutta Conference (CALCON), Kolkata, India, 2020, pp. 462-466, doi: 10.1109/CALCON49167.2020.9106427.**

**B4. Vishwanath Gupta, Biswarup Basak & Biswanath Roy. 2022. Fuzzy logic based closed-loop light controller for daylight responsive office lighting system. 2nd International Conference on Recent Advances in Modeling and Simulations Techniques in Engineering and Sciences (RAMSTES-22), Jaipur. Accepted for further processing and publication in Journal of Mines Metals and Fuels (JMMF).**

**B5. Vishwanath Gupta, Subham Kumar Gupta & Biswanath Roy. 2022. Experimental assessment of flicker in commercially available, white-LED indoor luminaires. Published as a chapter in the book titled Automation and Computation, pp: 66-73, doi:10.1201/9781003333500-8.**

**4. List of Patents: NIL**





## 5. List of Presentations in National/International/ Conferences/Workshops:

### A. International Conferences: 5

**A1.** Presented the paper on “Design topology based comparative study on electric and photometric parameters of commercially available LED lamp systems” in the **2nd International Conference for Convergence in Technology (I2CT), 2017** at Pune.

**A2.** Presented the paper, “Stability analysis of a universal LED driver” in the **IEEE Calcutta Conference (CALCON), 2017** at Kolkata.

**A3.** Presented the paper, “A Fault-Detecting and Motion-Sensing Wireless Light Controller for LED Lighting System” in the **IEEE Calcutta Conference (CALCON), 2020** at Kolkata.

**A4.** Presented the paper, “Fuzzy logic based closed-loop light controller for daylight responsive office lighting system” in the **2nd International Conference on Recent Advances in Modeling and Simulations Techniques in Engineering and Sciences (RAMSTES-22)** at Jaipur (Online mode).

**A5.** Presented the paper, “Experimental assessment of flicker in commercially available, white-LED indoor luminaires” in the **International Conference on Automation and Computation (AUTOCOM-22)** at Dehradun (Online mode).



# Statement of Originality

I, **Vishwanath Gupta** registered on **29.05.19** do hereby declare that this thesis entitled "**Studies on daylight responsive smart wireless driver for white LED modules**" contains literature survey and original research work done by the undersigned candidate as part of Doctoral studies.

All information in this thesis have been obtained and presented in accordance with existing academic rules and ethical conduct. I declare that, as required by these rules and conduct, I have fully cited and referred all materials and results that are not original to this work.

I also declare that I have checked this thesis as per the "Policy on Anti Plagiarism, Jadavpur University, 2019", and the level of similarity as checked by iThenticate software is **3%**.

*Vishwanath Gupta*

Signature of Candidate:

Date: 12/04/23

Certified by Supervisors:

*Biswanath Roy 12/04/2023*

1. **Biswanath Roy**

Professor

Electrical Engineering Department

Jadavpur University

Professor  
Electrical Engineering Department  
JADAVPUR UNIVERSITY  
Kolkata - 700 032

*B. Basak 12/04/2023*

2. **Biswarup Basak**

Former Professor

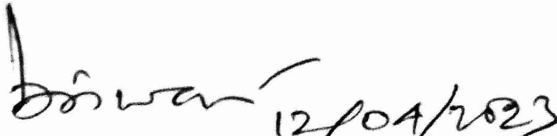
Department of Electrical Engineering

IEST, Shibpur

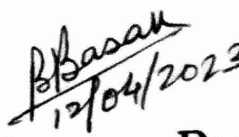


## Certificate from the Supervisors

This is to certify that the thesis entitled “**Studies on daylight responsive smart wireless driver for white LED modules**” submitted by **Vishwanath Gupta**, who got his name registered on **29.05.2019** for the award of **Ph.D.(Engg.)** degree of Jadavpur University is absolutely based upon his own work under the supervision of **Biswanath Roy and Biswarup Basak** and that neither his thesis nor any part of the thesis has been submitted for any degree/diploma or any other academic award anywhere before.

  
1. **Biswanath Roy**  
Professor  
Electrical Engineering Department  
Jadavpur University

Professor  
Electrical Engineering Department  
JADAVPUR UNIVERSITY  
Kolkata - 700 032

  
2. **Biswarup Basak**  
Former Professor  
Department of Electrical Engineering  
IEST, Shibpur



## Acknowledgements

The completion of this thesis is possible with the kind support and help of many individuals. I would like to extend my sincere thanks to all of them.

Foremost, I would like to thank The Almighty for blessing me with this opportunity to pursue higher studies.

I would like to express my sincere gratitude to my supervisors Prof. (Dr.) Biswarup Basak, Department of Electrical Engineering, IEST and Prof. (Dr.) Biswanath Roy, Electrical Engineering Department, JU for their invaluable guidance, continuous motivation and support throughout the study and research.

I would like to thank Prof. (Dr.) Saswati Mazumdar, Head of the EE Dept., JU, Dr. Suddhasatwa Chakraborty, Section In Charge, Illumination Engg. Laboratory, Mrs. Sangita Sahana, Asst. prof., EE Dept., Dr. Kamalika Ghosh, Ex-Director, SISED and Mr. Parthasarathi Satvaya, Asst. Prof., SISED for providing the necessary facilities for implementation of this work.

I also take this opportunity to pay my deepest regards to all my teachers from my school and colleges who imbibed in me the thirst for knowledge and were always ready to quench my curiosity. I remain indebted to them.

I want to thank DST PURSE II, RUSA 2.0, JU and SVMCM for providing research scholarship and financial support in purchasing necessary facilities for implementation of this work.

I would like to thank my fellow research scholars Dr. Pradip Kr Maiti, Dr. Purnima Mandal, Dr. Biswadeep Gupta Bakshi and Mr. Sourish Chatterjee for their encouragement and cooperation during my research work.





I would like to thank Mr. Sumit Paul and Mr. Subham Kumar Gupta who completed their M.E in Illumination Engineering from Electrical Engineering Department of Jadavpur University for their cooperation during my research.

I would also want to thank Mr. Pradip Pal and Mr. Samir Mandi, staff of Illumination Engg. Section, JU and all the faculty members and other staff members of the EE Dept. and SISED for their technical support.

Finally, I would like to express my heartfelt gratitude towards the pillars of my support, 'my family' and my friends, for their emotional support, love and, above all, for their encouragement and patience.



**Dedicated to**

*my Father, Mother, Wife and Son*



# Abstract

LED luminaires for modern day lighting application should be smart, wattage-independent in a given output power range, dimmable and fault adaptive to provide uninterrupted, energy-efficient, and cost-effective operation. On the other hand, the light controllers used in conjunction with the dimmable LED luminaires should be able to provide wireless control, fault-monitoring and spectral tuning to improve the features of the LED luminaire. However, all of these improvements should not come at the cost of electrical and photometric performance. Therefore, the performance of LED luminaires with or without light controllers should comply with the recommended standards. In this proposed research work, attempts are made to improve the features and performance of a LED luminaire and light controllers used in various lighting applications.

In the first stage, the design and performance evaluation of a smart, wattage-independent, fault-adaptive dimmable LED luminaire that has a wide output power range and is free from current imbalance of LED chips in the LED luminaire is performed. A Simulink model of the LED luminaire is simulated in Matlab-Simulink platform to test its electrical performance and verify its compliance with recommended standards. A mathematical model of the LED driver unit of the luminaire is also formulated to perform stability analysis. The operation of the simulated LED luminaire is satisfactory, stable in steady state and in compliance with relevant standards.

In the next stage, three light controllers with improved features and performance compared to previous light controllers are developed and tested.



The first one is a Fuzzy Logic Inference System (FIS) based closed-loop light controller that can control the position of window blind and amount of light output from artificial luminaires depending upon the amount of available daylight. The FIS is implemented inside a micro-controller and not on a computer, hence eliminating the need for dedicated computer and interfacing accessories. The developed FIS is validated through simulation in DIALux 4.13 lighting design software.

The second light controller is capable of varying the light output from the artificial luminaire based on ambient light and the presence of the user through wireless communication. It can also detect the place of origin of the fault (LED driver unit or lamp module unit) and convey the result to the operator. A hardware prototype of the designed controller is fabricated and tested in the laboratory and its performance is found to be satisfactory.

The third light controller possesses the ability to manually or automatically vary the luminous flux and CCT of light separately or simultaneously from multiple tunable-white LED luminaires using Bluetooth wireless communication with the help of a dedicated mobile app. The developed controller remains unaffected by wireless communication failure and input power failure. A hardware prototype of the light controller is developed and tested in real time for an indoor lighting scheme installed inside a test room. The results of the real-time testing show that the light controller is able to vary the luminous flux and CCT satisfactorily and has deviation within the recommended tolerable limits.





# Contents

List of Abbreviations	xxviii
List of Acronyms	xxx
List of Figures	xxxii
List of Tables	xxxvi
<b>1 General introduction</b>	<b>2</b>
1.1 Overview . . . . .	2
1.2 Development of LED lighting over the years . . . . .	2
1.3 Present status of LED lighting . . . . .	5
1.4 My thesis . . . . .	5
1.4.1 Problem statement . . . . .	5
1.4.2 Objective . . . . .	6
1.4.3 Methodology . . . . .	6
1.4.4 Steps of execution . . . . .	7
1.4.5 Original contributions . . . . .	9
1.4.6 Organisation of the thesis . . . . .	9
<b>2 Literature review</b>	<b>14</b>
2.1 LED lighting system . . . . .	15
2.1.1 LED chip and lamp module . . . . .	15
2.1.2 LED driver system . . . . .	18
2.2 Recent trends in LED lighting systems . . . . .	22
2.2.1 Daylight-actuated automatic control . . . . .	22
2.2.2 Fault monitoring and adaptation . . . . .	24
2.2.3 Spectral tuning . . . . .	25
2.2.4 Wireless light control . . . . .	28

<b>3</b>	<b>Performance evaluation of commercially available indoor pc-WLED luminaires</b>	<b>32</b>
3.1	Introduction . . . . .	33
3.2	Test luminaires . . . . .	33
3.3	Experimentation and performance parameters . . . . .	35
3.3.1	DC operation . . . . .	35
3.3.2	AC operation . . . . .	36
3.4	Results and analysis . . . . .	36
3.5	Chapter summary . . . . .	47
<b>4</b>	<b>Smart fault-adaptive LED luminaire: Design and Modelling</b>	<b>50</b>
4.1	Introduction . . . . .	51
4.2	Design and simulation . . . . .	52
4.2.1	Modeling of LED lamp modules . . . . .	54
4.2.2	Modeling of LED driver . . . . .	57
4.3	Principle of operation . . . . .	67
4.4	Results and analysis . . . . .	68
4.5	Chapter summary . . . . .	81
<b>5</b>	<b>Stability analysis of the designed smart LED luminaire</b>	<b>82</b>
5.1	Theoretical background . . . . .	83
5.2	Mathematical model . . . . .	84
5.3	Results and analysis . . . . .	86
5.4	Chapter summary . . . . .	93
<b>6</b>	<b>Daylight-responsive closed-loop light controllers: Design and Evaluation</b>	<b>94</b>
6.1	Fuzzy logic based closed-loop light controller . . . . .	95
6.1.1	Introduction . . . . .	95
6.1.2	Features and design . . . . .	95

6.1.3	Principle of operation . . . . .	100
6.1.4	Results and analysis . . . . .	102
6.2	Fault-monitoring and motion-sensing wireless light controller . . . . .	107
6.2.1	Introduction . . . . .	107
6.2.2	Features and design . . . . .	108
6.2.3	Principle of operation . . . . .	111
6.2.4	Laboratory testing . . . . .	112
6.2.5	Results and analysis . . . . .	113
6.3	Chapter summary . . . . .	115
<b>7</b>	<b>Design and real time evaluation of a wireless light controller for tunable-white LED luminaire</b>	<b>118</b>
7.1	Introduction . . . . .	119
7.2	Wireless light controller . . . . .	120
7.2.1	Features . . . . .	120
7.2.2	Design and development . . . . .	121
7.3	Principle of operation . . . . .	124
7.4	Real-time testing . . . . .	129
7.5	Results and analysis . . . . .	135
7.6	Chapter summary . . . . .	143
<b>8</b>	<b>Overall conclusions</b>	<b>146</b>
	<b>Prospective applications of the present study</b>	<b>150</b>
	<b>Future scope</b>	<b>152</b>
	<b>Annexures</b>	<b>154</b>
	<b>Bibliography</b>	<b>162</b>



## List of Abbreviations

AC	Alternating Current
ANFIS	Adaptive Neuro Fuzzy Inference System
BR	Blending Ratio
CCM	Continuous Conduction Mode
CCT	Correlated Colour Temperature
COB	Chip on Board
CRI	Colour Rendering Index
CW	Cool White
DAQ	Data Acquisition System
DC	Direct Current
DCM	Discontinuous Conduction Mode
DIP	Dual-in Package
DSO	Digital Storage Oscilloscope
EMI	Electro-magnetic Interference
FIS	Fuzzy Logic Inference System
I <sup>2</sup> C	Inter-Integrated Circuit
INR	Indian Rupee
IR	Infra-red
LED	Light Emitting Diode
MOSFET	Metal Oxide Semiconductor Field-Effect Transistor
NSO	National Statistical Organization
pc-WLED	Phosphor Converted White Light Emitting Diode
PFC	Power Factor correction
PI	Proportional-Integral
PIR	Passive Infra-red
PWM	Pulse Width Modulation
RF	Radio Frequency
RMS	Root Mean Square
RTC	Real Time Clock
SEPIC	Single-ended Primary Inductor Conductor
SMD	Surface Mounted Device
SMPS	Switched Mode Power Supply
SRC	Series Resonant Converter
SSL	Solid State Lighting
THD	Total Harmonic Distortion
TLA	Temporal Light Artefacts
WLED	White Light Emitting Diode
WW	Warm White



## List of Acronyms

$I_{Np}$	Current output of module sensor block
$V'_{\gamma}$	Critical voltage of LED lamp module
$I'$	Value of input current at $V'_{\gamma}$
$V_{rms}$	Root mean square value of input AC voltage
$V_D$	Rated voltage of single LED chip
$R_{Di}$	Dynamic resistance of single LED chip
$V_{\gamma i}$	Threshold voltage of single LED chip
$I_{Di}$	Current of single LED chip
$V_o$	Rated input voltage of an LED module
$R_D$	Dynamic resistance of an LED module
$I_o$	Rated input current of an LED module
$V_{\gamma}$	Threshold voltage of an LED module
$N_S$	Number of LED chips connected in series
$N_P$	Number of parallel strings in LED module
$N_H$	Number of healthy parallel strings in LED module
$D$	Duty cycle of flyback converter
$D_{max}$	Maximum value of duty cycle of flyback converter
$V_{min}$	Minimum RMS value of supply voltage
$L_m$	Mutual inductance of flyback converter
$f_s$	Switching frequency of flyback converter
$P_{omax}$	Maximum rated output power of LED driver
$C_o$	Capacitance of output capacitor of flyback converter
$I_c$	Output current of condition monitor block
$\phi_m$	Loop gain phase margin
$G_{PI}$	Transfer function of PI controller
$K_p$	Proportional constant
$K_i$	Integral constant
$V_M$	Maximum amplitude of carrier signal
$E_{set}$	Desired illuminance value on working plane
$x_c, y_c$	Chromaticity coordinates of CW LED array
$x_w, y_w$	Chromaticity coordinates of WW LED array
$E_W$	Individual illuminance contribution of WW LED array
$E_C$	Individual illuminance contribution of CW LED array
$DC_{CW}$	Duty Cycle of CW LED array
$DC_{WW}$	Duty Cycle of WW LED array





## List of Figures

1.1	Illustration of Haitz's law . . . . .	3
1.2	Block diagram representation of a general LED luminaire	4
1.3	Conceptual flow diagram of the thesis . . . . .	12
2.1	Operating principle of LED . . . . .	16
2.2	Types of LED chip arrangement . . . . .	17
2.3	Basic structural types of LED driver . . . . .	19
3.1	Test LED luminaires . . . . .	34
3.2	V-I characteristics of the test luminaires . . . . .	37
3.3	Comparison of relative lumen output of the test luminaires . . . . .	38
3.4	Comparison of CCT of the test luminaires . . . . .	38
3.5	Comparison of colour shift of the test luminaires . . . . .	39
3.6	Input current harmonic spectrum of System1 driver . . . . .	41
3.7	Input current harmonic spectrum of System2 driver . . . . .	42
3.8	Input current harmonic spectrum of System3 driver . . . . .	42
3.9	Comparison of input current harmonics of test luminaires	43
3.10	Laboratory experimental setup for flicker measurement	44
3.11	Flicker profile of System1 . . . . .	45
3.12	Flicker profile of System2 . . . . .	45
3.13	Flicker profile of System3 . . . . .	46
4.1	Block diagram of the LED luminaire . . . . .	52
4.2	Simulated LED luminaire . . . . .	53
4.3	Equivalent Circuit of an LED chip: Linear model . . . . .	54
4.4	Simulated LED module . . . . .	57
4.5	Block diagram of designed power circuit . . . . .	58
4.6	Control algorithm for the module sensor block . . . . .	63
4.7	Control algorithm for the dimmer block . . . . .	64
4.8	Control algorithm for the condition monitor block . . . . .	65

4.9	Control algorithm for the reference signal generator block	66
4.10	Output Current of LED luminaires having rated currents of 2A, 3A and 4A respectively at $230V_{rms}$	69
4.11	Variation of electrical parameters of LED driver with rated power at $230V_{rms}$	70
4.12	Output current waveform under dimmed operation	71
4.13	Variation of electrical parameters with output power for different dimming levels at $230V_{rms}$ (a) input power factor (b) efficiency (c) THD and (d) current ripple	73
4.14	Output current waveform under normal operation	76
4.15	Output current waveform when 90% dimming is required and one parallel string becomes faulty	77
4.16	Output current waveform when 50% dimming is required and two parallel strings becomes faulty	78
4.17	Variation of electrical parameters for fault occurrence at different dimming levels at $230V_{rms}$ (a) input power factor (b) efficiency (c) THD and (d) current ripple	80
5.1	Variation of Phase Margin with $N_s/N_p$ ratio at $230V_{rms}$	88
5.2	Variation of Phase Margin with input AC voltage for different $N_s/N_p$ ratio	89
5.3	Variation of settling time with $N_s/N_p$ ratio at $230V_{rms}$	89
5.4	Bode plot of loop gain for 72W LED luminaire with $N_s/N_p$ ratio of 1.5 at $230V_{rms}$	90
5.5	Bode plot of closed loop system for 72W LED luminaire with $N_s/N_p$ ratio of 1.5 at $230V_{rms}$	90
5.6	Step response of 72W LED luminaire with $N_s/N_p$ ratio of 1.5 at $230V_{rms}$	91
5.7	Simulated output current waveform for 72W LED luminaire with $N_s/N_p$ ratio of 1.5 at $230V_{rms}$	92
6.1	Simulated model test room	96

6.2	Block diagram of the complete light control system . . .	97
6.3	Operational flow diagram of the FIS based light-controller	101
6.4	Luminaire parts list . . . . .	102
6.5	Comparison of average illuminance before and after control . . . . .	105
6.6	Comparison of overall uniformity before and after control	106
6.7	Block diagram of the proposed system . . . . .	110
6.8	Control algorithm of the developed controller . . . . .	112
6.9	Developed hardware setup . . . . .	113
6.10	Variation of electrical parameters with output light of LED module . . . . .	114
7.1	Block diagram of the designed light controller . . . . .	121
7.2	Developed hardware prototype of the proposed light controller . . . . .	122
7.3	Screenshot of the developed mobile app . . . . .	123
7.4	Operating algorithm of the developed controller . . . . .	125
7.5	Variation of average illuminance on working plane with duty cycle . . . . .	128
7.6	Plan view of the installed lighting arrangement in test room . . . . .	130
7.7	Luminaire arrangement in the test room . . . . .	130
7.8	Polar diagram of the installed luminaire . . . . .	131
7.9	Block diagram of the test lighting system operated with developed controller . . . . .	132
7.10	Plan view of the measurement setup on the working plane	134
7.11	Illuminance and CCT measurement setup in the test room . . . . .	134
7.12	Measured CCT in AUTO mode for 10 different runs to check repeatability . . . . .	136

7.13 Measured illuminance in AUTO mode for 10 different runs to check repeatability . . . . .	136
7.14 Desired vs. measured mean values of CCT and illuminance in AUTO mode . . . . .	137
7.15 Percentage error in CCT and illuminance in AUTO mode	137
7.16 Minimum vs. mean calculated uniformity in AUTO mode	138
7.17 Illuminance measurement during power failure and subsequent restoration . . . . .	139
7.18 Variation of CCT at different constant illuminance values	140
7.19 Variation of illuminance at different constant CCT values	140
7.20 Reference vs. measured set points in MANUAL mode .	141
7.21 Percentage error in CCT and illuminance in MANUAL mode . . . . .	142
7.22 Minimum vs. mean calculated uniformity in MANUAL mode . . . . .	142

## List of Tables

2.1	List of important inferences from corresponding literature	29
3.1	Declared product ratings and cost . . . . .	34
3.2	Arrangement of LED chips inside test luminaires . . . . .	34
3.3	Comparison parameters for test luminaires . . . . .	36
3.4	Performance of test luminaires on AC supply . . . . .	40
3.5	Experimentally obtained THD values of test luminaires	43
3.6	Experimentally obtained %F of test luminaires . . . . .	46
4.1	Electrical parameters of LED modules . . . . .	55
4.2	Look-up table . . . . .	61
4.3	Output current and current in each parallel string at different dimming levels for single string fault . . . . .	75
5.1	Phase margin of the LED driver for different $N_s/N_p$ ratio	87
6.1	Designed fuzzy sets of the inputs and outputs . . . . .	99
6.2	Rule base for control group 1 . . . . .	99
6.3	Rule base for control group 2 . . . . .	100
6.4	Rule base for control group 3 . . . . .	100
6.5	Obtained results with only artificial lighting . . . . .	102
6.6	Outputs predicted by designed FIS . . . . .	104
6.7	Control voltages and pulse width of generated PWM signals . . . . .	114
7.1	Technical specifications of the installed LED luminaire	131
7.2	Desired time varying profile of CCT and illuminance for AUTO mode testing . . . . .	135
7.3	Set points for MANUAL mode testing . . . . .	141



# 1 General introduction

## 1.1 Overview

Light is electromagnetic radiation that has a wavelength in the range of 380-760nm [1]. Before the advent of artificial lighting sources, living creatures depended on natural sources to meet their need for light, but with the invention of incandescent lights in the nineteenth century, a revolution in artificial light sources began. The development of more energy-efficient fluorescent lamps led to their wide-scale production and use in general-purpose lighting. The invention of Solid State Lighting (SSL) in the late twentieth century was a major breakthrough and presently, LED luminaires have replaced conventional light sources used in almost all lighting applications [2].

## 1.2 Development of LED lighting over the years

Light Emitting Diodes (LEDs) started their journey in the 1960s as tiny infrared sources placed inside the computer circuit board and remote controls [3]. Commercially successful LED devices were produced by Fairchild Optoelectronics in the 1960s [4]. In the 1990s, high-brightness blue LEDs were developed[5]. After the development of high-efficiency blue LEDs, white LEDs were developed, leading to their use in general lighting [6] and today LED has become the most widely used light source. Its performance is increasing and cost is decreasing day by day. The improvement in the luminous flux and the reduction in cost over time is illustrated by Haitz's law, as shown in **Fig. 1.1** [7].

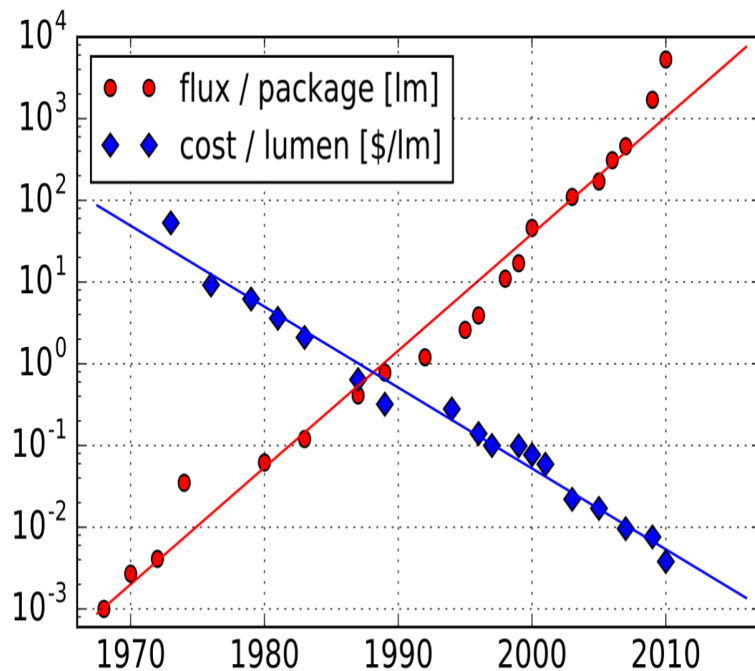


**Fig. 1.1:** Illustration of Haitz’s law

The progress in semiconductor physics and technology resulted in numerous varieties of LEDs available in almost all possible colours, sizes, power ratings, and spectral composition. The initial cost involved in large-scale production of LEDs is also being reduced exponentially, providing an additional advantage of a shorter payback period for consumers. In the last decade, LEDs were used in display panels, signage, street lighting and general purpose lighting due to its longer lifetime, absence of toxic mercury, reliability, wider colour gamut, smooth dimming characteristics and reduced energy consumption [8–11]. However, some technical issues needed to be tackled, such as temperature and moisture sensitivity, creation of discomfort glare [12], blue light hazards [13].

The operation of LEDs from a power source is carried out with the help of an LED driver as shown in **Fig. 1.2**. The LED driver incorporates a power circuit, feedback-sensing and control circuit to operate the connected LED load from a DC or AC supply.



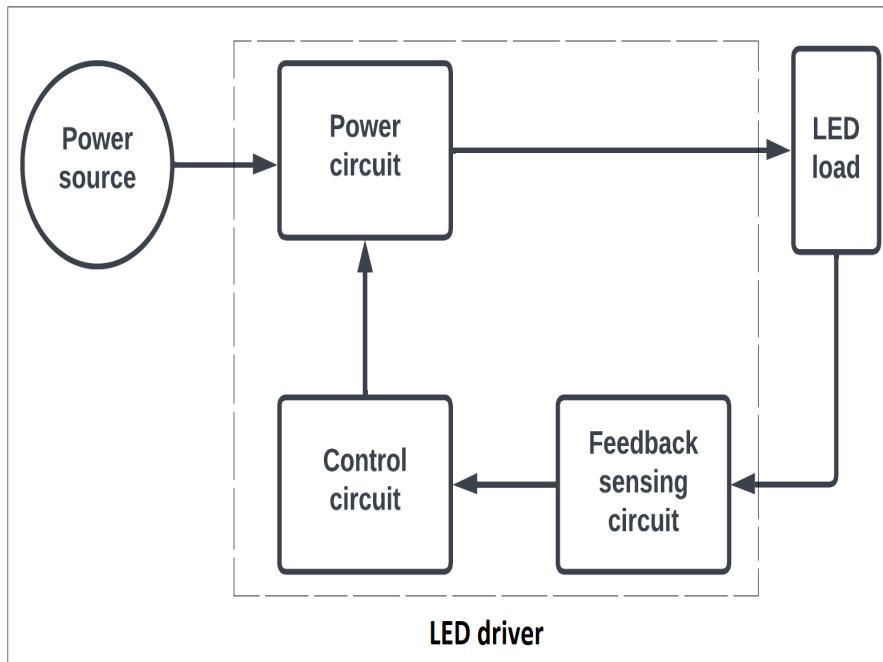


**Fig. 1.2:** Block diagram representation of a general LED luminaire

The power circuit consists of a power converter and a power switch. DC-DC converters used in LED drivers mostly include digital control boost converters [14], synchronous buck power converters [15], Cuk converters [16, 17], buck-boost converters [18] and tapped inductor converters [19, 20]. AC-DC converters used for LED driver circuits include flyback [21–25], boost-flyback [26] and SEPIC converters [27–29]. Additional electrical or electronics components are added to these general power converters to modify the LED driver circuit to achieve desired results.

The lighting applications employing LED luminaires are expected to maintain the required level of light output. This requires the sensing of light output which can be achieved through the use of external photosensors [30–32]. However, the use of an additional external light sensor is costly and the sensed value is easily influenced by ambient physical conditions such as temperature, humidity, etc. However, this limitation can be overcome by sensing the output current of the LED

driver rather than the light output, by modifying the converter design, since the light output closely follows the output current of the LED driver [33–37]. Despite the progress in LED chip and LED driver technologies, some challenges such as making them wattage-independent, increasing the efficiency, power factor, burning life, decreasing Total Harmonic Distortion (THD) and Temporal Light Artefacts (TLA), and development of fault-tolerant and spectrally tunable LED luminaires still remained.

### **1.3 Present status of LED lighting**

Recent efforts have been made to improve the LED driver and light controller technologies to make LED lighting systems low flicker or flicker-free. [38–41], more efficient with an improved power factor [42–46] and incorporate fault monitoring and spectral tuning capabilities. Still, a single LED driver is unable to operate LED modules of different power ratings satisfactorily. In addition, most LED or light controllers for fault monitoring are capable of detecting only the fault or predicting the fault time, but are incapable of operating the LED load after the occurrence of the fault [47–51]. Furthermore, the dynamic light controllers developed in recent times [52–57] are inept in operating multiple LED luminaires in real-time lighting applications. The present work attempts to overcome the shortcomings of previous research work.

## **1.4 My thesis**

### **1.4.1 Problem statement**

To design, simulate and evaluate the performance of wattage-independent, fault-adaptive dimmable multi-string LED luminaire that remains unaffected by imbalance of current in parallel strings and simultaneously develop and test hardware prototypes of automatic wireless light con-

trollers for daylight-responsive LED luminaires that provide fault monitoring and spectral tuning capabilities.

#### **1.4.2 Objective**

Up-gradation of the existing LED driver design topology to incorporate fault-adaptation and output power independence features and improve the features and performance of light controller technologies.

#### **1.4.3 Methodology**

##### **A. Testing commercially available pc-WLED indoor luminaires in the laboratory**

- A1. To observe the topology of LED drivers and LED modules;
- A2. To test LED luminaires to compare their performance and verify their compliance with recommended standards.

##### **B. Conceptualisation and design of a wattage-independent, fault-adaptive dimmable LED luminaire**

- B1. To simulate the proposed LED luminaire in Matlab-Simulink platform;
- B2. To test the performance of the simulated LED luminaire for all possible scenarios of dimming and fault occurrences in the wide output power range;
- B3. To perform the stability analysis of the simulated LED luminaire.

##### **C. Design and development of wireless light controllers for daylight-responsive, fault-monitoring and spectrally tunable LED luminaires**

- C1. To design an fuzzy logic inference system (FIS) based light controller for the daylight-integrated artificial indoor lighting scheme and test it using DIALux 4.13 lighting design software;

C2. To develop a daylight responsive, motion-sensing and fault-monitoring wireless light controller and testing it in the laboratory for performance evaluation;

C3. To develop a wireless dynamic light controller and test it in real time for an indoor lighting application.

#### **1.4.4 Steps of execution**

##### **Step 1: Performance evaluation of commercially available indoor pc-WLED luminaires**

1.1. Procurement of commercially available pc-WLED luminaires of different makes;

1.2. Study of the LED driver and lamp module topologies;

1.3. Testing of test luminaires for performance assessment.

##### **Step 2: Simulation and testing of a smart, fault-adaptive dimmable LED luminaire**

2.1. Development of a control algorithm for the proposed LED luminaire to achieve the desired features;

2.2. Simulation of a Matlab-Simulink model of the LED luminaire to implement the developed control algorithm;

2.3. Testing of the simulated LED luminaire model to evaluate fault-adaptive and dimming features;

2.4. Performing stability analysis of the simulated LED luminaire.

##### **Step 3: Design and implementation of an FIS-based light controller for a daylight integrated artificial lighting system**

3.1. Designing a model test room in DIALux 4.13 lighting design software;

3.2. Designing a FIS to achieve the desired quantity and quality of light on the working plane of the model test room;

3.3. Direct implementation of FIS inside a micro-controller eliminating the requirement of a dedicated computer and compatible interfacing accessories;

3.4. Testing the designed FIS for the model test room to determine its performance.

#### **Step 4: Design and fabrication of a fault-monitoring and motion sensing light controller**

4.1. Development of a control algorithm for the proposed light controller to achieve fault-monitoring and daylight-responsive features;

4.2. Fabrication of a hardware prototype to implement the developed algorithm;

4.3. Incorporation of RF modules to achieve wireless connectivity in the hardware prototype;

4.4. Laboratory testing of the developed hardware prototype to evaluate its performance.

#### **Step 5: Development and real-time testing of a light controller for multiple tunable-white LED luminaires based indoor lighting scheme**

5.1. Installation of multiple tunable-white LED luminaires in a test room to achieve dynamic lighting;

5.2. Development of a control algorithm for the proposed light controller for manual and automatic variation of illuminance and CCT;

5.3. Fabrication of a hardware prototype to implement the developed algorithm;

5.4. Development of a compatible mobile application to operate the developed light controller;

5.5. Testing the developed hardware prototype in real time to ascertain its performance.

### 1.4.5 Original contributions

Following are the original contributions of the proposed work:

- 1) Design, performance evaluation and stability analysis of an automatic wide output power range and fault-adaptive dimmable multiple-string LED luminaire free from current imbalance issue.
- 2) Development of a Fuzzy Logic Inference System (FIS) based light controller implemented on Arduino Mega micro-controller using C++ programming language instead of simulation in Matlab environment to make it cost effective by obliterating the need of a dedicated computer and additional interfacing accessories.
- 3) Development of a closed-loop wireless light controller to monitor the occurrence of faults in the LED driver and the LED module separately so that the labour and cost of dismantling the entire luminaire in case of fault occurrence is eliminated.
- 4) Development and real-time performance evaluation of a smart phone-operated automatic dynamic light controller for multiple tunable-white LED modules based indoor lighting installation that remains unaffected by communication error and power failure.

### 1.4.6 Organisation of the thesis

The details of the work done in the present thesis are organised as follows:

In **Chapter 2**, an extensive review of available technical literature and resources on LED chip, LED driver technology and currently in-demand technologies of light controllers in LED lighting systems is conducted and their research gaps are identified. The addressal of

these research gaps led to the formulation of the research objectives.

In **Chapter 3**, laboratory experiments are carried out on three different commercially available indoor pc-WLED luminaires to obtain their electrical and photometric performance during DC and AC operation. The topology of the LED drivers and LED modules is also studied. The experimental results obtained are also compared with the Indian and International standards recommended to verify the compliance of individual LED luminaires.

The concept and design of a smart fault-adaptive LED luminaire are introduced in **Chapter 4**. The LED luminaire model is first simulated on the Matlab-Simulink platform and then tested to assess its electrical performance, dimming and fault-adaptive capabilities in the complete output power range of 18W-72W, suitable for commercial and industrial indoor lighting applications.

**Chapter 5** deals with the stability analysis of the LED luminaire discussed in **Chapter 4**. A mathematical model, in the form of a transfer function, of the LED luminaire is developed first and then its stability is determined by performing the phase margin test. Stability is defined in terms of the phase margin of the simulated model. The optimised arrangement of LED chips in the LED lamp modules is also determined for the optimised performance of the LED luminaire in the given output power range.

**Chapter 6** describes the design, development and performance assessment of two numbers of daylight-responsive closed-loop light controllers. The first section deals with the design and implementation of a Fuzzy Logic Inference System (FIS) based light controller on Ar-

duino Mega micro-controller that predicts the amount of light output required from artificial lamps and the position of window roller blinds. The simulated light controller is tested offline by modelling a test office room using DIALux 4.13 lighting design software. The second section explains the design and development of a wireless fault-monitoring and motion-sensing light controller for an indoor LED luminaire. A hardware prototype of the designed controller is developed and tested in the laboratory to evaluate its performance.

**Chapter 7** discusses the development and real-time testing of a wireless light controller for multiple spectrally tunable-white LED luminaires installed in a test room. A mobile app is developed to provide wireless communication support to the light controller. The developed controller operated through the mobile app can manually or automatically vary the CCT and illuminance as per the user's requirement. The operation of the developed controller is also observed during communication failure and power failure scenarios.

**Chapter 8** contains the overall conclusions, prospective applications and the future scope of the research work carried out in this thesis. The conceptual flow diagram of the thesis is shown in **Fig. 1.3**



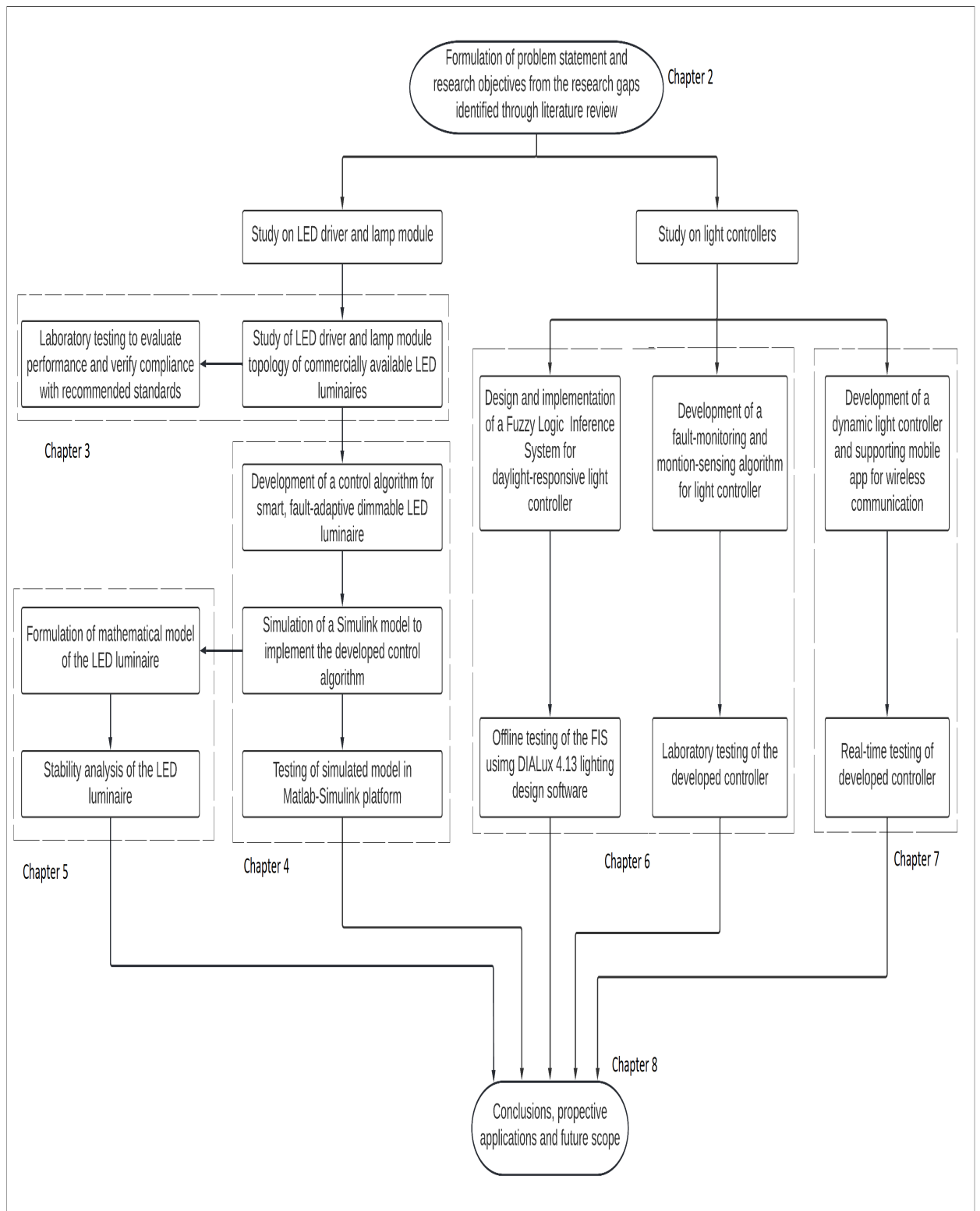


**Fig. 1.3:** Conceptual flow diagram of the thesis



## 2 Literature review

In this chapter, a review of available national and international technical literature and resources on LED chip, LED driver technology and recent trending control techniques in LED lighting systems, surveyed before and during the time of carrying out the research work, is presented. The evolution of design features of the LED lamp module and the LED driver over the years is reviewed. The LED lighting system controllers with the following trending control techniques are considered in this research work: a) daylight-actuated automatic light control, b) fault monitoring and adaptation, and c) wireless light control. The addressal of the research gaps that were identified during the course of literature survey prompted the establishment of the research objectives.

## 2.1 LED lighting system

An LED lighting system or LED luminaire constitutes a lamp module and a compatible driver system. The lamp module assembled with LED chips generates the light and the driver unit helps in the satisfactory operation of the LED lamp.

### 2.1.1 LED chip and lamp module

An LED is a crystalline, solid, two-terminal, p-n junction device that emits light by a principle called electroluminescence [58]. In an unbiased condition, an LED chip consists of a p-type and a n-type layer segregated by a depletion layer. In the p-type layer, electrons are the minority carriers and in the n-type layer, electrons are the majority carriers. When a forward voltage is applied beyond the threshold voltage, the barrier energy of the depletion layer is reduced, initiating the flow of the charge carriers. The electrons shift from the n-layer to the p-layer, the holes shift from the p-layer to the n-layer, and they recombine at the junction. A relatively smaller fraction of the band-gap energy appears as heat during recombination. Fast and efficient dissipation of this heat into the atmosphere through a properly designed heat sink is important to avoid some serious problems such as thermal runaway, deteriorated performance, and reduced life expectancy. The process of recombination is simultaneously radiative and non-radiative. In radiative recombination, a large part of the band gap energy is radiated as photons with visible wavelengths according to Planck-Einstein theory, while only a smaller part of the band gap energy generates heat ('phonons') in non-radiative recombination [59]. The working principle of an LED chip can be explained with the help of a forward biased pn junction diode as shown in **Fig. 2.1**[60] .

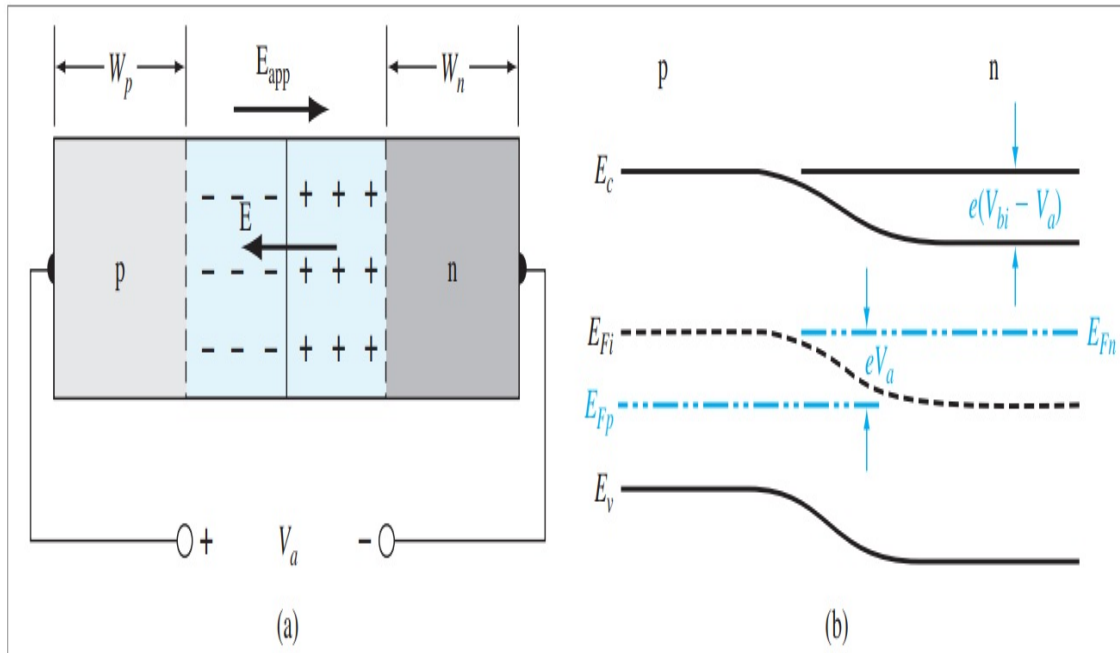


**Fig. 2.1:** Operating principle of LED

Currently, LED chips of different colour and power ratings are available in the market in four packages, that is, conventional or dual-in package (DIP), surface mounted device (SMD), chip-on-board (COB) and MicroLED. MicroLEDs are not used for general lighting purposes, but for defining pixels in flat panel televisions. DIP is mostly used as an indicator light in electronic applications. SMD and COB packages are used mostly for general purpose lighting, as they offer better thermal management, reduced size, and higher density of the luminous surface [61]. The spectral composition of visible radiation of an LED chip is determined by doping materials [62]. An LED module is used as the source of artificial light in almost all lighting applications instead of single LED chips because the maximum allowable output power of an individual LED chip is 20W due to packaging limitations [11]. The LED module is an assembly of LED chips connected together in series, parallel or series-parallel combination as shown in **Fig. 2.2**.

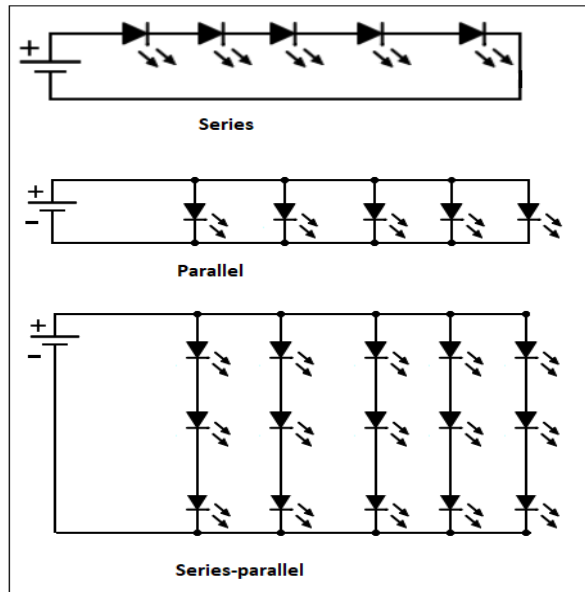


**Fig. 2.2:** Types of LED chip arrangement

The lighting application in which the luminaire is going to be used decides the choice of chip arrangement in the LED module. In an LED module with series arrangement of LED chips, the same current is delivered to each LED chip as it is operated by a constant current driver. The series arrangement ensures the same brightness and current consumption from each LED chip and thereby eliminates the issue of thermal runaway. However, the disadvantage of the series arrangement is that the entire LED module will fail if any of the LED chips becomes faulty [63–74]. On the other hand, an LED module with parallel arrangement of LED chips provides the same voltage to each LED chip as it is operated using a constant voltage driver. The advantage of parallel arrangement is that, in the event of a fault in any LED chip, the LED module still provides light output, although it is reduced. However, the parallel arrangement requires a large amount of current for high-wattage LED modules, making the selection of the LED driver component difficult. Therefore, it is better to have an LED module with series-parallel arrangement that provides

continuous operation and reduces the current requirement of the LED module [72, 75–88]. The series-parallel arrangement of single LED chips is used for the design of the LED lamp module mentioned in **Subsection 3.2.1**.

### 2.1.2 LED driver system

LED driver is essential for the LED lighting system during AC operation. It provides the required voltage and current to the LED modules for satisfactory performance. The LED driver makes the LED luminaire more reliable, efficient, flexible, compact, safe from surge protection and comply with relevant standards [89–92]. But LED products with nearly similar ratings from different manufacturers differ in electrical and photometric performance because of the difference in driver topology and LED load modelling. Therefore, it is desirable to test and verify some of the commercially available LED lighting systems. *This experimental testing and consequent analysis of commercially available LED luminaires is carried out and described in details in Chapter 3.*

LED lighting systems employ single-stage or two-stage LED drivers [93]. The single-stage LED driver contains a DC / DC converter with additional circuitry for constant output current and power factor correction (PFC). However, it has the disadvantage of a larger volume due to the bulky storage capacitor. The two-stage LED driver has separate DC/DC converter and PFC blocks. The design is simple and gives better control, but the use of extra electronics components makes this type of driver costly and less reliable. Constant current control is achieved using a current loop in the DC/DC converter stage [94–96].

In addition to single-stage and two-stage LED drivers, integrated-stage drivers are being used recently to increase efficiency and reduce

cost. In integrated-stage drivers, through the sharing of active power switches and control circuits, the PFC stage and the DC/DC stage can be combined into a single stage, thereby reducing the cost and size of the driver while increasing the efficiency, reliability and dynamics of the system [63, 97–99]. Different types of LED drivers based on structure are shown in **Fig. 2.3**.

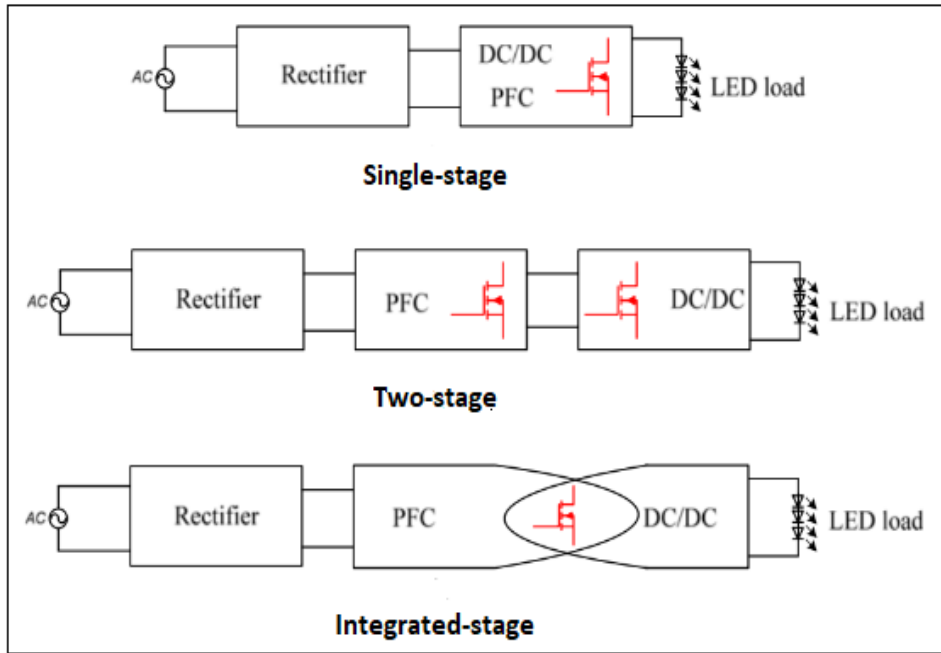


**Fig. 2.3:** Basic structural types of LED driver

In general practise, the topology of the LED driver is selected on the basis of electrical parameters. The single-stage LED driver topology with a flyback converter is preferred for the design of the smart fault-adaptive LED driver mentioned in **Subsection 3.2.2** of this work, as it is suitable for LED luminaires of wide output power range with the lowest component count compared to other isolated converters.

Different LED drivers employ different control algorithms to achieve the desired performance [63–74]. *Chiu et. al.* designed an adaptive feedback control algorithm to predict the reference voltage in the feedback loop. The algorithm measured the drain voltage of the dimming



transistors and reduces the power losses of the dimming transistors [72]. In another work, *Lohaus et al.* proposed an adaptive voltage regulation algorithm to minimise power loss in the linear current regulator of the proposed single channel LED driver. Self-adaptive voltage regulation techniques have been obtained using digital control mechanisms with resistive feedback control [74]. *Moon et al.* presented a method for feedback control to minimise the steady-state error of a LED driver [73]. The control methods presented in the above research work and many others are only suitable for driving a fixed power output LED module that has a series arrangement of LED chips.

Multiple string LED luminaires were considered in some works, but the output power of the LED luminaire was fixed [76, 79, 83, 87, 88]. Some research works deal with multiple-string LED luminaires with variable output power [80–82, 84–86]. A current controller for a universal LED driver using a single-ended primary inductor converter (SEPIC) DC/DC converter was presented by *Chiu et. al.*. The controller employs a T–S fuzzy model capable of operating unknown connected LED arrays from DC source [84]. *He et. al.* in their work proposed a control methodology in which the voltage of the bidirectional converter storage capacitor used in the LED driver was adaptively decreased as the load became lighter to reduce converter power losses and maintain power efficiency at lighter loads [85]. In their research work, *Gucin et. al.* designed a multichannel LED driver in the output range of 14W-58W *Gucin et. al.*. The LED driver mentioned is highly efficient and uses the series resonant converter (SRC) topology [86]. The LED drivers in the above mentioned works did not take into consideration the current mismatch among same-rated LED chips. The compliance of values of electrical parameters was not reported for the LED drivers mentioned above on universal AC supply, so their compliance with recommended standards is unknown. This is the first

research gap that needs to be addressed because it will be appropriate to use one single driver for wide output range multiple-string LED modules that are free from current imbalance among connected LED chips and comply with relevant standards.

*The multiple-string wattage-independent LED luminaires designed in **Chapter 4** with the distinct features of wattage independence in a broad operating range is a decent effort to address the research gap mentioned above. The designed driver is free of the current imbalance in the parallel LED strings that occurs due to the disparity among the LED chips of the same ratings.*

Stability analysis is another important aspect of LED driver design. The operation of the LED driver must be stable for its satisfactory performance. Stability analysis is carried out by developing its mathematical model and obtaining the characteristics of the system by any one of the available methods, such as the root locus method, nyquist diagrams or bode plots as reported in the following research works [73, 100–102]. The stability analysis of the LED luminaires at different input voltages was presented by *Jia et. al.* using Bode plots of loop gain. In this work, stability was defined in terms of DC gain. Stability analysis showed that the designed driver was less stable when driving LED modules with fewer LED chips and driver operation was more stable at higher input voltages [100]. In another work by *Moon et. al.*, the stability of the LED driver was analysed by comparing their loop gain Bode plots with the conventional LED driver having PI controller [73]. The root locus method was used by *Kim* to assess the performance of the linearised buck LED driver in transient state [101]. The stability issue for the N+1 redundancy system based on the small signal model was analysed by *Jiang et. al.* in their research study. The study showed that if the phase margin is small, the system becomes unstable during parallel operation [102]. However, the

LED drivers mentioned in the above works operate the lamp modules having a series arrangement of LED chips. Research works that considered LED luminaires having multiple strings in parallel have not reported steady-state analysis of the LED luminaire.

*This is the second research gap whose solution is provided in **Chapter 5** by performing stability analysis of the wattage-independent multiple-string LED luminaire designed in **Chapter 4**.*

## **2.2 Recent trends in LED lighting systems**

LED lighting systems are suitable for diverse lighting applications, unlike their preceding lighting technologies, and thus reduce substantial energy costs. Research has been going on since their advent to improve light quality and quantity of light from LED lighting systems. The features of LED lighting that are reviewed in this work are automatic dimming, fault analysis and wireless control.

### **2.2.1 Daylight-actuated automatic control**

In today's context of energy savings, increased focus on energy efficiency and visual comfort has emphasised the use of daylight in commercial buildings. In a natural daylight-assisted artificial light control scheme, controlling the light output of the luminaire and window blinds can be achieved by manual or automatic controls, or both. However, manual control is better suited as an additional option rather than the main control option. Automated control of LED luminaires in conjunction with available daylight should be the preferred control technique to achieve the desired results within an indoor environment [103–122].

Photosensor, controller and actuator are the basic blocks of any automatic daylight-responsive artificial lighting scheme. The different lighting schemes differ from each other on the basis of the usage of

these basic blocks. Various controllers were used to control integrated artificial lighting with daylight, but, being dynamic in nature, the Fuzzy Logic Inference System (FIS) is advantageous for the appropriate integration of available daylight to improve the light quality and quantity [114–118, 120–122].

The adaptive predictive techniques to control artificial lights using ANFIS were shown by *Kurian et al.* in their research work [121]. *Kurian et al.* further upgraded their work on the integrated daylight lighting scheme by optimising the visual and thermal comfort of users and electrical energy consumption using a FIS-based window blind controller and an adaptive predictive artificial light controller [122]. In the study by *Lah et al.*, a fuzzy controller was developed to determine the position of a roller blind to achieve automatic illuminance control within a test chamber. In this work, only roller blinds were controlled and artificial light sources were not used [116]. Another research by *Colaco et al.* presents an online predictor for adaptive daylight illuminance, an algorithm to control artificial light and an FIS for window blinds to reduce glare and solar heat gain [117]. In their work, *Liu et al.* designed an FIS controller to regulate the luminous flux of LED luminaires. The FIS considered daylight, user movement, and visual comfort to achieve the desired results [115]. *Verghese et al.* designed a daylight integrated lighting system using a novel camera-based fuzzy controller to control window blinds. Based on the extracted image parameters, the controller optimises the illuminance and uniformity within a test space considering the thermal and visual comfort of the users [118]. However, in all the above mentioned works, the FIS is designed in MATLAB environment in a computer that must be connected to the controller and actuator using suitable interfacing accessories like PLC, DAQ, FPGA etc. The inclusion of computer and related accessories make the control scheme complex,

space-consuming and costly. It would be better if the FIS was implemented directly inside the controller, as it would eliminate the need for a dedicated computer and connection accessories.

*This is the third research gap that paved the way for the development of a Fuzzy logic based light controller for daylight responsive office lighting system discussed in **Section 6.1 of Chapter 6.***

### **2.2.2 Fault monitoring and adaptation**

At present, a typical LED module has a lifespan of up to 25,000 hours in terms of maintaining luminous flux [123, 124]. However, the driver unit has a shorter life expectancy than the LED module due to the presence of electrolytic capacitors [125]. But in currently available commercial LED lighting systems and the LED luminaires mentioned in previous works [53, 126–129], if the operation is hampered, it is not possible to infer whether the driver is faulty or the LED module without dismantling the complete LED lighting system and testing the driver and the LED module individually. However, this strenuous exercise can be excluded by the introduction of a fault detection module inside a light controller for the LED lighting system, which will indicate whether the driver or the LED module is faulty and the same can be easily replaced.

*This gap in research sets the need for the development of a fault-detecting light controller mentioned in **Section 6.2 of Chapter 6.***

However, mere monitoring or fault detection is not enough for the continuous and unhindered operation of the LED luminaire. The research work carried out **Section 6.2 of Chapter 6** and most of the available research [48, 130–132] discuss only the fault monitoring part. *Ding and Zhang* proposed a data analysis method that assessed the amount of damage to the LED and predicted the remaining life of the LED luminaire [130]. In another study by *Laadjal et. al.*, a novel

condition monitoring system is discussed to detect capacitor failures of a fault-tolerant LED driver [48]. *Suttharssan et. al.* in their research work demonstrated the use of condition monitoring strategies for high-power LEDs to predict the probable time of occurrence of failure [131]. The controllers designed and developed in the above works are incapable of operating the LED luminaires after a fault occurrence. These controllers also detect the occurrence of faults in LED modules that have a series arrangement of LED chips. Monitoring faults and subsequent adaptation to faults in series-parallel LED luminaires have not yet been reported.

*The solution of this research gap led to the design of smart fault-adaptive LED luminaire in **Chapter 4** that can monitor, detect and adapt to the failure of any connected LED chip and provide uninterrupted operation of the LED luminaire.*

### **2.2.3 Spectral tuning**

Nowadays, research related to the non-visual affect of light is gaining momentum. Light from LED luminaires is used to improve the well-being of the end-users with the use of white-tunable LEDs and compatible controllers. The amount and colour of light from an LED luminaire can be regulated automatically in a predefined pattern throughout the day or manually depending on the needs of the end-users. This is the basic principle of dynamic lighting, which is achieved by controlling the amount of light output along with spectral tuning. The luminaires used in dynamic lighting are white-tunable LEDs. White-tunable LED luminaires are mostly used in lighting applications employed in health, education and work sectors [133]. In health-care applications, white-tunable LED based dynamic lighting is used to generate light output from the artificial lamps that follows the outside

daylight pattern closely. This helps to realign the circadian rhythms and sleep-wake patterns of end users to achieve the most positive results [134–136]. The usage of tunable-white LEDs in lighting applications related to the education sector is activity driven and their objective is to increase the focus and improve the behaviour of the students[137–139]. Tunable-white LED luminaires are used in workplace lighting applications to prevent or reduce the risk of disrupted circadian rhythm. Spectral adjustment of white light is very beneficial for office workers whose circadian rhythm is interrupted because they work continuously at constant light levels throughout the day and is still more desirable for night workers who are at increased risk of disrupting the circadian rhythm [140–143].

Some of the commercially available tunable-white LED luminaires with integrated control are Philips iW Fuse Powercore [144], Philips FloatPlane [145], Philips BoldPlay [146] and Acuity Brands Slot LED-Dynamic Recessed Tunable White [147]. White-tunable LED lamps with wireless control designed to upgrade end-user personal lighting are also commercially available, such as Philips Hue white ambiance A19 [148], TP-Link LB120 [149], Sengled Element Plus [150], Ilumni A19 LED Smart Light Bulb [151] and Kasa Smart Wi-Fi LED Light bulb-Tunable White [152]. These commercially available products provide wireless control of CCT and illuminance using compatible mobile applications, but all these products are preferred only for domestic lighting applications, as they are stand-alone units with a single controller for single LED lamp. Academically, various light controllers are developed to spectrally tune white-tunable LED lamp modules for specific outcomes [52, 153–157]. In the work published by *Gilman et al.*, a wired, simple and manual control strategy for a single module of prototype tunable-white LED are proposed to maintain stable colour quality fidelity score compared to a standard daylight source

with an equivalent CCT [153]. Non-linear techniques are introduced to manually control the intensity and CCT of a single bicolor WLED source in the study conducted by *Chen and Tan* [157] and these non-linear control techniques were modified and improved by *Lee et al.* in their research work [156]. In another investigation carried out by *Qiao et al.*, only the CCT of a bicolor LED is manually varied using a single PWM signal [154]. In the work published by *Maiti and Roy*, a simple manual dynamic light controller is developed that provides variable CCT but constant illuminance from a single tunable-white LED light source at a vertical distance of 1m. The control logic based on Grassman's colour mixing law is embedded in a PIC 18F4550 microcontroller and wirelessly controlled by an infrared (IR) remote in the range of 4m. The limitations of the above-reviewed research articles are that the control logic is developed for a single luminaire. In another work by *Maiti and Roy* [52], the controller developed in their previous work [155] was modified to control multiple tunable-white LED sources manually as well as automatically using IR remote. The limitations of the updated work are that the number of set points for CCT and illuminance is limited to the number of remote keys and if the end-user desires to have a different set point other than the assigned ones, then the controller is to be reprogrammed. Also, the real-time testing results of the operation of the developed controller when driving multiple light sources is not presented.

*This research gap of limited number of set points and lack of experimental results in real-time lighting application prompted the fabrication and real-time testing of a updated light controller in **Chapter7**. The developed light controller can automatically or manually control and spectrally tune the light output from multiple tunable-white LED luminaires independently or collectively.*



## 2.2.4 Wireless light control

The different operating components of typical automatic lighting control applications are installed separately and signals from one component to another are sent through dedicated low-voltage wire. This type of communication between the different components of the lighting system is called hardwired communication. A more recent approach to wireless control that communicates by radio waves has gained popularity, eliminating the need for dedicated control wiring. The advantages of wireless control are greater installation flexibility, good scalability, and lower installation labour cost [158]. Advancement in wireless technology led to its use in automatic lighting control applications. Initially, wireless communication using infrared (IR) Radio Frequency (RF) was used in LED light control [52, 53, 159]. However, limited range and communication disruption due to the presence of obstructions are some of the limitations of infrared RF control. This paved the way for the use of the RF Zigbee wireless protocol [160] with the advantage of a relatively long range and a low data rate [161–164]. Currently, with the advent of Bluetooth and Wi-Fi technologies, wireless control of the LED luminaire can be achieved through a smartphone. The light from the luminaires can be turned on/off, dimmed, and its CCT can be varied according to the needs of the end user [165–170].

*The fault-monitoring and motion-sensing light controller developed in **Section 6.2** of **Chapter 6** incorporates the Zigbee wireless protocol through Xbee wireless modules and the dynamic light controller developed in **Chapter 7** is operated via a smartphone using Bluetooth wireless technology.*

**Table 2.1:** List of important inferences from corresponding literature

Inference	Publications
An LED module having LED chips in series-parallel combination is used as the source of artificial light in almost all lighting applications instead of single chip as it provides continuous operation and reduces current requirement of the LED module	<p>N. Ning, W. Chen, D. Yu, C. Feng, and C. B. Wang, "Self-adaptive load technology for multiple-string led drivers," <i>Electronics Letters</i>, vol. 49, pp. 1170–1171, 2013.</p> <p>W. Chen and S. Hui, "A dimmable light-emitting diode (led) driver with mag-amp postregulators for multistring applications," <i>Power Electronics, IEEE Transactions on</i>, vol. 26, pp. 1714 – 1722, 07 2011</p> <p>C. Chiu, C. Shen, and G. Hsieh, "Universal lighting control of unknown connected light emitting diode arrays via a t-s fuzzy model-based approach," <i>IET Power Electronics</i>, vol. 8, no. 2, pp. 151–164, 2015.</p> <p>J. He, X. Ruan, and L. Zhan, "Adaptive voltage control for bidirectional converter in flicker-free electrolytic capacitorless ac-dc led driver," <i>IEEE Transactions on Industrial Electronics</i>, vol. 64, no. 1, pp. 320–324, 2017.</p>
The compliance of the electrical performance of the LED drivers, operating multiple string LED modules on Universal AC supply, with recommended standards was not reported	<p>N. Ning, W. Chen, D. Yu, C. Feng, and C. B. Wang, "Self-adaptive load technology for multiple-string led drivers," <i>Electronics Letters</i>, vol. 49, pp. 1170–1171, 2013.</p> <p>C. Chiu, C. Shen, and G. Hsieh, "Universal lighting control of unknown connected light emitting diode arrays via a t-s fuzzy model-based approach," <i>IET Power Electronics</i>, vol. 8, no. 2, pp. 151–164, 2015.</p> <p>J. He, X. Ruan, and L. Zhan, "Adaptive voltage control for bidirectional converter in flicker-free electrolytic capacitorless ac-dc led driver," <i>IEEE Transactions on Industrial Electronics</i>, vol. 64, no. 1, pp. 320–324, 2017.</p>
Stability analysis of the LED driver should be carried out to ascertain the performance of the LED lighting system through out the operating voltage range	<p>S. Moon, G. Koo, and G. Moon, "Dimming-feedback control method for triac dimmable led drivers," <i>IEEE Transactions on Industrial Electronics</i>, vol. 62, no. 2, pp. 960–965, 2015</p> <p>M.G. Kim, "Proportional-integral (pi) compensator design of duty-cycle-controlled buck led driver," <i>IEEE Transactions on Power Electronics</i>, vol. 30, no. 7, pp. 3852–3859, 2015</p> <p>L. Jia, Y. Liu, and D. Fang, "High power factor single stage flyback converter for dimmable led driver," 2015 IEEE Energy Conversion Congress and Exposition (ECCE), pp. 3231–3238, 2015.</p>
Various controllers are used to control integrated artificial lighting with daylight, but, being dynamic in nature, the Fuzzy Logic Inference System (FIS) is advantageous for the appropriate integration of available daylight to improve the light quality and quantity	<p>J. Liu, W. Zhang, X. Chu, and Y. Liu, "Fuzzy logic controller for energy savings in a smart led lighting system considering lighting comfort and daylight," <i>Energy and Buildings</i>, vol. 127, pp. 95–104, 2016.</p> <p>S. Colaco, C. Kurian, V. George, and A. Colaco, "Integrated design and real-time implementation of an adaptive, predictive light controller," <i>Lighting Research Technology</i>, vol. 44, no. 4, pp. 459–476, 2012.</p>

**Table 2.1:** List of important inferences from corresponding literature  
(Continued)

Inference	Publications
Almost all research works in the field of fault monitoring and adaptation of LED lighting system deals only with mere detection and monitoring of fault but mere monitoring and detection is not enough for continuous and unhindered operation of LED luminaires	K. Laadjal, F. Bento, and A. J. M. Cardoso, "On-line diagnostics of electrolytic capacitors in fault-tolerant led lighting systems," <i>Electronics</i> , vol. 11, no. 9, 2022
	C. Ding and T. Zhang, "Research on health monitoring of led lighting system," in <i>2016 Prognostics and System Health Management Conference (PHM-Chengdu)</i> , 2016, pp. 1–5
	T. Sutharssan, S. Stoyanov, C. Bailey, and Y. Rosunally, "Prognostics and health monitoring of high power led," <i>Micromachines</i> , vol. 3, no. 1, pp. 78–100, 2012.
Many light controllers were developed for spectral tuning of tunable-white LED modules but there was lack of real-time experimental results	P. K. Maiti, A. D. Singh, and B. Roy, "Design and development of daylight responsive rf light controller," in <i>2017 IEEE Calcutta Conference (CALCON)</i> , 2017, pp. 309–313
	J. Gilman, M. Miller, and M. Grimaila, "A simplified control system for a daylight-matched led lamp," <i>Lighting Research and Technology</i> , vol. 45, pp. 614–629, 10 2013
	P. K. Maiti and B. Roy, "Development of dynamic light controller for variable cct white led light source," <i>LEUKOS</i> , vol. 11, no. 4, pp. 209–222, 2015
	A. T. L. Lee, H. Chen, S.-C. Tan, and S. Y. Hui, "Precise dimming and color control of led systems based on color mixing," <i>IEEE Transactions on Power Electronics</i> , vol. 31, no. 1, pp. 65–80, 2016.
	H. Kim, W. Yang, Y. S. Cho, and D. Park, "Design of led lighting system using bluetooth wireless communication," <i>Journal of the Korean Institute of Illuminating and Electrical Installation Engineers</i> , vol. 29, pp. 1–7, 02 2015.
The quality and quantity of light from LED luminaires can be controlled through wireless communication using a smartphone	Y. Peng, K. Xia, and J. Wang, "Lighting control system based on smart phone and bluetooth," <i>Applied Mechanics and Materials</i> , vol. 602-605, pp. 1260–1263, 08 2014.



### **3 Performance evaluation of commercially available indoor pc-WLED luminaires**

In this chapter, the electrical and photometric performance of three different commercially available indoor pc-WLED luminaires is carried out along with verification of their compliance with relevant national and international standards. Tear-down of each LED luminaire is carried out to study their respective topology. The V-I characteristics of the LED modules under test are obtained experimentally. Laboratory experimentation is carried out to obtain their electrical and photometric performance. The electrical and photometric performance is determined from the experimental results. The results are also compared with relevant national and international standards to verify the compliance of individual LED luminaires.

### 3.1 Introduction

LED luminaires are currently used in almost all lighting applications, indoor or outdoor. The use of LED lighting ranges from high power rating applications like industrial and outdoor lighting to low power rating applications like decorative lighting. For each and every lighting application, a vast number of LED luminaires, varying in design topology and performance, are manufactured and marketed by a large number of companies and the product count is increasing every year. This fast development of LED technology has led to easy availability, increased efficiency and lower cost of LED luminaires [171]. Products from different manufacturers are required to comply with relevant local or international standards and regulations to ensure parity among products of different brands [172]. But LED products of ratings nearly similar to those of different manufacturers differ in electrical and photometric performance from each other. The cause of this variation is the difference in the driver topology and LED load modeling. In this chapter, comparative studies of three commercially available indoor pc-WLED luminaires with nearly similar ratings are carried out to ascertain the effect of design topology on electrical and photometric performance.

### 3.2 Test luminaires

For this study, three numbers of indoor pc-WLED downlighters are procured from the market as per availability. The three test luminaires are shown in **Fig. 3.1**. The declared product ratings and cost of the test luminaires are given in **Table 3.1**. The lamp modules and the drivers of the three luminaires are dismantled and their topology is studied. In each of the samples, 0.2W LED chips were arranged in a series parallel combination. The arrangement is given in **Table 3.2**.

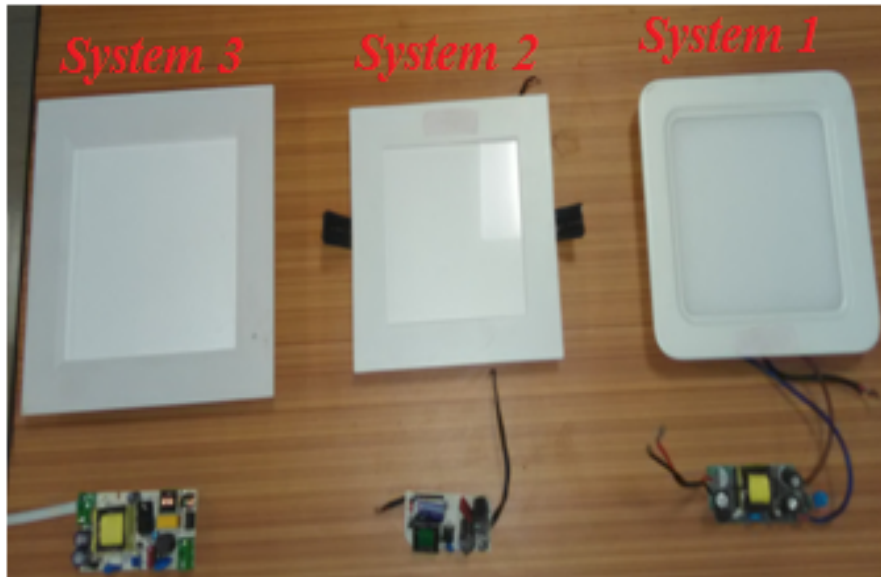


**Fig. 3.1:** Test LED luminaires

**Table 3.1:** Declared product ratings and cost

Parameters	System1	System2	System3
Rated AC Supply Voltage (V)	240 (100-265)	220-240	220-240
Rated Input Current (mA)	50	55	80
Rated Input Power (W)	10	12	12
Rated Power Factor	0.5	0.9	0.95
Rated DC Voltage (V)	30-38	40	27-42
Rated DC Current (mA)	270	250	270
Correlated Colour Temperature (CCT)(K)	6000	3000	6000
Colour Rendering Index) (CRI)	80-89	80-89	80-89
Approx. Market Price (INR)	1000	1200	1500

**Table 3.2:** Arrangement of LED chips inside test luminaires

Test luminaires	Number of LED chips	
	Series	Parallel
System1	9	5
System2	13	4
System3	12	5

### 3.3 Experimentation and performance parameters

The test luminaires are operated first on the DC supply and then on the AC supply. The experimental procedure and the considered performance parameters are mentioned in the following sections.

#### 3.3.1 DC operation

For DC operation, the maximum allowable limit for the ripple voltage is 2% of the DC output voltage [173]. The DC voltage is supplied from GwInstek make GPR – 6060D (0-60V, 0-6A) [174] DC supply which has a ripple voltage of 400mV in the range of 20-50V DC. So the ripple voltage has a range of 2% to 0.8% which is less than the maximum allowable limit of 2% in the entire operating region, as recommended by IS 16105:2012 [173].

When tested on DC supply, the driver becomes redundant and the DC supply is directly given to the LED modules. On DC operation, the input voltage in volts and input current in milliamperes supplied to the LED modules and their photometric parameters: relative lumen output in percent, CCT in kelvin and colour shift in terms of MacAdam ellipse size are measured. Relative lumen output and CCT are measured using an integrating sphere and Konica Minolta make chromameter CL-200A [175]. The absolute lumen output cannot be measured due to the unavailability of standard lamp. The colour shift of the LED modules with the variation of current is specified using MacAdam ellipse step size. Colour shift corresponding to MacAdam ellipse step size of 8 is within the allowable limits according to CIE [90]. The  $u'-v'$  chromaticity coordinates are measured with the help of Spectroradiometer JETI make SPECBOS1200 [176]. .



### 3.3.2 AC operation

According to IS 16105:2012, during AC operation, the maximum allowable %THD is 3% of the fundamental for the input voltage. For experimentation, the Agilent 6812B AC Power Source / Analyser (300V, 6.5A, 750VA, 45 Hz to 1 kHz) [177] is used from which the rated input AC voltage is supplied. The %THD of the AC power supply is 0.3% of the fundamental, which is well below the maximum allowable limit of 3%.

When AC operation is performed, the complete LED luminaire (lamp module together with the driver) is tested. The three sets of test luminaires are compared based on the parameters mentioned in **Table 3.3**.

**Table 3.3:** Comparison parameters for test luminaires

Electrical	Photometric
Input power factor	Relative lumen output in %
Efficiency	CCT in Kelvin
%THD	%flicker
Output power in watts	Colour shift in MacAdam ellipse size

### 3.4 Results and analysis

The experimental results obtained from laboratory testing are analysed to compare the performance of the test luminaires and to check their compliance with relevant standards.

\*DC operation During DC operation, the supplied input voltage and current are measured to obtain the V-I characteristics of the three test luminaires, as shown in **Fig. 3.2**, from which it is seen that the threshold voltage is maximum for System2 and minimum for System1. This experimental observation is in accordance with the LED chip arrangement of the test luminaires shown in **Table 3.2**. System2 had 13 numbers of LED chips and System1 had only 9 numbers of LED

chips connected in series.

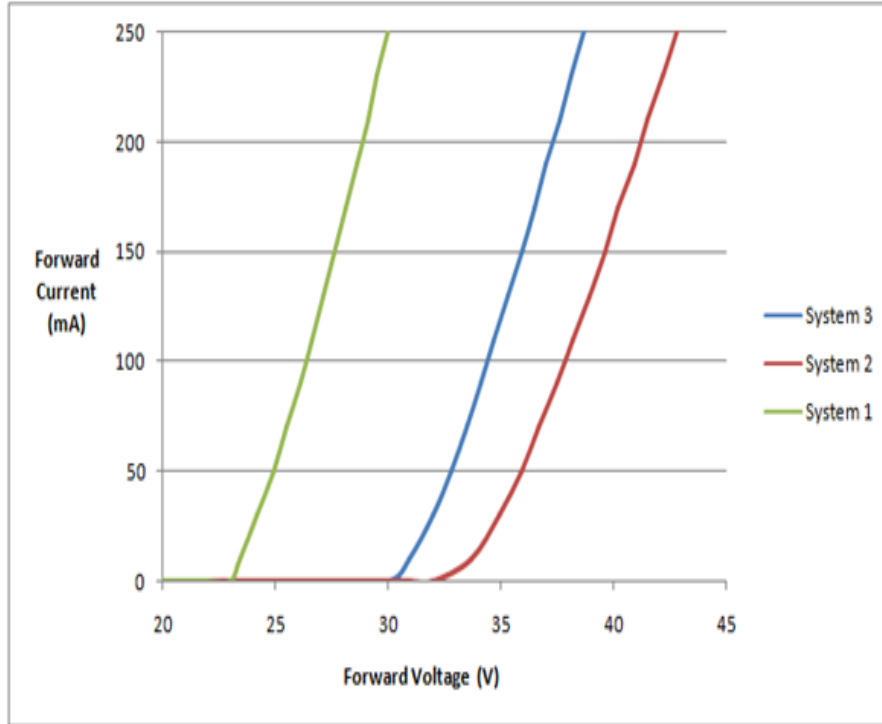


**Fig. 3.2:** V-I characteristics of the test luminaires

The photometric parameters are measured for a given range of input current for the three test luminaires. The variation in relative lumen output (%) and CCT (K) with input current of the three LED modules is shown in **Figs. 3.3- 3.4**. It is observed from **Fig. 3.3** that the variation of the relative lumen output with the input current is almost the same for System1 and System3, while for System2 it is slightly steeper than for the other two systems. From **Fig. 3.4**, it is observed that the CCT of the test luminaires remains constant throughout the input current range, except at low current values.

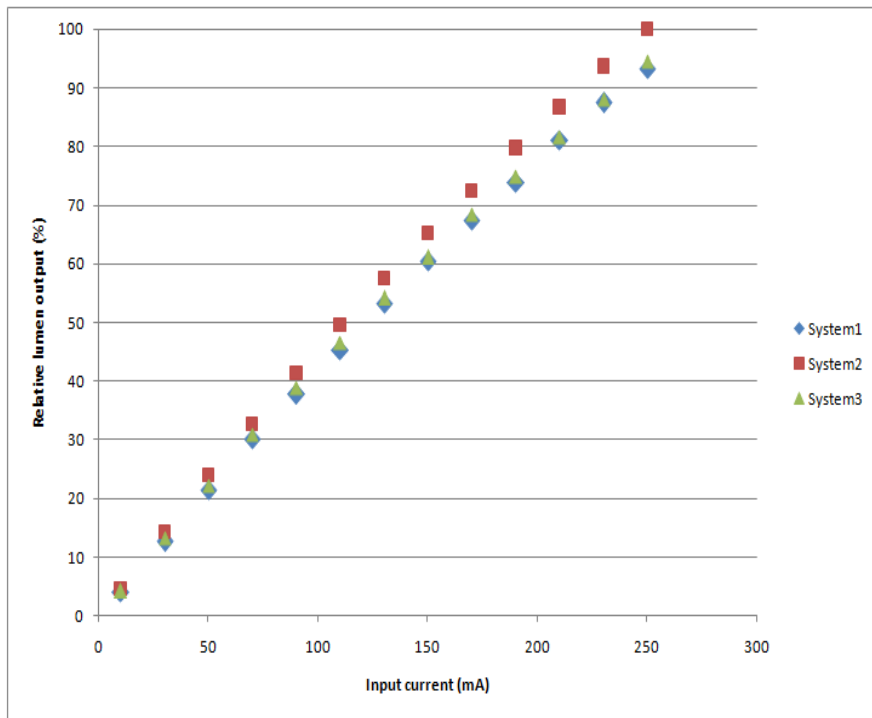


Fig. 3.3: Comparison of relative lumen output of the test luminaires

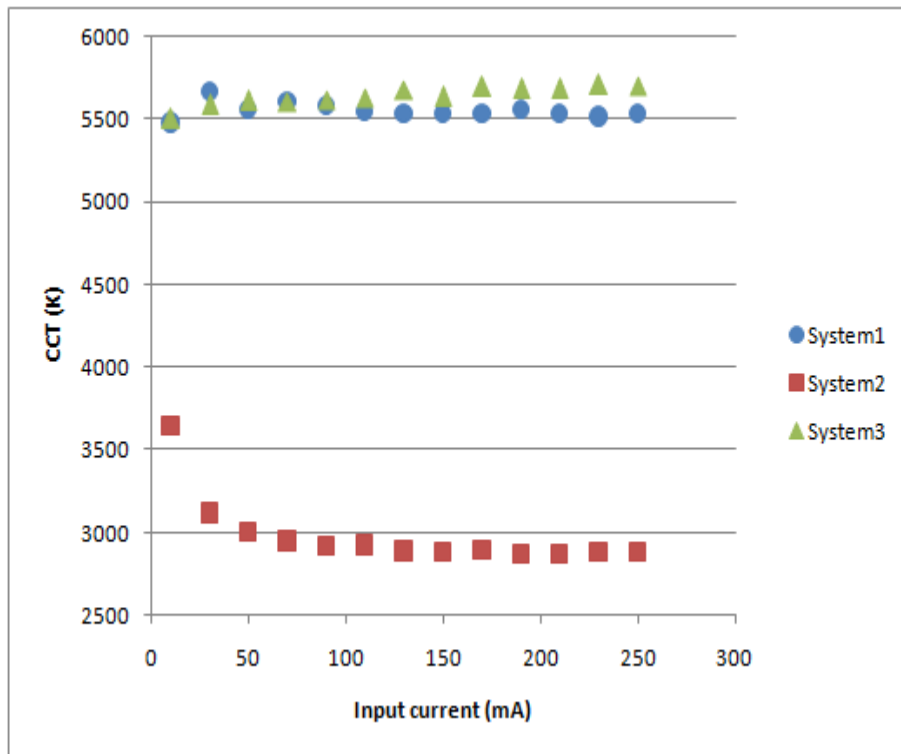
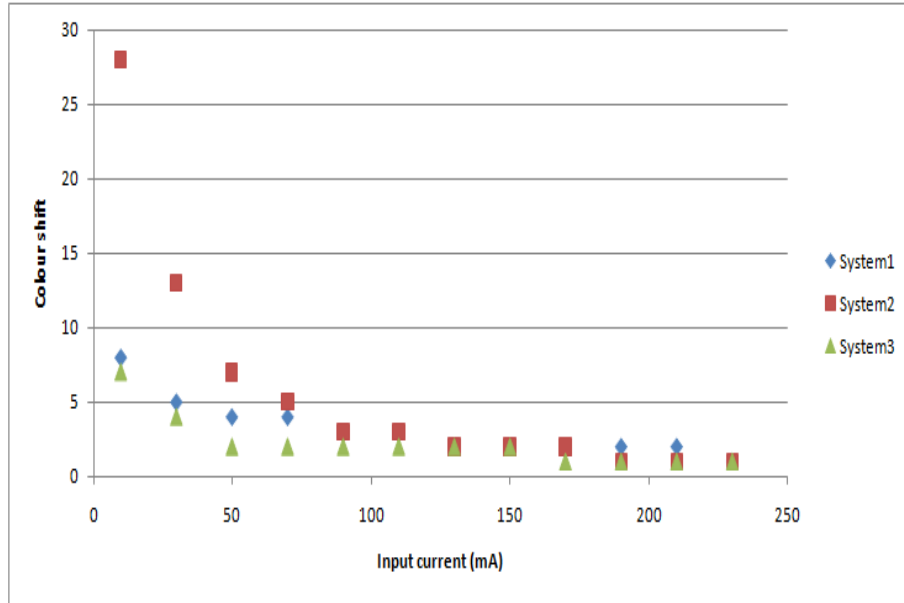


Fig. 3.4: Comparison of CCT of the test luminaires

The variation of colour shift of the test luminaires with the input current is shown in **Fig. 3.5**. The color shift should remain within the MacAdam ellipse step size of 8 [90]. From **Fig. 3.5** it is seen that the colour shift of System 1 and System 3 remains within 8 step and 7 step, respectively, throughout the operating current range, but that of System 2 is higher than 8 steps for low operating currents.



**Fig. 3.5:** Comparison of colour shift of the test luminaires

## AC operation

The electric and photometric results of different LED luminaires on AC supply are given in **Table 3.4**.

**Table 3.4:** Performance of test luminaires on AC supply

Test luminaires	Input voltage (V)	Input power factor	Output current (mA)	Output power (W)	Efficiency	Relative lumen output (%)	CCT (K)	Colour shift (Step size)
System1	240	0.42	276	7.6	0.80	100.0	5208	1
	230	0.42	275	7.6	0.81	99.4	5208	1
	210	0.44	272	7.5	0.81	98.4	5232	1
	190	0.45	270	7.4	0.82	97.6	5220	1
System2	240	0.88	247	9.8	0.77	100.0	2915	1
	230	0.88	246	9.8	0.76	100.0	2967	1
	210	0.89	247	9.8	0.76	100.0	2947	1
	190	0.89	247	9.8	0.76	100.0	2923	1
System3	240	0.95	274	9.7	0.80	100.0	5400	1
	230	0.95	272	9.7	0.80	99.0	5412	1
	210	0.96	271	9.6	0.81	98.5	5406	1
	190	0.97	269	9.5	0.82	97.7	5406	1

The following observations are made from the experimental results shown in **Table 3.4**:

- a) LED luminaires are designed such that their photometric parameters (relative lumen output, CCT and colour shift) show an insignificant variation through out the input supply voltage range of  $190V_{rms}$  to  $240V_{rms}$ .
- b) The input power factor of System 3 is 0.95, System2 has a power factor of 0.88 and System 1 has a very poor power factor of around 0.4. Therefore, only System1 complies with the International Standard IEC-610003-2 [89] which requires the minimum power factor to be greater than or equal to 0.9.
- c) The efficiency of System1 and System3 is more than 0.8 but that

of System2 is less than 0.8, implying that the driver of System2 has the maximum power loss.

In order to ascertain the %THD of the test luminaires, the harmonic spectrum of the input current of the individual drivers of the test luminaires at  $230V_{rms}$  is measured in the laboratory using Digital Storage Oscilloscope Tektronix TBS1072B (70MHz, 1GS/s) [178] as shown in **Figs. 3.6 - 3.8**. From the harmonic spectrum, amplitudes of second and odd harmonics are calculated and compared with the values specified by the international standard IEC-61000-3-2 [89] as shown in **Fig. 3.9**. Finally, the %THD values calculated from the experimental results are given in **Table 3.5**. From **Table 3.5** it can be concluded that the calculated %THD of System3 complies only with the relevant standards. The high value of THD of System1 implies that the driver of System1 consists of non-linear electronic components which draw more reactive power from the supply and hence draws an input current containing more amounts of harmonics than System2 and System3.

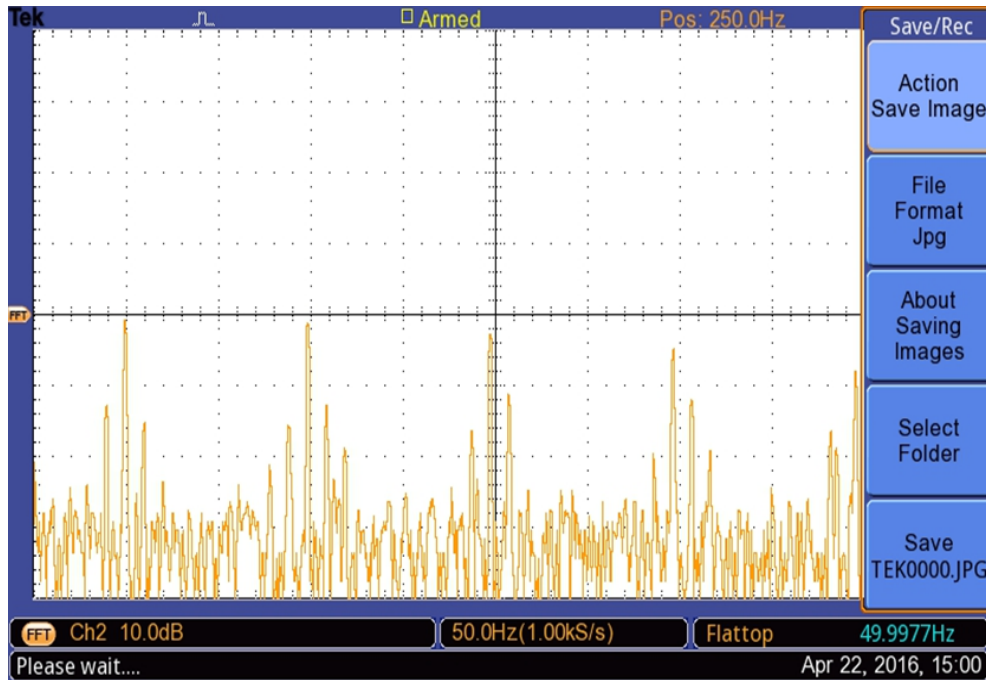


**Fig. 3.6:** Input current harmonic spectrum of System1 driver

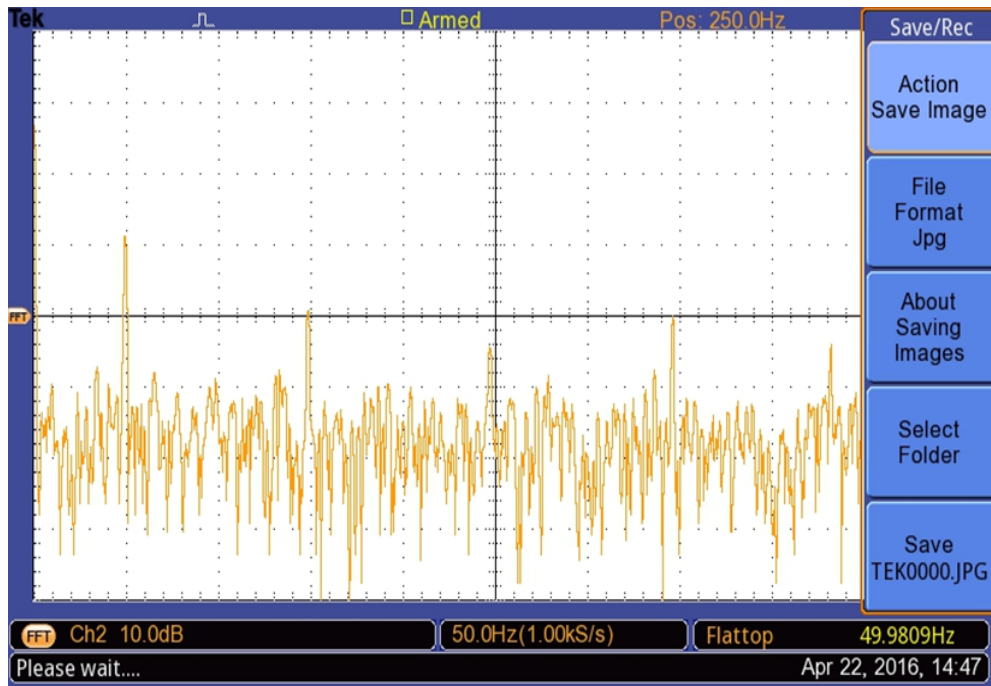


Fig. 3.7: Input current harmonic spectrum of System2 driver

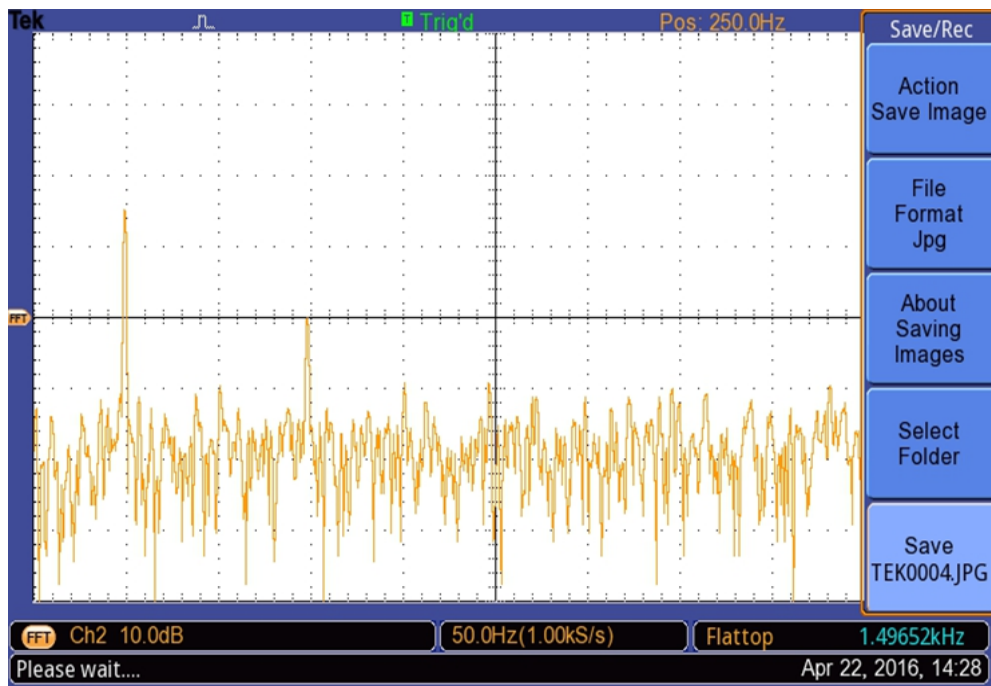
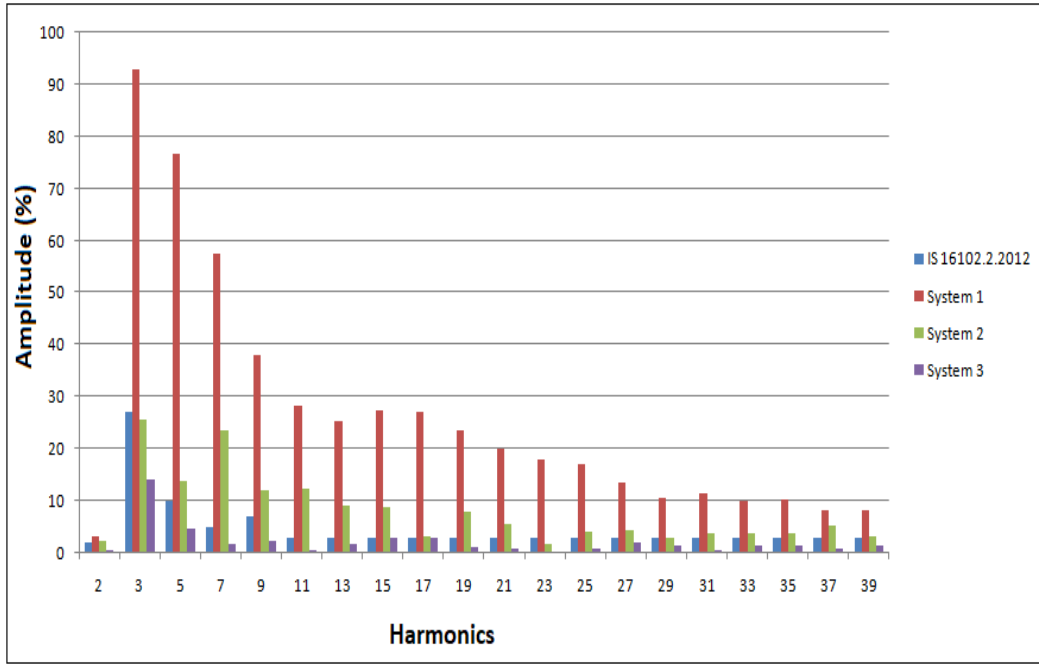


Fig. 3.8: Input current harmonic spectrum of System3 driver



**Fig. 3.9:** Comparison of input current harmonics of test luminaires

**Table 3.5:** Experimentally obtained THD values of test luminaires

Test luminaires	THD (%)
System1	160.35
System2	59.18
System3	24.73

The flicker phenomenon in test luminaires is measured in the laboratory in terms of %F given by (3.1) [91]

$$\%F = (A - B) * 100 / (A + B) \quad (3.1)$$

where, A is the peak light output value and B is the trough light output value.

A programmable power supply GwINSTEK APS 1102 [179] that complies with IS 16105:2012 is used to power the test luminaires. The light from the test luminaire, whose flicker measurement is to be measured, is made to fall on an ambient light sensor TEMT6000 [180] placed at a



set point below the luminaire. TEMT6000 has a special ambient light detector whose spectral responses match the human eye response, and it converts the light falling on it to a proportionate voltage. The variation of voltage, corresponding to the light output, with time is then observed using a GwINSTEK make Digital Storage Oscilloscope (DSO GDS 2202-E) [181]. In addition, a voltage waveform proportionate to the input current ripple is observed. The experimental setup installed for flicker assessment is shown in **Fig. 3.10**.

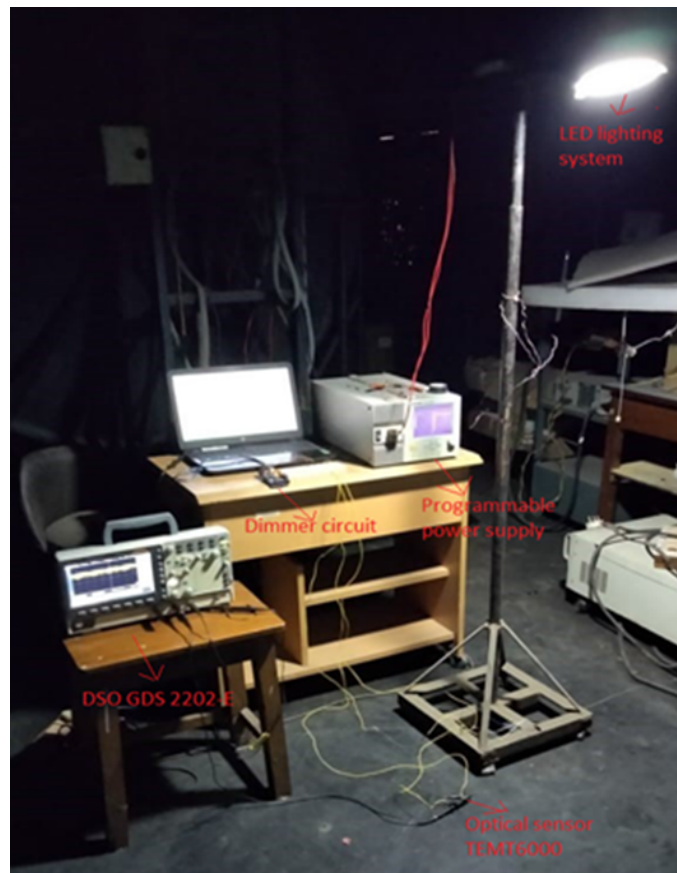


**Fig. 3.10:** Laboratory experimental setup for flicker measurement

The flicker profiles of input current and light output, obtained as the corresponding voltage waveforms, of the test luminaires are shown in **Figs. 3.11- 3.13** and the measured %F is given in **Table 3.6**. The maximum allowable upper limit of %F is 30% as recommended by the IEEE standards PAR 1789 [91] so it can be concluded from **Table 3.6**

that only System1 complies with the recommended standard value.

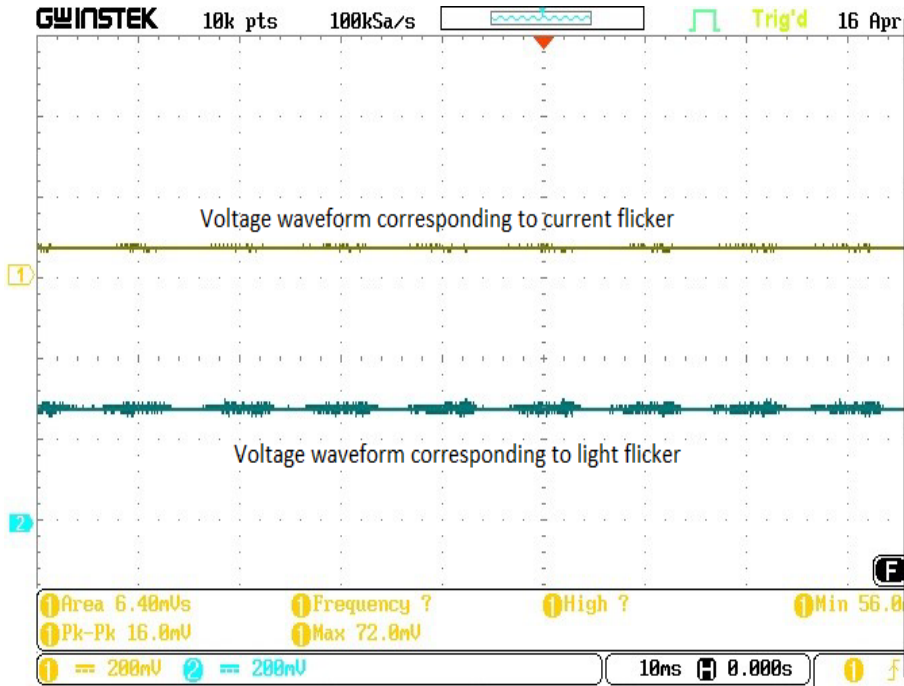


Fig. 3.11: Flicker profile of System1

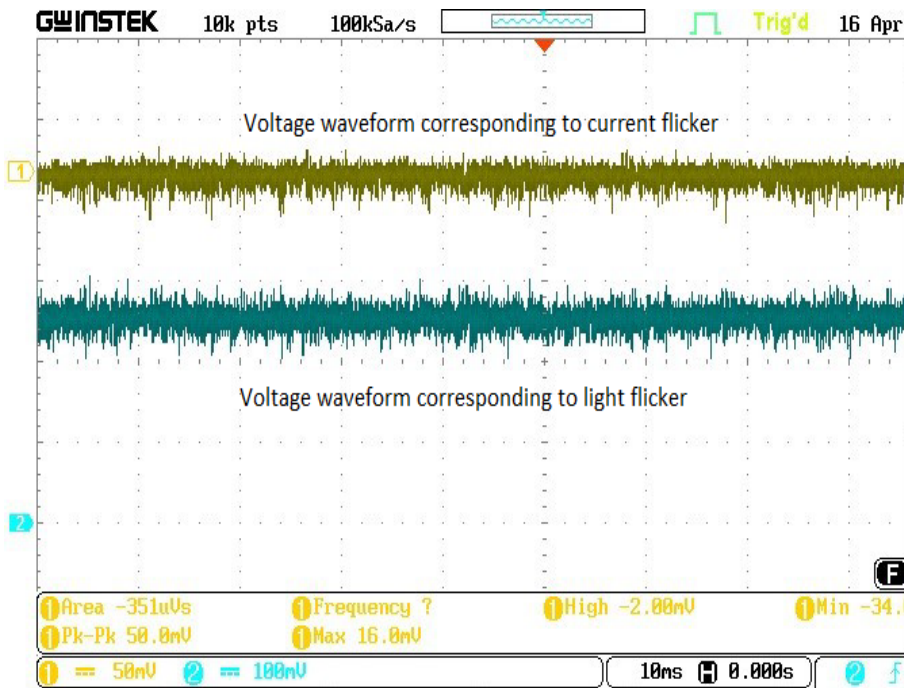
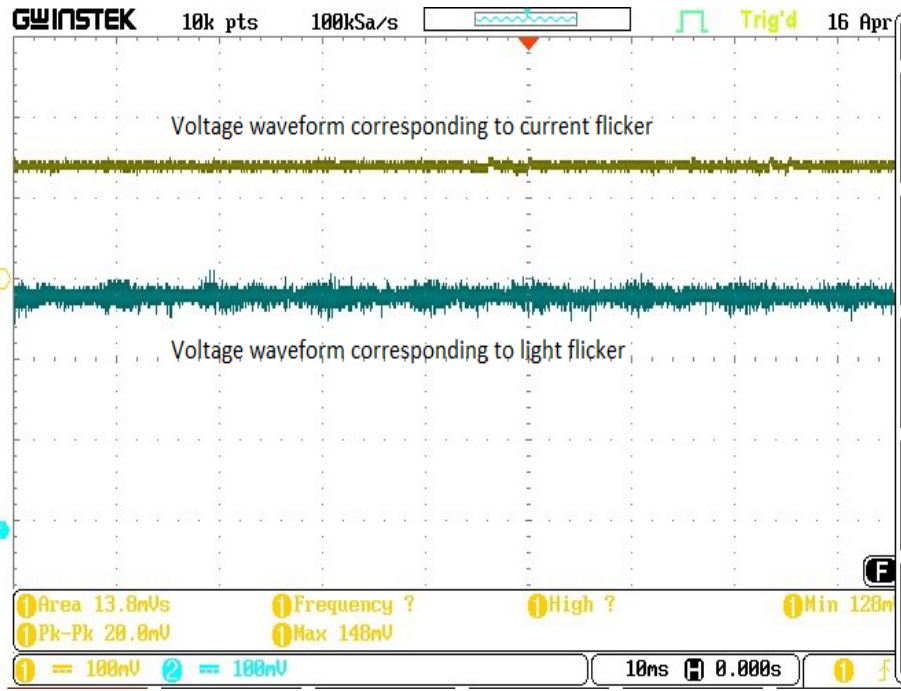


Fig. 3.12: Flicker profile of System2



**Fig. 3.13:** Flicker profile of System3

**Table 3.6:** Experimentally obtained %F of test luminaires

Test luminaires	%F
System1	12.5
System2	36.0
System3	33.3

### 3.5 Chapter summary

In this chapter, comparison of the electric and photometric performance of three pc-LED luminaires of fairly the same ratings is done by laboratory testing. During DC operation, the variation in input current affects the photometric performance of the lamp modules, but during AC operation, the variation in input voltage does not affect the photometric parameters of the lamp modules significantly, because the input current to the lamp modules remains constant even with the variation in input voltage. From the experimentally obtained results, the following conclusions are drawn:

- i) Lamp module of System2 has the highest forward voltage drop of 33.95V compared to that of lamp module of System 1 (23.51V) and System3 (31.13V).
- ii) Among the three test luminaires, only System3 with a power factor of approximately 0.95 and %THD of 24.73 complies with the recommended standards.
- iii) System2 has an efficiency of 0.76, which is less than the efficiency of System1 (0.80) and System3 (0.80).
- iv) System1 shows a significant colour shift at lower input currents than System2 and System3, which is undesirable.
- v) System1, however, compared to the other test luminaires, has a very small %F value of 12.5 which is below the recommended maximum value of 30%.

### Publications

The publications related to this work are as follows:

## Conference Publications: 2

1. **Vishwanath Gupta**, Kamalika Ghosh & Biswanath Roy. **2017**. Design topology based comparative study on electric and photometric parameters of commercially available LED lamp systems. **2nd International Conference for Convergence in Technology (I2CT), Mumbai, India, 2017, pp. 116-123**, doi: 10.1109/I2CT.2017.8226105.

2. **Vishwanath Gupta**, Subham Kumar Gupta & Biswanath Roy. **2022**. Experimental assessment of flicker in commercially available, white-LED indoor luminaires. Published as a chapter in the book titled **Automation and Computation, pp: 66-73**, doi:10.1201/9781003333500-8.



## 4 Smart fault-adaptive LED luminaire: Design and Modelling

The concept and design of a smart fault-adaptive LED luminaire is introduced in this chapter. The unique features of the n-string LED luminaire are as follows:

- a) wattage-independent operation in the 18-72W output power range
- b) unaffected current imbalance in the parallel LED strings, which occurs because of disproportionate current sharing among LED chips of same ratings
- c) ability to dim the light output from the connected LED module as well as monitor, detect and adapt to the failure of any connected LED chip.

The designed LED luminaire provides optimised light output even under faulty conditions, thereby ensuring unhindered improved operation. The LED luminaire model is simulated and tested in the Matlab-Simulink platform and its electrical performance for 100% to 30% of the rated light output and during the occurrence of faults is found to be satisfactory and in compliance with relevant standards.

## 4.1 Introduction

LED luminaires generally employ an LED lamp module having a series combination of single LED chips and a driver to achieve the desired electrical and photometric performance. These general LED luminaires are suitable for fixed power output lighting applications and suffer from the disadvantage of complete disruption of continuous operation even if a single LED chip becomes dysfunctional [63–71]. Some of the previous works [48, 130–132] dealt with fault monitoring in LED modules having series arrangement of LED chips prior to actual failure. But these systems cannot operate LED luminaires after a fault occurs. However, in one of the research work carried out by *Hsia and Ciou*, a power chip was proposed that can automatically identify faulty LED chips and bypass them without affecting the performance of other chips, but this requires complex electronics circuitry to be connected to the LED luminaire [47]. Therefore, this drawback of the series connection prompted the use of an arbitrarily series-parallel combination of LED chips to design an LED lamp module. However, the imbalance of current in series-parallel combination is one of its disadvantages [77, 78]. Some of the research articles [84–87] presented controllers for n-string LED luminaires operating in a wide output power range, but there were no dimming and condition monitoring capabilities, which, if present, will decrease the demand for light energy, provide visual comfort to the end user [73, 127, 182] and at the same time provide uninterrupted optimised operation of LED luminaires.

Hence, it will be appropriate to use n-string LED luminaires in future illumination applications such as industrial indoor, commercial indoor and road lighting that require features such as wide operating range, automatic dimming actuated by daylight and fault adaptation. Furthermore, the electrical performance of the LED driver should comply



with relevant standards [89, 91] when operated on universal AC supply.

So, a n-string LED luminaire is designed and simulated that operates automatically in the range of 18W-72W on universal AC supply, varies the light output according to requirements and adapts to the failure of any LED chip at rated conditions or during dimmed operation to provide uninterrupted optimised light output and delay the immediate replacement of the faulty LED luminaire.

## 4.2 Design and simulation

The block diagram of the smart LED luminaire is given in **Fig.4.1** and the simulated model in Matlab-Simulink is shown in **Fig. 4.2**.

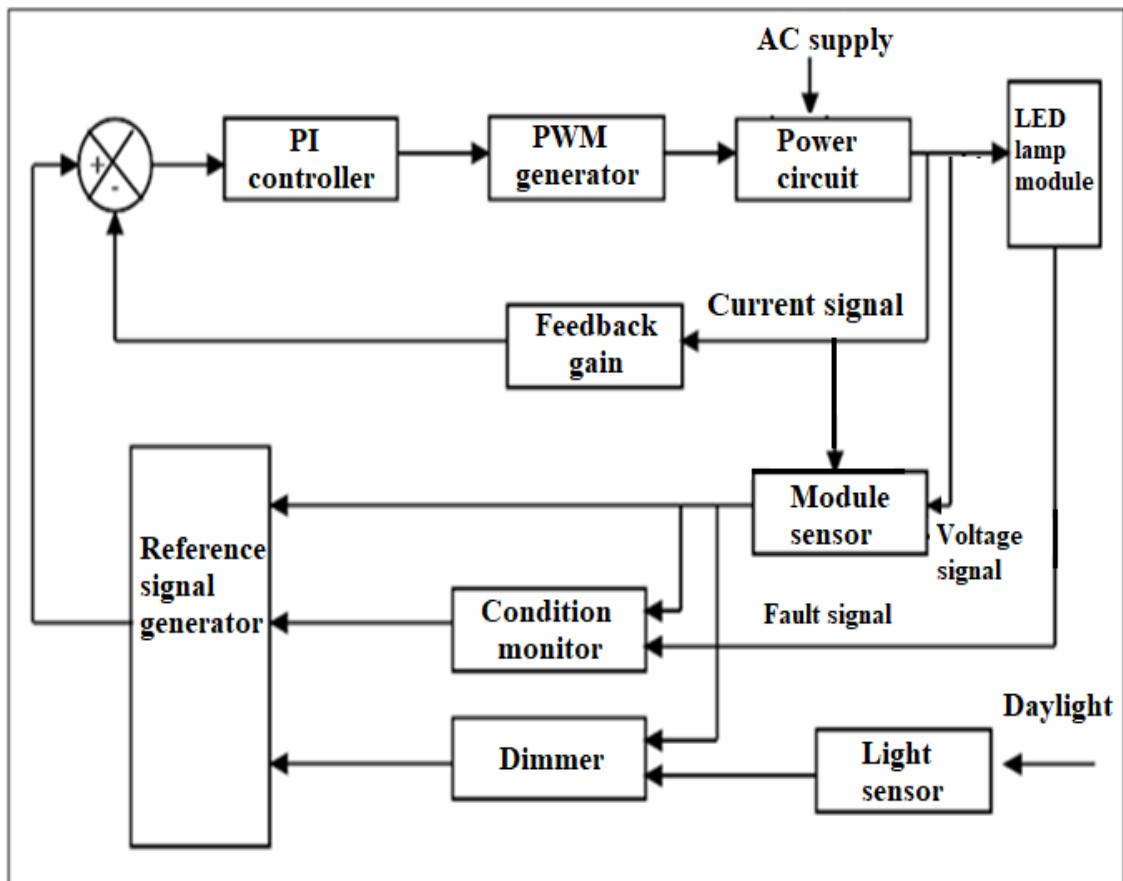


**Fig. 4.1:** Block diagram of the LED luminaire

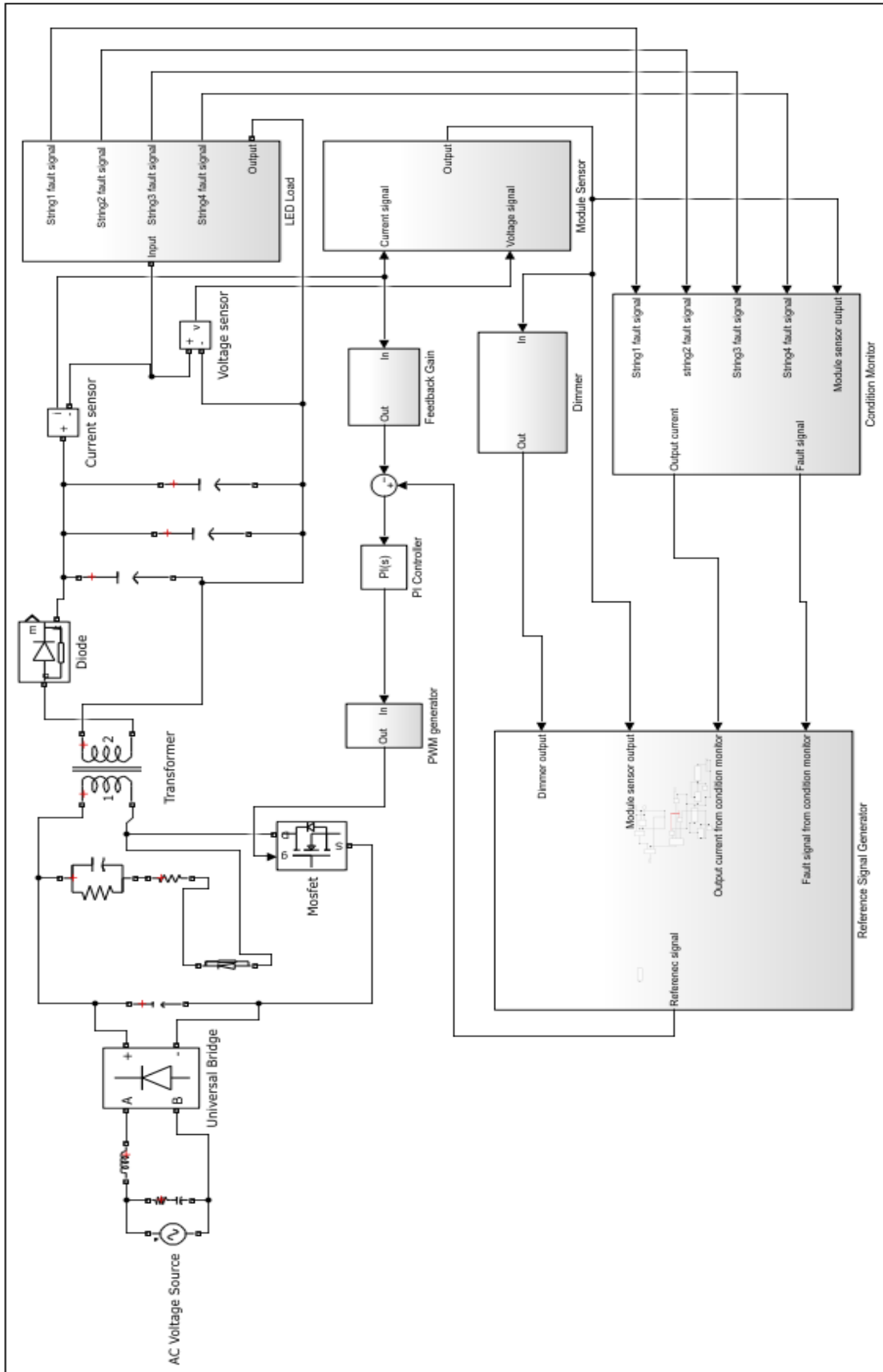
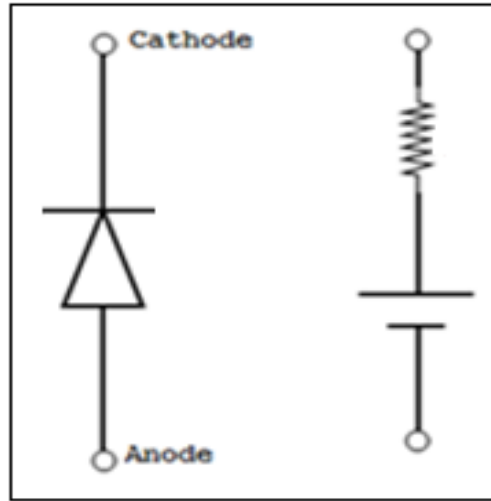


Fig. 4.2: Simulated LED luminaire

### 4.2.1 Modeling of LED lamp modules

At first, the 18W-72W LED lamp modules were designed using a piecewise-linear modelling technique. Each lamp module is assembled with 3W LED chips, as shown in **Fig. 4.3** [63].



**Fig. 4.3:** Equivalent Circuit of an LED chip: Linear model

The I-V model of single LED chip is given by (4.1) and that of the entire module is given by (4.2)

$$V_D = R_{Di}I_{Di} + V_{\gamma i} \quad (4.1)$$

$$V_o = \frac{N_s}{N_p}(R_{Di}) \cdot N_p I_{Di} + N_s V_{\gamma i} = R_D I_o + V_{\gamma} \quad (4.2)$$

In the present work, Lumileds make (LXML-PWC2) 3W white LED chips [183] having a rated voltage of 3V at 1000mA and threshold voltage of 2.4V are used to design the 18W-72W LED lamp modules. The lamp modules are then simulated in Matlab-Simulink platform using the obtained electrical parameters as given in **Table 4.1**.

**Table 4.1: Electrical parameters of LED modules**

Power rating (W)	LED chips in series	LED chips in parallel	Dynamic resistance (Ohms)	Threshold voltage (V)	Rated voltage (V)	Rated current (A)
18	3	2	0.9	7.2	9	2
	2	3	0.4	4.8	6	3
24	4	2	1.2	9.6	12	2
	2	4	0.3	4.8	6	4
27	3	3	0.6	7.2	9	3
30	5	2	1.5	12	15	2
	2	5	0.24	4.8	6	5
36	6	2	1.8	14.4	18	2
	4	3	0.8	9.6	12	3
	3	4	0.45	7.2	9	4
	2	6	0.2	4.8	6	6
42	7	2	2.1	16.8	21	2
	2	7	0.17	4.8	6	7
45	5	3	1	12	15	3
	3	5	0.36	7.2	9	5
48	8	2	2.4	19.2	24	2
	4	4	0.6	9.6	12	4
	2	8	0.15	4.8	6	8
	9	2	2.7	21.6	27	2
54	6	3	1.2	14.4	18	3
	3	6	0.3	7.2	9	6
	2	9	0.13	4.8	6	9
	10	2	3	24	30	2
	5	4	0.75	12	15	4
60	4	5	0.48	9.6	12	5
	2	10	0.12	4.8	6	10
	7	3	1.4	16.8	21	3
	3	7	0.26	7.2	9	7
	11	2	3.3	26.4	33	2
66	2	11	0.11	4.8	6	11
	12	2	3.6	28.8	36	2
72	8	3	1.6	19.2	24	3
	6	4	0.9	14.4	18	4
	4	6	0.4	9.6	12	6
	3	8	0.23	7.2	9	8
	2	12	0.1	4.8	6	12

Combinations having all LED chips in series or in parallel are not considered because if all LEDs are connected in series, the module will be inoperable if any one LED chip is destroyed and if all LEDs are connected in parallel large output current will flow for high-power modules, which makes component selection for the LED driver difficult and costly as well. Since, the minimum number of parallel branches is 2 in the modelled LED modules, 2A is set as the minimum rated current value.

The fault detection is done by measuring the voltage in any one of the LED chips in each parallel string during operation. If the voltage across that chip is within the rated operating range, then the whole parallel string is considered healthy; otherwise, it is considered faulty. This is because, if that particular chip is faulty, it becomes open circuited and therefore, the voltage across that LED chip will be the voltage applied to that parallel string, which will be greater than its rated voltage and if any other LED chip of that particular parallel string becomes faulty, then this chip gets open circuited and the voltage across the LED chip under measurement will become less than the minimum rated value, ideally zero. Therefore, one voltage sensor is connected in parallel with any one of the LED chips in each parallel string for condition monitoring and fault detection. Hence, to detect fault in each parallel string of an LED lamp module having 'n' parallel strings, only 'n' number of voltage sensors are required, which is the minimum requirement for fault detection. The designed LED lamp module is shown in **Fig. 4.4**.

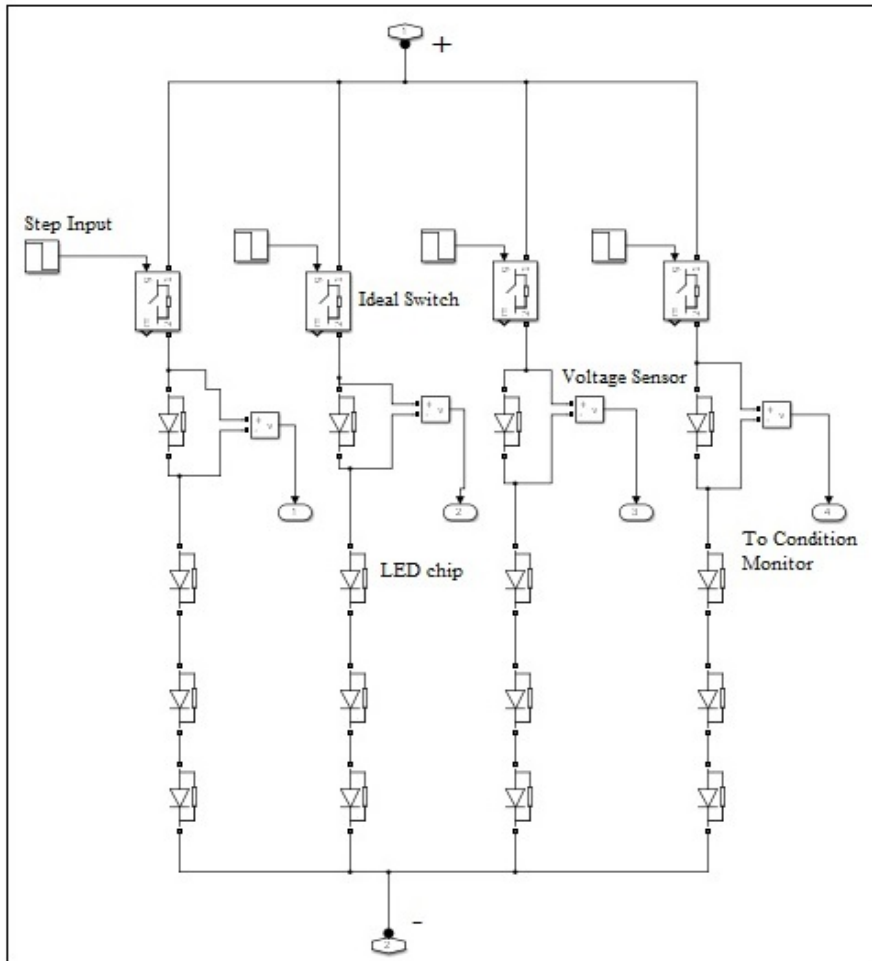


**Fig. 4.4:** Simulated LED module

### 4.2.2 Modeling of LED driver

The simulated LED driver model consists of the power circuit and the control circuit model.

#### Power circuit model

The power circuit is responsible for powering the LED lamp modules from AC supply. It incorporates an EMI filter across the input AC supply to decrease the input current harmonics, bridge rectifier to rectify the AC input to corresponding DC and flyback converter to obtain regulated DC supply for operating the LED modules on universal AC

supply. The designed block diagram of the power circuit is shown in **Fig. 4.5**.

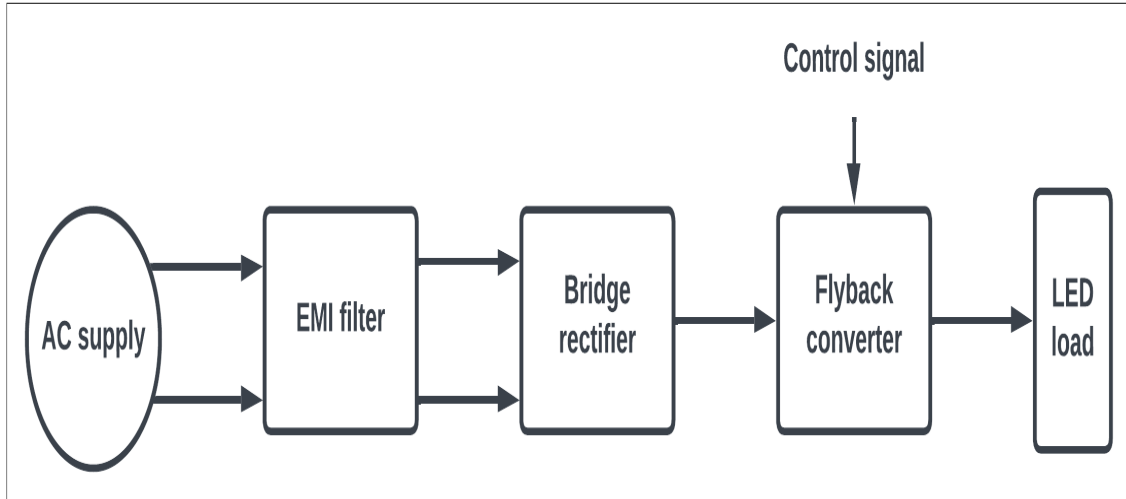


**Fig. 4.5:** Block diagram of designed power circuit

The power circuit of the LED driver is designed to operate LED lamp modules whose  $N_s/N_p$  ratio is greater than 1 in the power range of 18W-72W on Universal AC supply. This is because  $N_s/N_p$  ratio  $\leq 1$  will require higher amount of current and therefore, higher values of inductances and capacitances are required which will be costly, space consuming and commercially not viable. It is also observed that the  $N_s/N_p$  ratio for most commercial LED modules is greater than 1 [184].

### **Control circuit model**

The control circuit of the designed LED driver has two basic functions:

- A) Generation of reference signal
- B) Generation of control signal for power circuit

### **Generation of Reference Signal**

The generation of reference signal, corresponding to the values of the electrical parameters required at the input of the LED load, is carried

out using the following subsystem blocks: a) Module sensor block, b) Dimmer block, c) Condition monitor block and d) Reference signal generator block. Each block uses a dedicated control algorithm to generate the required signals. The control algorithms are shown in **Figs. 4.6-4.9**.

### **Module sensor block**

The module sensor block determines the number of parallel strings within the connected LED lamp module ( $N_p$ ) and the corresponding rated current ( $I_{N_p}$ ) by taking the instantaneous values of the output voltage and current of the power circuit as input and comparing them with predetermined values for each series-parallel combination of LED chips in the power range of 18-72W presented as a look-up table and given in **Table 4.2**. The look-up table is based on the operating point of the LED lamp module at the critical voltage ( $V'_\gamma$ ) slightly greater than their threshold voltage ( $V_\gamma$ ). When the input voltage of the LED lamp module connected as load is between  $V_\gamma$  and  $V'_\gamma$ , the corresponding rated current ( $I_o$ ) is set as the module sensor signal. The devised algorithm provides the simulated LED driver with the following unique features:

- 1) It makes the LED driver wattage independent in a output power range of 18-72W
- 2) It keeps the LED driver performance unaffected if there is a current imbalance in the parallel strings due to disparity among connected LED chips
- 3) It eliminates any possibility of transient instability in the LED driver system as it regulates the current of the connected LED load in small steps rather than a sudden change over. A large sudden current change can make the output current unbounded due to decrease in transient stability, whereas increasing the input current in small steps



does not affect the transient stability.

The look-up table is formulated as follows:

a) The values of the corresponding threshold voltage ( $V'_\gamma$ ) for all the LED modules are obtained from **(4.3)**

$$V'_\gamma = V_\gamma + \Delta V \quad (4.3)$$

where  $\Delta V$  is a small voltage value that theoretically lies in the range ( $0 < \Delta V \leq [V_D - V_\gamma]$ ).  $V_D$  is the rated voltage of a single LED chip.

b) The voltage range of the designed LED lamp modules (except those having minimum value of rated current) is set as  $V_\gamma$  to  $V'_\gamma$

c) The value of input current ( $I'$ ) at  $V'_\gamma$  volts for each LED lamp module (except those having minimum value of rated current) is calculated.

d) A tolerance value ( $\Delta I$ ) is estimated and the current range of the LED modules is set as  $(I' - \Delta I)$  to  $(I' + \Delta I)$ .  $\Delta I$  should be such that the current limiting values of any two LED modules do not overlap.

e) The required look-up table is generated with these limiting values of voltage and current and the corresponding rated current for all LED lamp modules in the given power range.

Table 4.2: Look-up table

LED chips in series in one string	Number of parallel strings	Rated power (W)	Rated current (A)	Reference signal (V)	Minimum voltage value (V)	Maximum voltage value (V)	Minimum current value (A)	Maximum current value (A)
8	3	72	3	0.3	19.2	19.5	0.14	0.24
7	3	63	3	0.3	16.8	17.1	0.16	0.26
6	3	54	3	0.3	14.4	14.7	0.2	0.3
	4	72	4	0.4			0.3	0.4
5	3	45	3	0.3	12	12.3	0.25	0.35
	4	60	4	0.4			0.35	0.45
4	3	36	3	0.3	9.6	9.9	0.33	0.43
	4	48	4	0.4			0.45	0.55
	5	60	5	0.5			0.58	0.68
	6	72	6	0.6			0.7	0.8
3	3	27	3	0.3	7.2	7.5	0.45	0.55
	4	36	4	0.4			0.62	0.72
	5	45	5	0.5			0.78	0.88
	6	54	6	0.6			0.95	1.05
	7	63	7	0.7			1.1	1.2
	8	72	8	0.8			1.29	1.39
2	3	18	3	0.3	4.8	5.1	0.7	0.8
	4	24	4	0.4			0.95	1.05
	5	30	5	0.5			1.2	1.3
	6	36	6	0.6			1.45	1.55
	7	42	7	0.7			1.71	1.81
	8	48	8	0.8			1.95	2.05
	9	54	9	0.9			2.26	2.36
	10	60	10	1			2.45	2.55
	11	66	11	1.1			2.68	2.78
	12	72	12	1.2			2.95	3.05

## Dimmer block

The dimmer block determines the amount of dimming (100% dimming indicates the rated light output and 0% dimming indicates no light output) required based on available daylight, which can be measured with the help of a light sensor. Based on the amount of dimming ( $X$ ) required, it modifies  $I_{Np}$  (from the module sensor block) to generate the dimmer output signal ( $D$ ) as given in (4.4).

$$D = X.I_{Np} \quad (4.4)$$

The simulated dimmer block is capable of dimming the light output (by varying the output current) from 100% to 10%.

## Condition monitor block

This block determines the number of healthy parallel strings of LED chips during operation ( $N_H$ ) and modifies the module sensor output signal ( $I_{Np}$ ) based on the number of healthy strings ( $N_H$ ). It takes the output of the voltage sensor, connected in parallel with any one of the LED chip for each parallel string, and processes it to ascertain the number of healthy parallel strings. The information about the number of healthy parallel strings is used to modify the module sensor output signal ( $I_{Np}$ ) to  $I_c$  which is given as input to the reference signal generator block.

## Reference signal generator block

This block determines the final reference signal using the outputs of the module sensor block ( $I_{Np}$  and  $N_p$ ), dimmer block ( $D$ ) and condition monitor block ( $I_c$  and  $N_H$ ) for continuous operation of the connected LED load under all possible operating conditions.

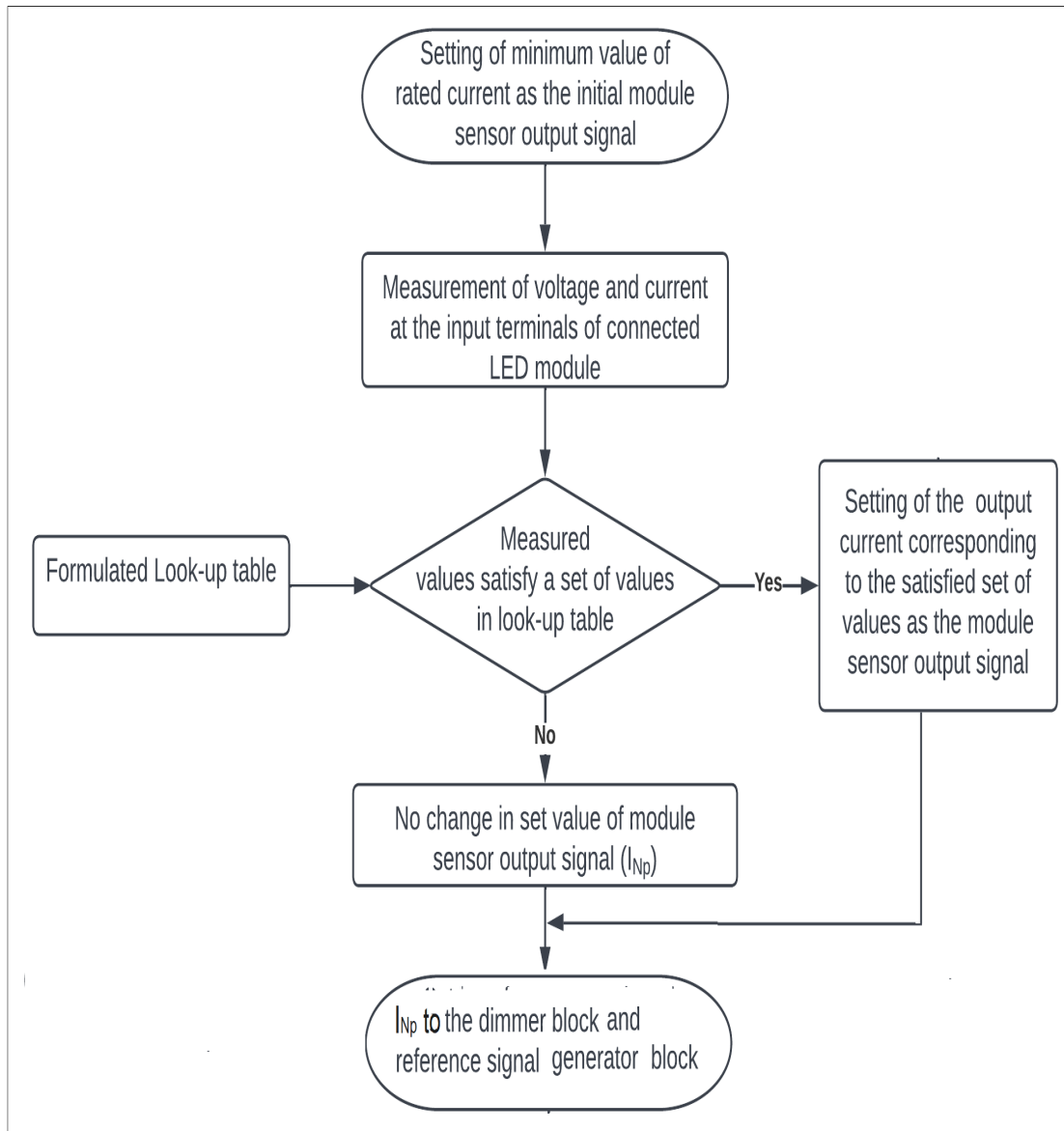


**Fig. 4.6:** Control algorithm for the module sensor block

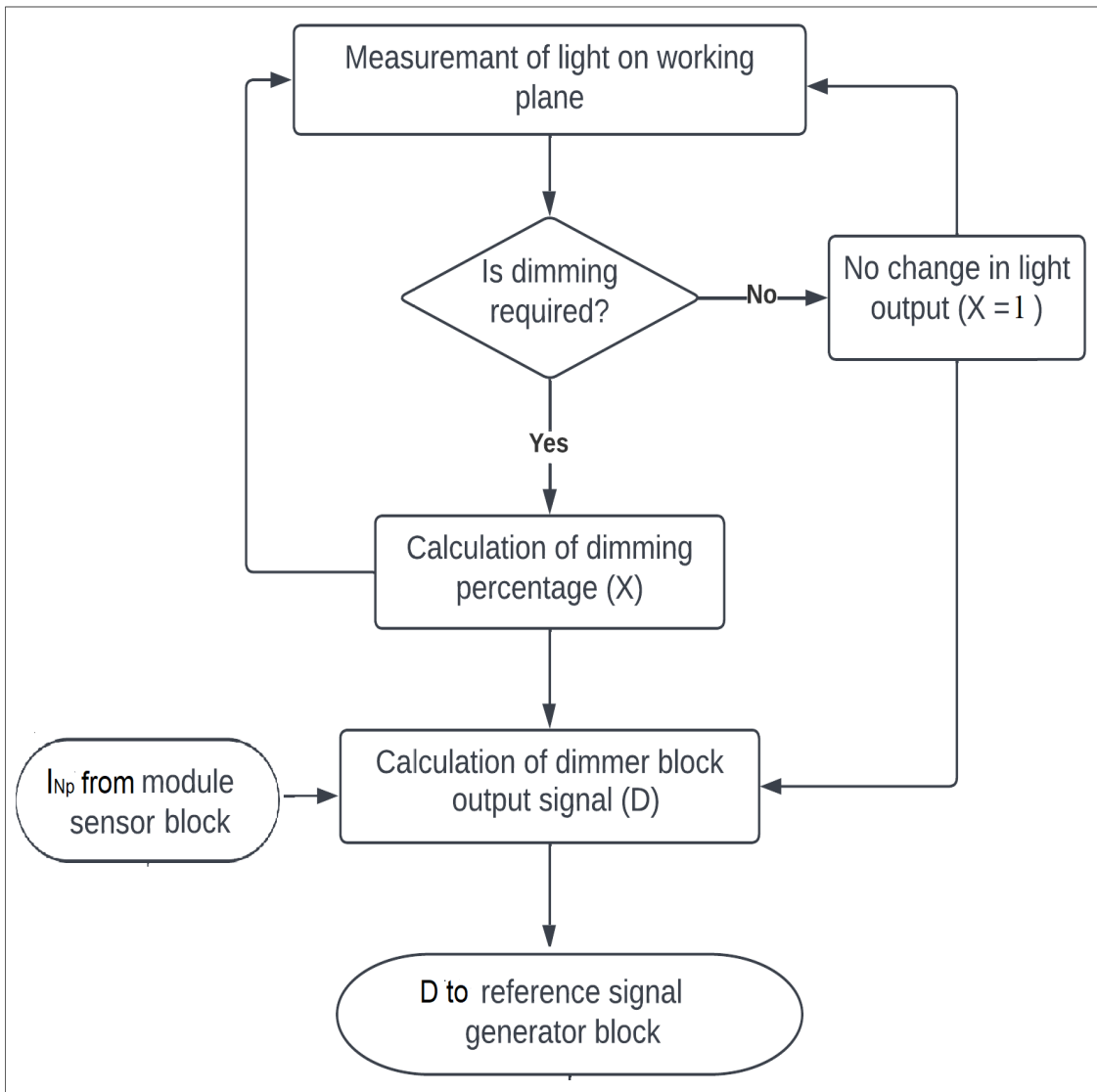


**Fig. 4.7:** Control algorithm for the dimmer block

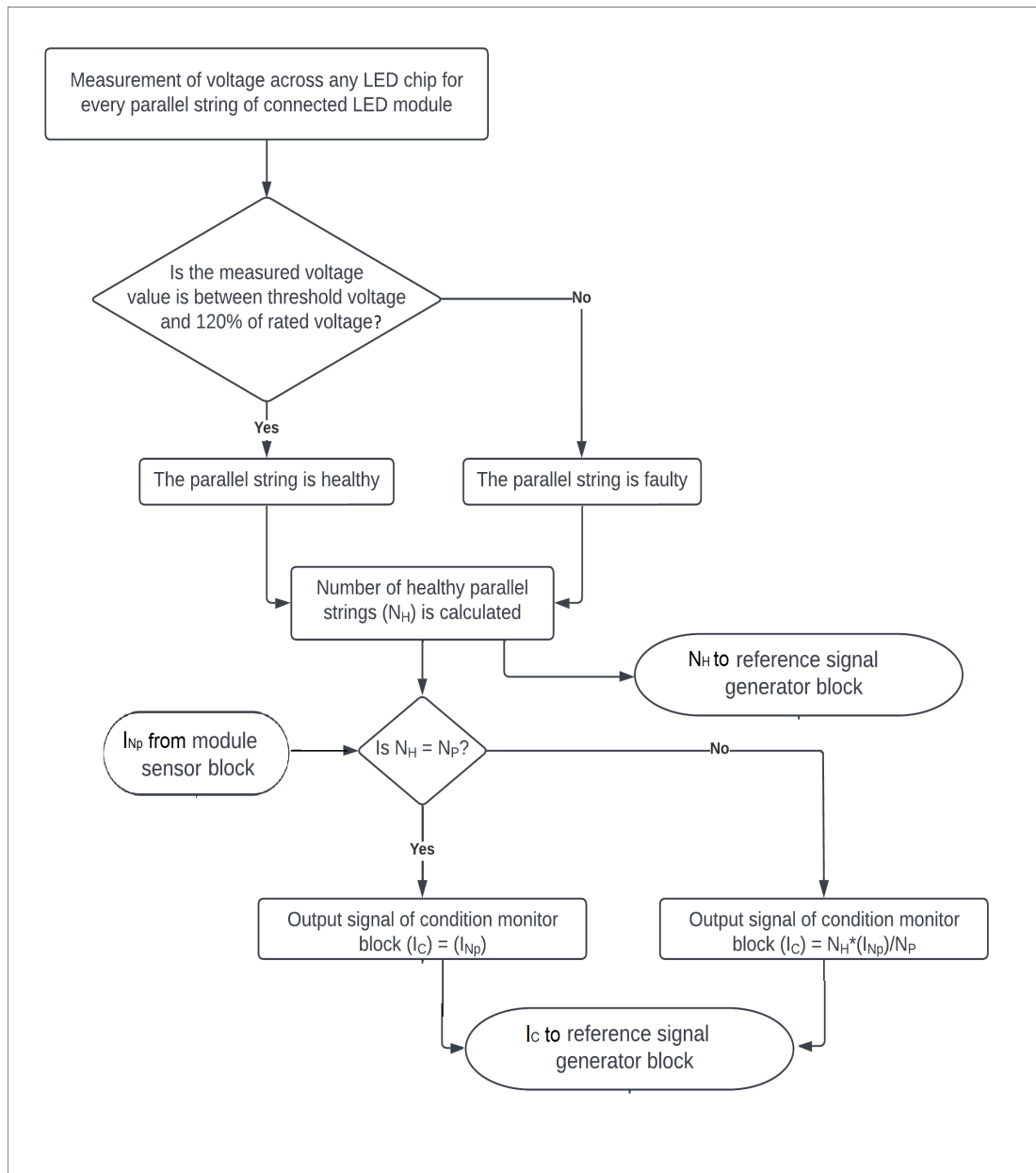


**Fig. 4.8:** Control algorithm for the condition monitor block

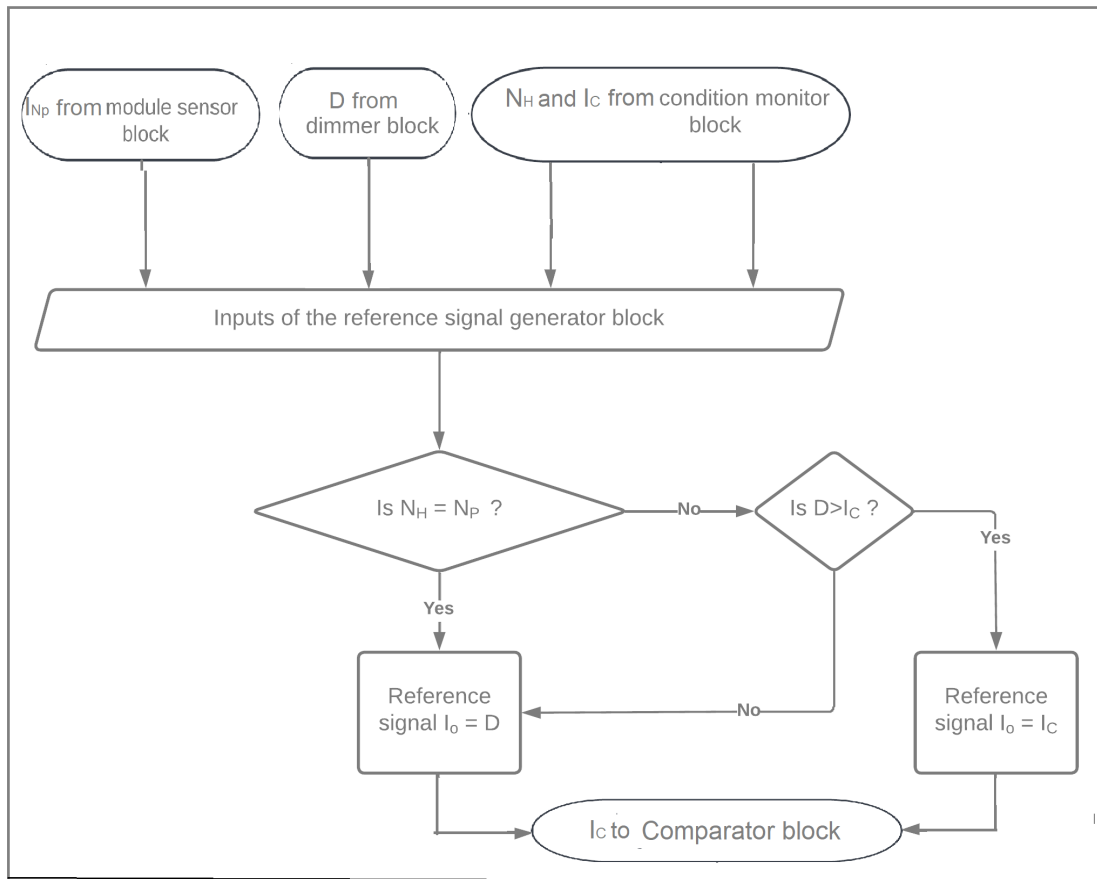


**Fig. 4.9:** Control algorithm for the reference signal generator block

### Generation of Gate Signal

Once the reference signal is generated, the gate signal is generated using conventional control blocks: PI controller, PWM generator block and feedback gain block. The error signal is generated by comparing the reference signal with the output signal of the feedback gain block. The gain of the feedback gain block is taken as 0.1. This gain value is the scaling factor that relates the rated current of the LED modules with the corresponding reference signal. A corresponding control signal is generated as the output of the PI controller using the error signal as the input. The PWM generator block, with the help of this control signal and a carrier signal (saw-tooth waveform of 100 kHz), generates gate pulse of required width.

### 4.3 Principle of operation

When power is given to the LED luminaire, the reference signal is set to the minimum value (0.2) by the reference signal regulator. At this instant, the output current is zero and so the value of error signal is equal to the value of reference signal. The PI compensator generates a control signal based on this error signal, which is compared with a 100kHz sawtooth carrier signal to generate the required PWM gate pulse. When the gate pulse is obtained, the MOSFET becomes ON, and as a result the output voltage starts to build up to make the output current follow the reference signal. However, current starts flowing in the LED module only when the driver output voltage becomes more than the threshold voltage of the connected LED module. During this period, when the driver output voltage is between  $V_\gamma$  and  $V'_\gamma$ , the output current is measured by the module sensor block, which generates the corresponding module sensor signal. The generated module sensor output acts as input to the condition monitor block and dimmer block. The amount of dimming required ( $X$ ) is determined by the dimmer whose output is the required dimmer signal given by (4.4). If no dimming is required, that is,  $X = 1$ , the required dimming signal  $D = I_{Np}$ . Meanwhile, the voltage across the LED chips of the connected LED load is measured and given as input to the condition monitor block. The condition monitor has the required signal  $I_c = N_H * I_{Np} / N_P$  as its output. However, if there is no faulty string, then  $I_c = I_{Np}$ . Finally, outputs of the module sensor block ( $I_{Np}$  and  $N_p$ ), dimmer block ( $D$ ) and condition monitor block ( $I_c$  and  $N_H$ ) are given as inputs to the reference signal generator block to set the reference signal ( $I_o$ ). If no dimming is required and there are no defective strings, then  $I_{Np}$  is set as the reference signal  $I_o$ . If dimming is required but there are no faulty strings, then the reference signal generator makes  $D$  (equal to  $X * I_{Np}$ ) the reference signal. However, if dimming is required and one or more



parallel strings become faulty, then the reference signal is made equal to  $I_c$  or  $D$ , whichever is lower for optimised operation. This ensures that the maximum current in each parallel branch is equal to or less than their rated current, thereby providing optimised operation under fault occurrence by preventing avalanche breakdown.

#### 4.4 Results and analysis

The simulated LED luminaire is tested in the output power range of 18W-72W at 5 input voltages, viz. the maximum ( $265V_{rms}$ ), the minimum ( $90V_{rms}$ ), intermediate input voltages ( $180V_{rms}$  and  $130V_{rms}$ ) and the nominal European and Indian input voltage ( $230V_{rms}$ ). There are three operating scenarios for the LED luminaire:

Scenario 1: No dimming required and no fault occurs

Scenario 2: Dimming is required but no fault occurs

Scenario 3: Dimming is required and fault occurs

##### Scenario 1

In this scenario, the LED luminaire operates at its rated conditions. No dimming is required and the connected LED lamp module is healthy. The dimmer block and the condition monitoring block are bypassed and the output of the module sensor block and the reference signal generator block determine the value of the reference signal. The LED driver output current waveforms obtained from simulation during the operation of LED modules having rated currents of 2A (48W), 3A (27W) and 4A (48W) respectively at  $230V_{rms}$  are shown in **Fig. 4.10**. When the number of connected healthy parallel strings ( $N_p$ ) are 4, 3 and 2 then the required output currents are 4A, 3A and 2A respectively and it is observed from **Fig. 4.10**, depicting the simulation result, that the output current meets the requirement of the connected LED load.

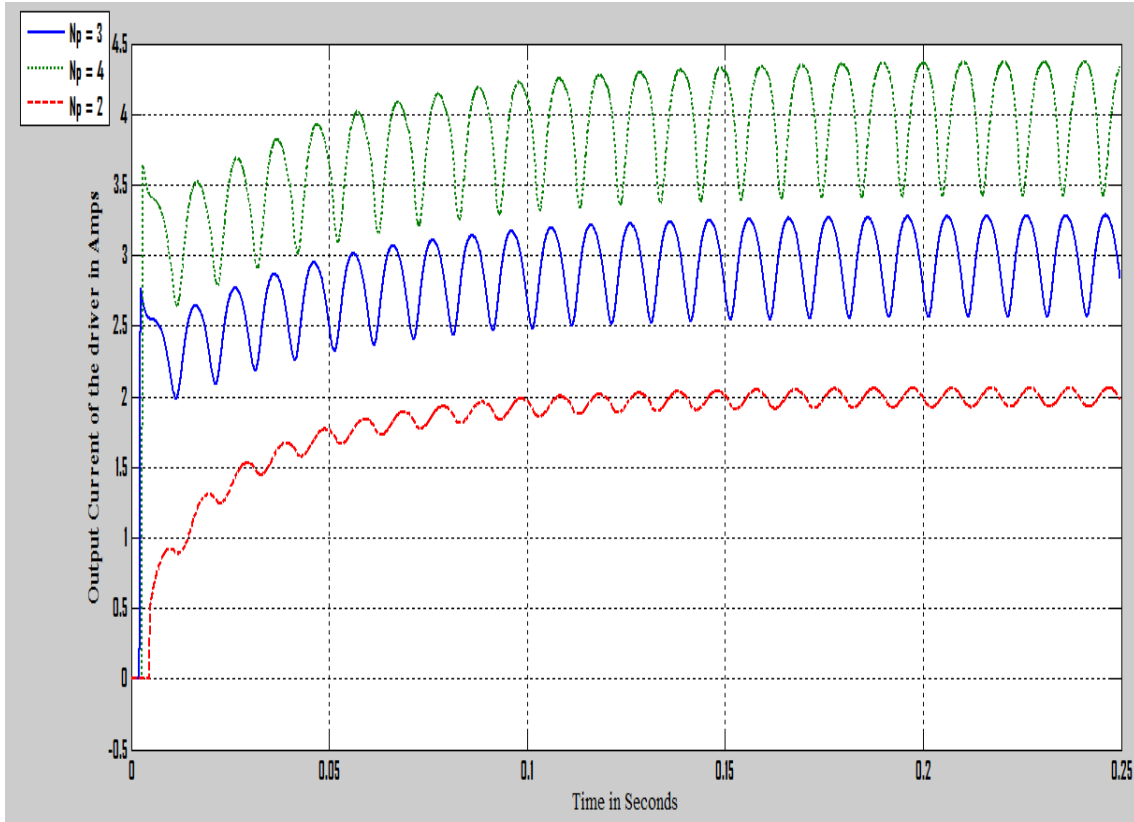


**Fig. 4.10:** Output Current of LED luminaires having rated currents of 2A, 3A and 4A respectively at  $230V_{rms}$

The electrical performance of the modelled LED driver throughout the entire output range under rated conditions is obtained through simulation. The variation of efficiency, Total Harmonic Distortion in percent(%THD), output current ripple in percent (%ripple) and input power factor in the output power range of 18-72W at  $230V_{rms}$  is shown in **Fig. 4.11**. %THD and %ripple are scaled down 20 times for ease of representation in a single diagram.

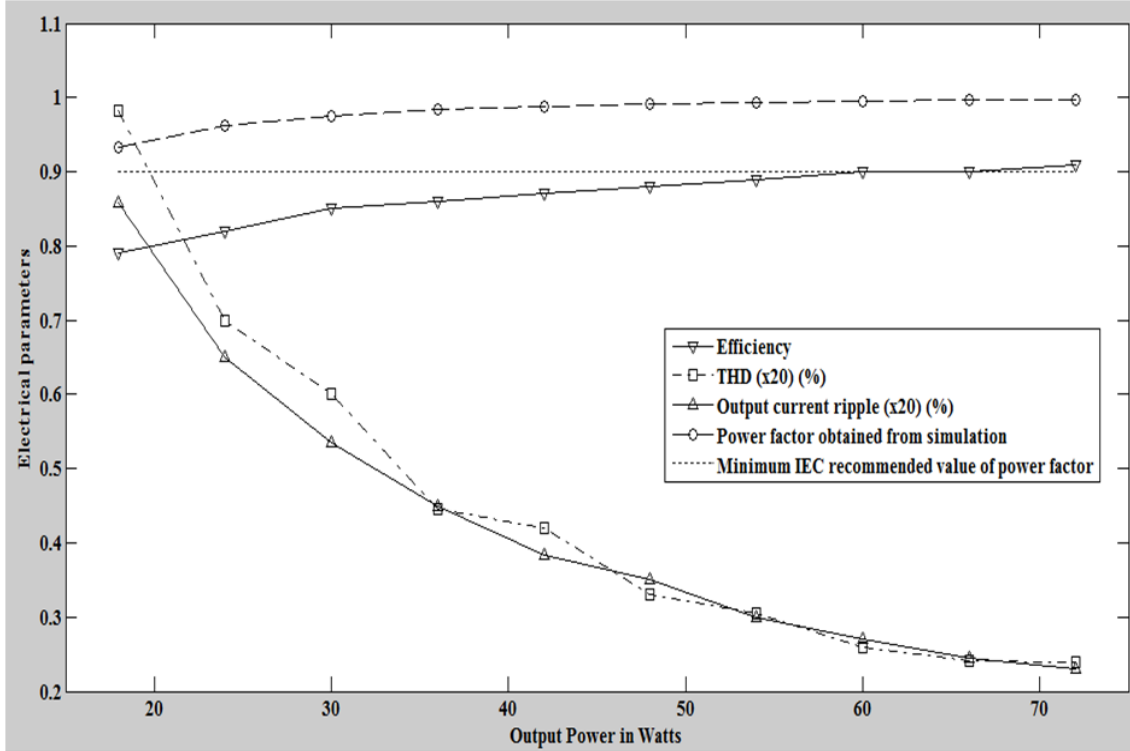


**Fig. 4.11:** Variation of electrical parameters of LED driver with rated power at  $230V_{rms}$

From **Fig. 4.11**, the following observations are made:

- 1) Input power factor varies from 0.933 to 0.996, always higher than the minimum recommended value of 0.9 [89]
- 2) efficiency varies from 0.79 to 0.91
- 3) THD varies from 19.63% to 4.8%
- 4) the output current ripple varies from 17.15% to 4.6%, which is within the maximum prescribed value of 42% [71] and IEEE Standard P1789 [91].

It is observed from **Fig. 4.11** that the input power factor and efficiency increase while %THD and the output current ripple decrease with the increase in rated output power. This happens because the LED driver supplies higher output power at comparatively higher voltages (current remaining constant), resulting in relatively low power loss.

## Scenario 2

In this scenario, the simulated LED luminaires are operated under dimmed conditions. However, no fault occurs in this scenario. The designed LED driver is made to operate a 6\*4 LED lamp module at  $230V_{rms}$  under dimmed conditions. During operation, the driver is required to vary the light level to 70%, 30% and 100% of rated value at 0.3, 0.45 and 0.65 seconds respectively. The obtained output current waveform of the LED driver is shown in **Fig. 4.12** and it is observed from **Fig. 4.12** that after 0.3 seconds the output current is 2.8A, after 0.45 seconds it is 1.2A and after 0.65 seconds it is again 4A, which are the required output currents for 70%, 30% and 100% of rated light output (considering linear relationship between LED luminaire light output and output current of LED driver). Hence, it can be concluded that the LED driver satisfactorily sets the required output current.

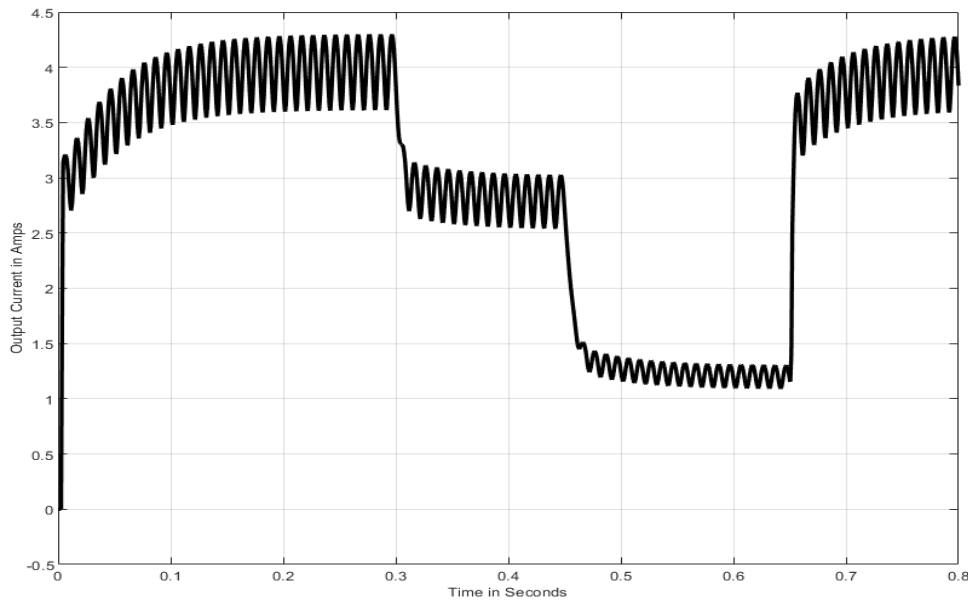
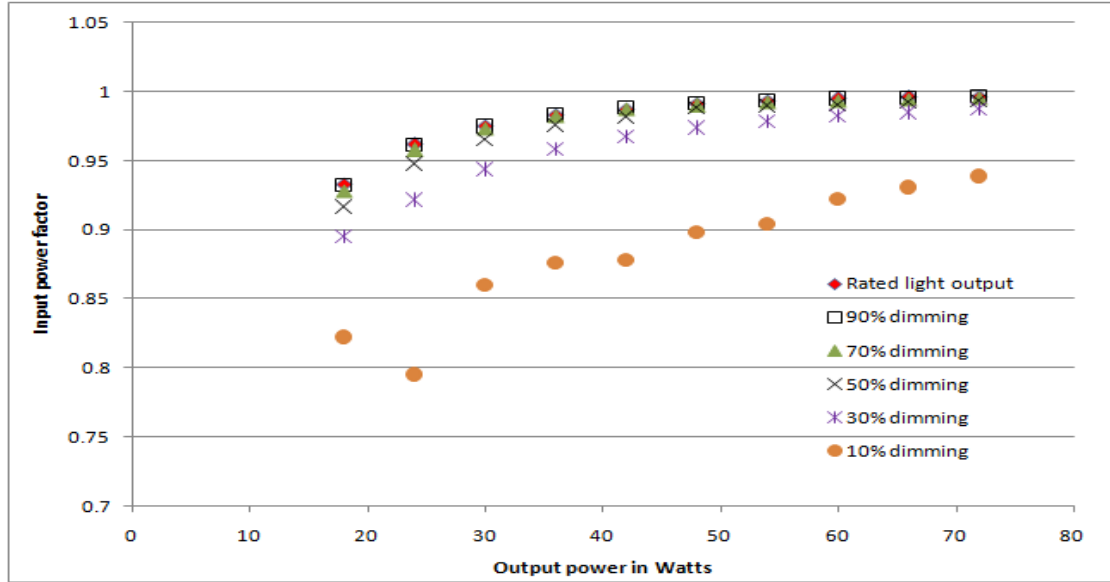


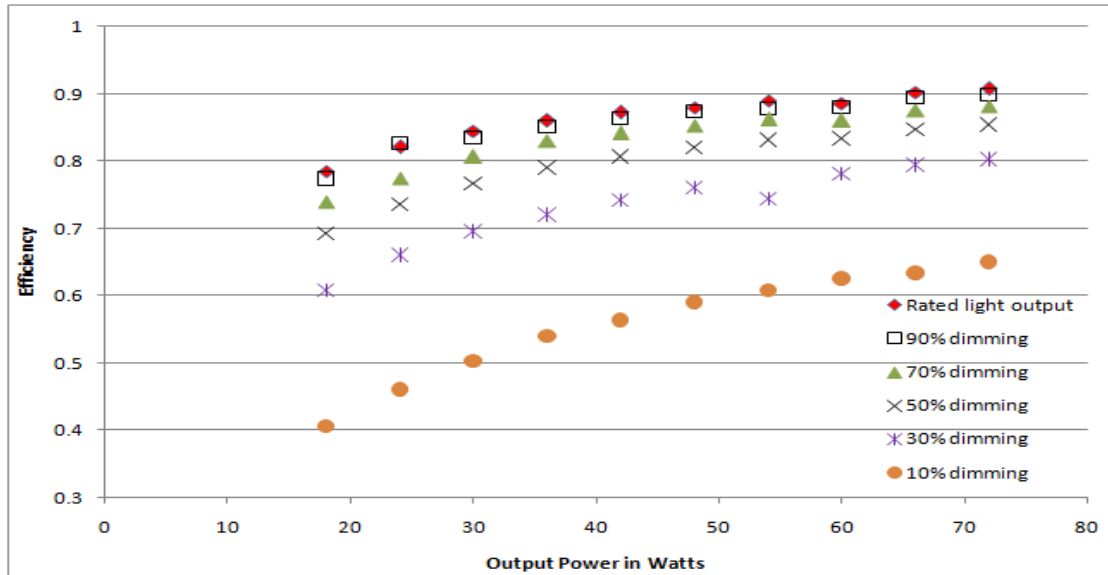
**Fig. 4.12:** Output current waveform under dimmed operation

The electrical performance of the modelled LED driver under different operating conditions is also obtained through simulation. A comparative study of the electrical performance of the simulated driver in

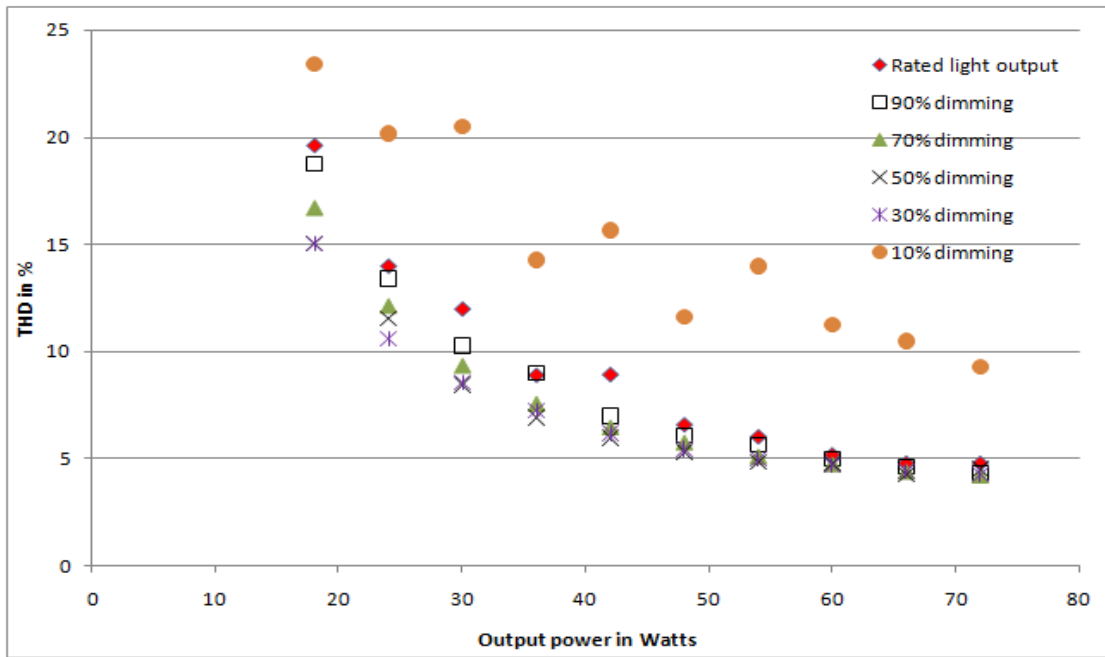
the entire output power range, for different dimming levels at  $230V_{rms}$ , is shown in **Fig. 4.13**.



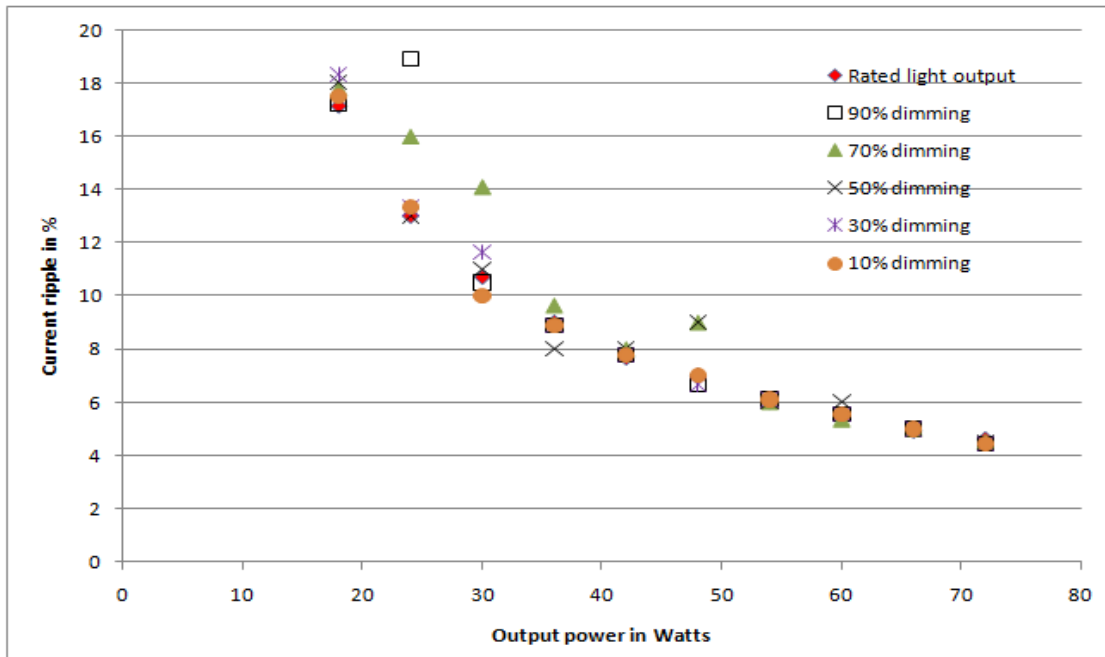
(a)



(b)



(c)



(d)

**Fig. 4.13:** Variation of electrical parameters with output power for different dimming levels at  $230V_{rms}$  (a) input power factor (b) efficiency (c) THD and (d) current ripple

From **Fig. 4.13** the following observations are made:

- 1) The input power factor varies from 0.93 to 0.99 for 100% and 70% light output and from 0.9 to 0.99 for 30% light output.
- 2) Efficiency varies from 0.79 to 0.91 for 100% light output, 0.74 to 0.88 for 70% light output and 0.61 to 0.8 for 30% light output
- 3) THD varies from 19.63% to 4.8% for 100% light output, 16.7% to 4.2% for 70% light output and 15% to 4.3% for 30% light output
- 4) Current ripple varies from 17.15% to 4.6% for 100% light output, 17.8% to 4.5% for 70% light output and 18.3% to 4.5% for 30% light output

The recommended minimum value of input power factor is 0.9 and the maximum allowable limits for %THD and %ripple are 30% and 20% respectively. So, it can be concluded that the electrical parameters are within their prescribed limits for 100% to 30% dimming levels. However, for a dimming level less than 30%, the electrical parameters are not within the prescribed limits. This deterioration of the electrical performance is due to high proportional conduction losses at currents lower than the rated current of the connected LED load. It is observed from **Fig. 4.13** that the input power factor and efficiency increase while %THD and the output current ripple decrease with the increase in rated output power. This happens because the LED driver supplies higher output power at comparatively higher voltages (current remaining constant), resulting in relatively low power loss. The same observations have been made for different dimming levels, at other supply voltages.

### **Scenario 3**

Under this scenario, during operation dimming is required as well as there is occurrence of fault. The values of output current and current in each parallel string after application of dimming and fault adaption

are shown in **Table 4.3**. From **Table 4.3**, it is seen that the current in each healthy parallel string after dimming and fault adaptation is always equal to or less than the rated current value.

**Table 4.3:** Output current and current in each parallel string at different dimming levels for single string fault

Light output (%)	Number of healthy parallel strings before fault	Output current corresponding to light output before fault (A)	Number of healthy parallel strings after fault	Output current after fault adaption (A)	Current in each parallel string after fault adaption (A)
100	4	4	3	3	1
	3	3	2	2	1
90	4	3.6	3	3	1
	3	2.7	2	2	1
70	4	2.8	3	2.8	0.93
	3	2.1	2	2	1
50	4	2	3	2	0.67
	3	1.5	2	1.5	0.75
30	4	1.2	3	1.2	0.4
	3	0.9	2	0.9	0.45
10	4	0.4	3	0.4	0.13
	3	0.3	2	0.3	0.15

**Figs. 4.14-4.16** show the output current waveforms of the simulated LED driver during the operation of 6\*4 72W LED lamp module at  $230V_{rms}$ . **Fig. 4.14** shows the output current waveform under normal operation, i.e. no parallel string is faulty and no dimming is required. The average output current is 4A, which is equal to the average value of rated current required when 4 healthy parallel strings are operating.



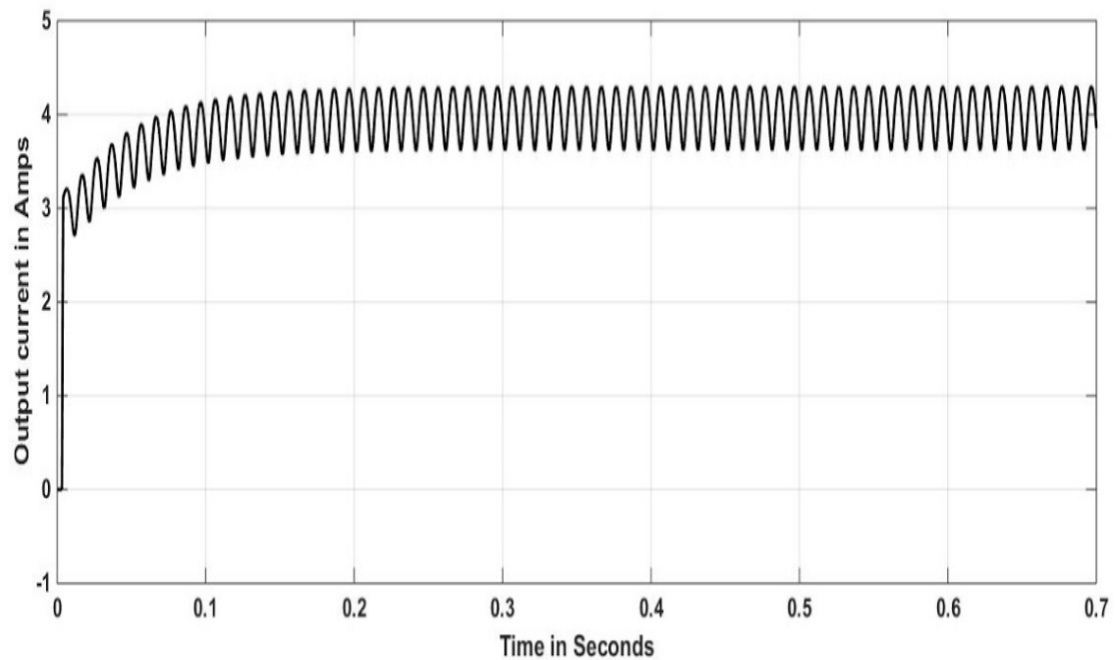


**Fig. 4.14:** Output current waveform under normal operation

**Fig. 4.15** shows the output current waveform of the LED driver when the 6 \* 4 72W LED lamp module is operated at rated conditions up to 0.25 seconds. After 0.25 seconds, 90% of rated light output is required so the output current should be 3.6A which is exactly what is obtained from simulation. Now, at 0.5 seconds, one of the parallel strings becomes faulty, so the output current should be 3A according to **Table 4.3**, which is the maximum rated current of the 6\*4 LED load with single string fault and 90% of rated light output.

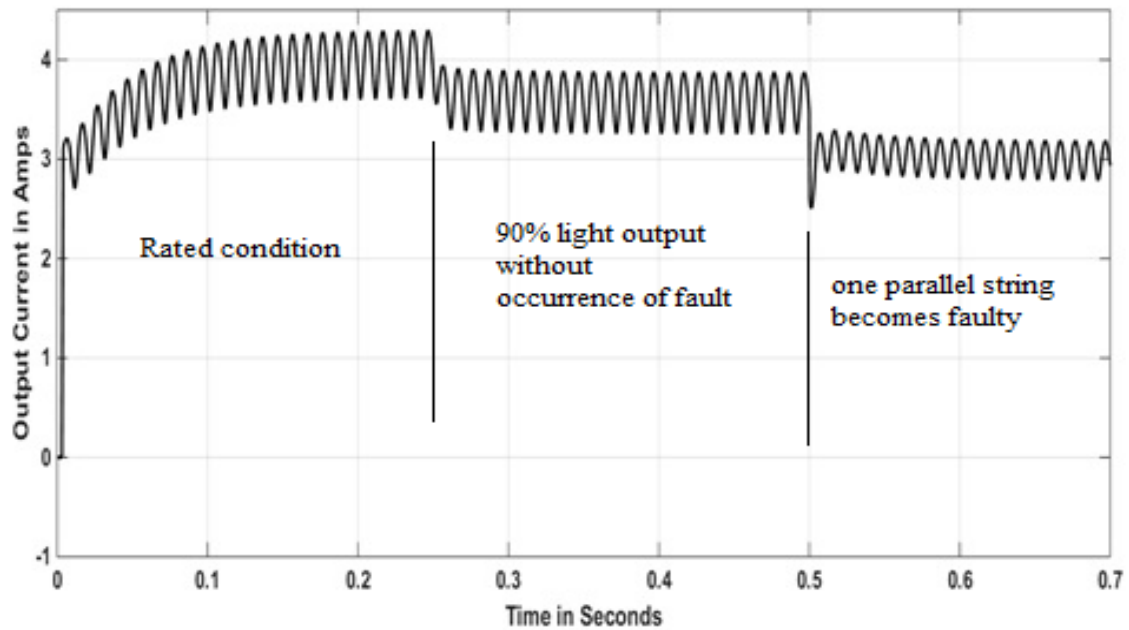


**Fig. 4.15:** Output current waveform when 90% dimming is required and one parallel string becomes faulty

**Fig. 4.16** shows the output current waveform of the LED driver when operating 6\*4 72W LED lamp module at rated condition up to 0.25 seconds. After 0.25 seconds, 50% of rated light output is required so the output current should be 2A which is exactly what is obtained from simulation. Now, at 0.5 seconds, two parallel strings becomes faulty, so the output current should remain unchanged at 2A because, it is the maximum rated current of the 6\*4 LED load with double string fault and 50% of rated light output.

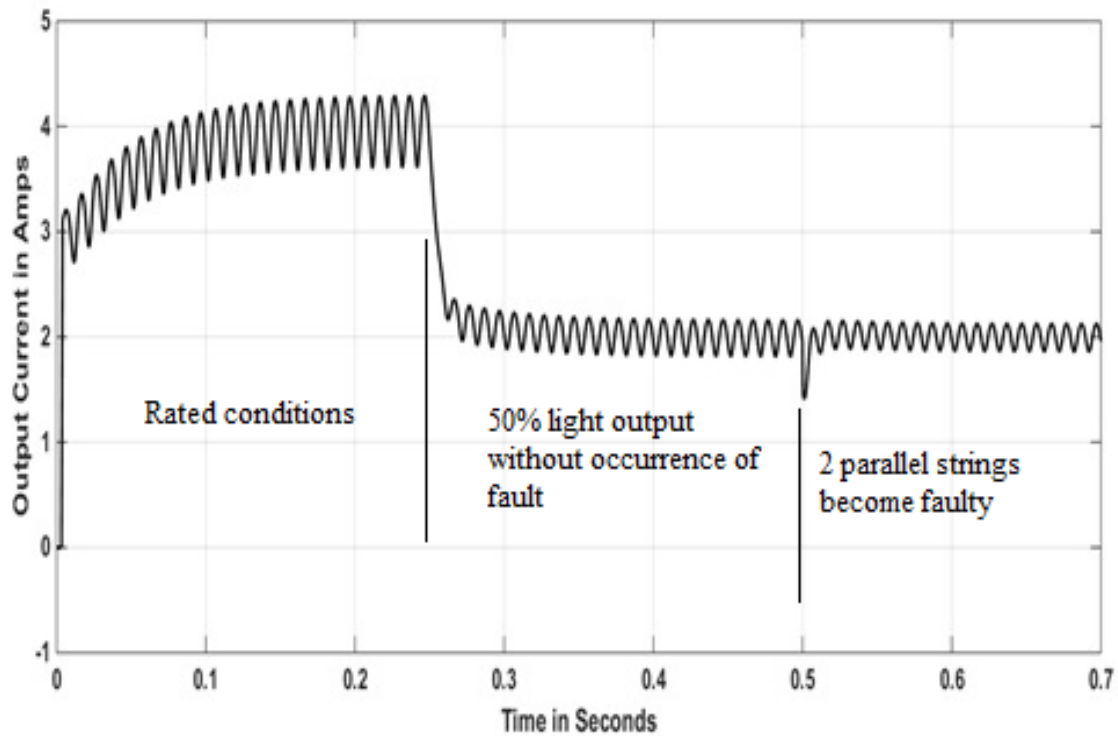


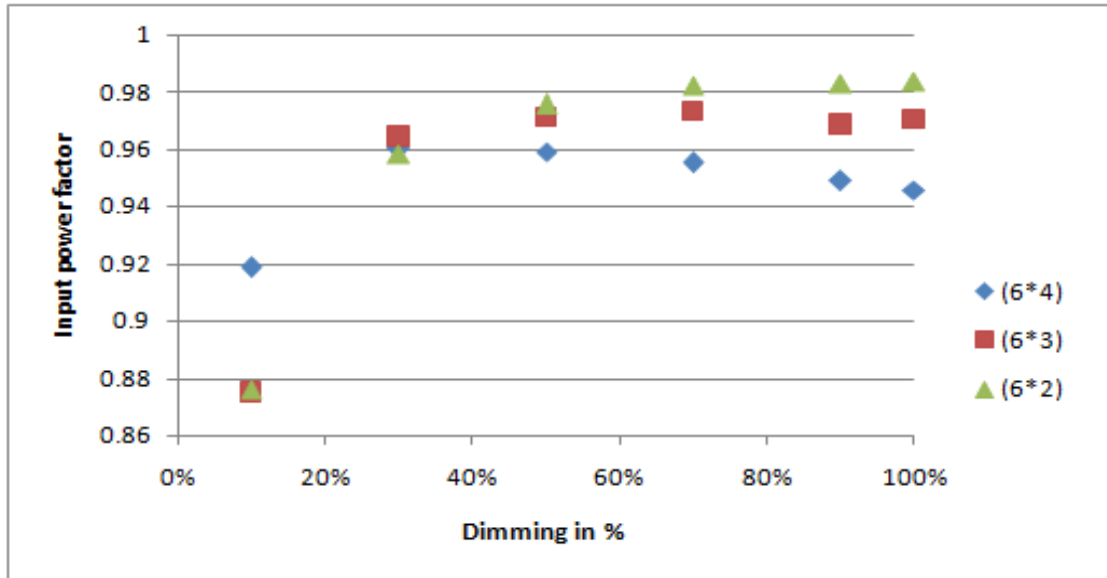
**Fig. 4.16:** Output current waveform when 50% dimming is required and two parallel strings becomes faulty

From **Figs. 4.14-4.16**, it can be concluded that the simulated LED luminaire works satisfactorily during the occurrence of a fault under dimmed operation.

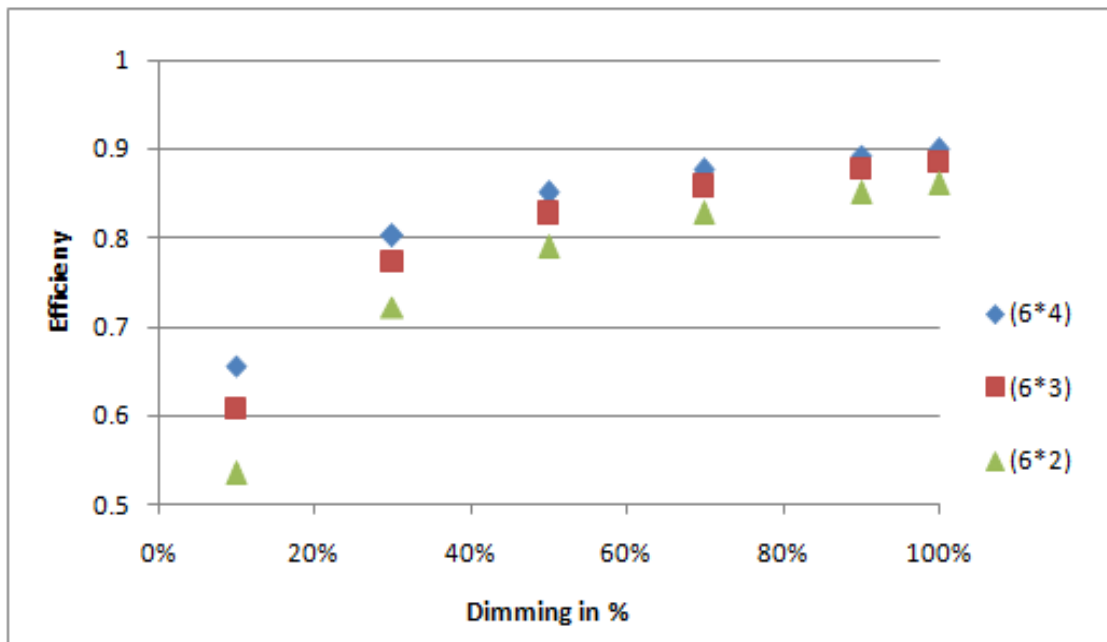
The variation of the driver's electrical performance parameters when fault occurs in the 72W LED lamp module ( $6 \times 4$ ), at  $230V_{rms}$  for the rated and dimmed conditions is shown in **Fig. 4.17**.

It is observed from **Fig. 4.17** that the efficiency remains almost constant; %THD and the %ripple decrease and the input power factor increases, if a fault occurs in  $6 \times 4$  LED module at any dimming level up to 30%. This happens because when a fault occurs in any connected LED lamp module, the slope of the V-I characteristics decreases and the LED driver has to supply the same output voltage but at a lower value of output current. As a result, conduction loss decreases. The same observations have been made for ( $5 \times 4$ ) 60W and

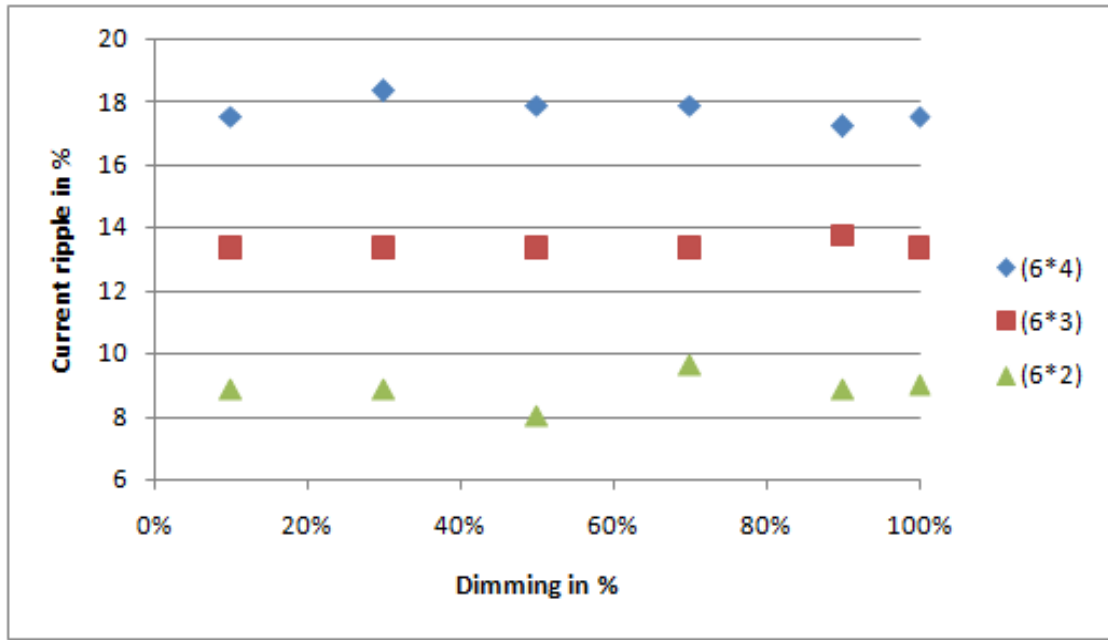
(4\*4) 48W LED module under fault occurrence at various dimming levels for other input voltages. This implies that the electrical performance of the simulated LED luminaire is satisfactory under fault conditions as well.



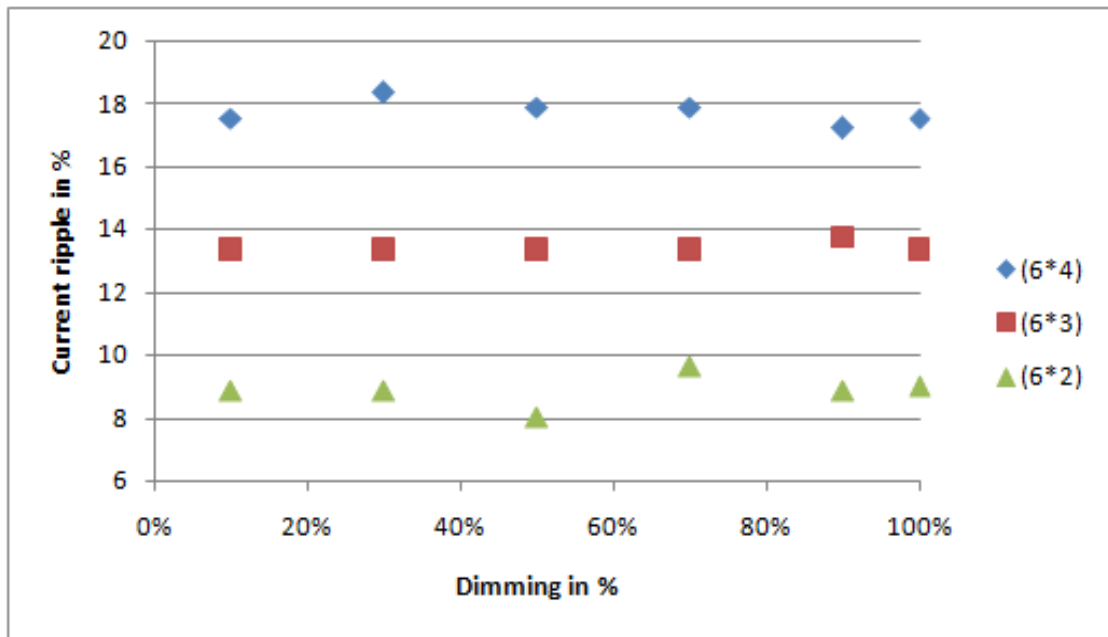
(a)



(b)



(c)



(d)

**Fig. 4.17:** Variation of electrical parameters for fault occurrence at different dimming levels at  $230V_{rms}$  (a) input power factor (b) efficiency (c) THD and (d) current ripple

## 4.5 Chapter summary

In this chapter, the design and performance analysis of a smart, fault-adaptive LED luminaire is performed using a simulation model on the Matlab-Simulink platform. The simulation results of the LED luminaire at different dimming levels and during fault occurrence show that the designed LED driver circuit provides the required voltage and current to connected LED lamp modules on  $90V_{rms}$ - $265V_{rms}$  AC supply for optimised unhindered operation. The electrical performance of the LED driver circuit in the output power range of 18-72W, input supply range of  $90V_{rms}$  to  $265V_{rms}$  and for dimming range of 100% to 30% and during the occurrence of a fault, is satisfactory and in compliance with the recommended standards. Input power factor as high as 0.999, %THD as low as 3.33%, efficiency as high as 0.94 and %ripple as low as 4.6% are obtained for the simulated LED driver.

## Publications

The publications related to this work are as follows:

### Journal Publications: 2

1. **Vishwanath Gupta**, Biswarup Basak, Kamalika Ghosh & Biswanath Roy. **2020**. Universal control algorithm for automatic current regulated LED driver. **International Journal of Power Electronics**. **12(2):169-180**, doi: 10.1504/IJPELEC.2020.10029994.

2. **Vishwanath Gupta**, Biswarup Basak, & Biswanath Roy. **2022**. Design and performance evaluation of an automatic dimmable fault-adaptive LED driver circuit. **Light and Engineering**. **31(4):40-49**, doi: <https://doi.org/10.33383/2022-062>.

## 5 Stability analysis of the designed smart LED luminaire

In this chapter, stability analysis of the LED luminaire, discussed in the previous chapter, in the output power range of 18W-72W on universal AC supply is carried out. Stability analysis is done by formulating the mathematical model of the LED luminaire, then obtaining the system characteristics from the loop gain bode plots and step response of the closed-loop system and finally performing the phase margin test. Stability is defined in terms of phase margin. The nature of step response of the modelled LED luminaire is found to be similar to the corresponding current waveforms obtained from Matlab-Simulink simulation. The fluctuation in phase margin and settling time with  $N_s/N_p$  ratio are studied to ascertain the  $N_s/N_p$  ratio of the LED lamp modules for the optimal performance of the LED luminaire in the given output power range.

## 5.1 Theoretical background

LED driver is a vital part of the LED luminaire when it is operated on AC supply. The operation of the LED drivers should be stable on AC supply; otherwise, the complete system will become inoperable. Therefore, stability analysis becomes an important part of any LED luminaire design. The stability analysis is done by formulating the mathematical model and obtaining the system characteristics by any one of the available methods such as the root locus method, nyquist diagrams or bode plots as reported in the following research works [73, 100–102]. However, the LED drivers mentioned above cannot operate the variable wattage n-string LED lamp modules. There are LED luminaires with multiple strings in parallel, but their steady-state stability analysis during operation is not reported [80–87].

### Phase margin test

According to phase margin test, 'a system is stable if phase margin of the loop gain (T) is positive and unstable if it is negative'. However, a small positive phase margin is not adequate, since a small positive phase margin gives rise to resonant poles with high closed-loop peaking factor (Q) near crossover frequency. This leads to the occurrence of overshoot and ringing phenomenon in the transient response [185]. The interrelation between the loop gain phase margin ( $\phi_m$ ) and Q is given by (5.1).

$$\phi_m = \tan^{-1} \sqrt{\frac{1 + \sqrt{(1 + 4Q^4)}}{2Q^4}} \quad (5.1)$$

Overshoot can be prevented by making the response critically damped or over damped. This requires Q to be equal to or less than 0.5. The



minimum value of phase margin for this value of Q is 76 degrees as obtained from (5.1). Therefore, the phase margin should be greater than 76 degrees for each case [185].

## 5.2 Mathematical model

Referring to the block diagram of the LED luminaire shown in **Fig. 4.1** in Chapter 4, its transfer function and the loop gain are obtained from the transfer function of each block.

The PI controller transfer function ( $G_{PI}$ ) is given by (5.2). The proportional constant ( $K_p$ ) value is considered equal to 1 and the integral constant ( $K_i$ ) value equal to 25 for the considered LED luminaires.

$$G_{PI} = \frac{sK_p + K_i}{s} \quad (5.2)$$

A gate signal of the required duty cycle is produced by the PWM generator by comparing the PI controller output signal with the high-frequency sawtooth carrier signal. The PWM generator transfer function ( $G_{PWM}$ ) is given by (5.3). The carrier signal has a maximum value ( $V_M$ ) of 2 Volts for the simulated LED luminaire.

$$G_{PWM} = \frac{1}{V_M} \quad (5.3)$$

The flyback converter in the present work operates in DCM and its average value is given by (5.4) [63].

$$I_o = \frac{V_g^2 D^2}{2L_m f_s V_o} \quad (5.4)$$

The flyback converter transfer function ( $G$ ) (output current versus duty cycle) is obtained with the help of averaging technique as given by (5.5) which is similar to the transfer function obtained in [63].

$$G = \frac{i_o(s)}{d(s)} = \frac{2 \frac{I_o}{DR_D C_o}}{S + \frac{V_o + I_o R_D}{V_o R_D C_o}} \quad (5.5)$$

The feedback gain block in the feedback loop converts the output current to the corresponding voltage feedback signal. The feedback gain has a constant value of 0.1. Therefore, the loop gain of the simulated LED luminaire is given by (5.6).

$$T = 0.1 G_{PI} G_{PWM} G \quad (5.6)$$

Putting (5.3), (5.4) and (5.5) in (5.6) and rearranging, the loop gain is obtained as given by (5.7).

$$T = \frac{\frac{0.2 K_p I_o}{DV_M R_D C_o} \cdot \left( s + \frac{K_i}{K_p} \right)}{s \cdot \left( s + \frac{V_o + I_o R_D}{V_o R_D C_o} \right)} \quad (5.7)$$

The transfer function of the simulated LED luminaire is given by (5.8).

$$G_{CL} = \frac{G_{PI} G_{PWM} G}{1 + T} \quad (5.8)$$

In terms of the model parameters, the transfer function is expressed by (5.9).

$$G_{CL} = \frac{\frac{2K_p I_o}{DV_M R_D C_o} \cdot (s + \frac{K_i}{K_p})}{s^2 + \frac{DV_o V_M + DI_o R_D V_M + 0.2K_p I_o V_o}{V_o V_M R_D C_o D} s + \frac{0.2I_o K_i}{DV_M R_D C_o}} \quad (5.9)$$

### 5.3 Results and analysis

The mathematical model of the LED luminaire is simulated in Matlab-Simulink. The stability is tested at 5 input voltages: the maximum ( $265V_{rms}$ ), the minimum ( $90V_{rms}$ ), intermediate input voltages ( $180V_{rms}$  and  $130V_{rms}$ ) and the European and Indian nominal input voltage ( $230V_{rms}$ ). The gain margin is infinite for the LED luminaire operating on universal AC supply. The phase margins of the simulated LED driver obtained for all the considered  $N_s/N_p$  ratios are given in **Table 5.1**. It is observed from **Table 5.1**, that the phase margins of the LED luminaire operating on universal AC supply are greater than 76 degrees, which is required for satisfactory stable operation. The phase margin is directly proportional to the  $N_s/N_p$  ratio until the value of  $N_s/N_p$  ratio is 1 at any particular input voltage, and then the phase margin becomes inversely proportional to the  $N_s/N_p$  ratio as shown in **Fig. 5.1**.

**Table 5.1:** Phase margin of the LED driver for different  $N_s/N_p$  ratio

$N_s/N_p$ ratio	Output Power (W)	Margin (degrees)				
		$265V_{rms}$	$230V_{rms}$	$180V_{rms}$	$130V_{rms}$	$90V_{rms}$
6	72	81.6	81	80	79	78.7
5.5	66	83.8	83.2	82.3	81.5	81.2
5	60	85.9	85.5	84.9	84.2	83.9
4.5	54	88.1	87.9	87.5	87.1	86.9
4	48	90.2	90.2	90.2	90.3	90.3
3.5	42	92	92.4	92.9	93.5	94
3	36	93.9	94.5	95.5	96.9	98.1
2.67	72	94.9	95.6	96.9	98.8	101
2.5	30	95.5	96.2	97.7	100	103
2.33	42	95.8	96.6	98.2	101	104
2	54	96.6	97.5	99.4	102	106
2	24	96.7	97.6	99.6	103	107
1.67	45	97.2	98.2	100	104	108
1.5	72	97.3	98.3	100	104	108
1.5	18	97.5	98.6	101	104	110
1.33	36	97.6	98.6	101	104	110
1.25	60	97.6	98.6	101	104	109
1	48	97.5	98.7	101	105	112
1	27	97.5	98.7	101	105	112
0.8	60	97.2	98.3	101	105	111
0.75	36	97	98.1	100	104	111
0.67	18	96.8	97.9	100	104	110
0.67	72	96.8	97.9	100	104	110
0.6	45	96.6	97.6	99.7	104	110
0.5	24	96.2	97.1	99.1	103	108
0.5	54	96.2	97.1	99.1	103	108
0.43	63	95.9	96.7	98.6	102	107
0.4	30	95.7	96.6	98.4	102	107
0.38	72	95.6	96.4	98.2	101	107
0.33	36	95.3	96.1	97.8	101	106
0.29	42	95	95.7	97.3	100	105
0.25	48	94.7	95.4	96.9	99.6	104
0.22	54	94.4	95.1	96.5	99.1	103
0.2	60	94.2	94.9	96.3	98.7	103
0.18	66	94.1	94.7	96	98.3	102
0.17	72	93.9	94.5	95.8	98	102

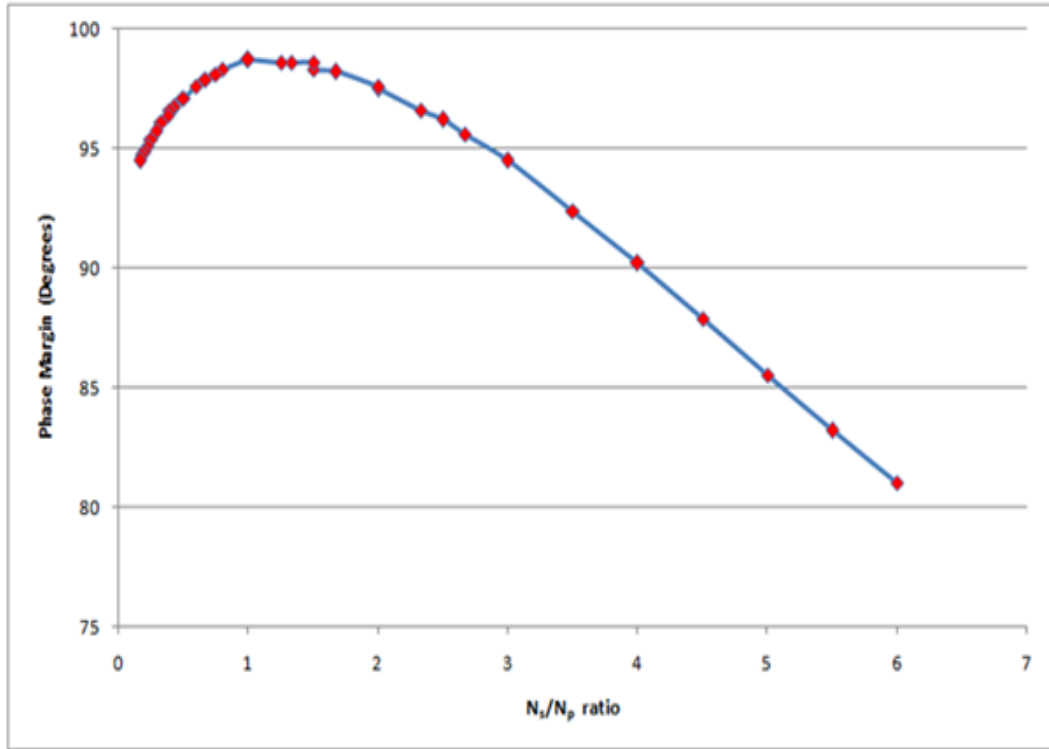


**Fig. 5.1:** Variation of Phase Margin with  $N_s/N_p$  ratio at  $230V_{rms}$

The phase margin increases with a decrease in the input voltage for LED luminaires having a  $N_s/N_p$  ratio less than 4. If  $N_s/N_p$  ratio is equal to 4, then the phase margin does not vary with the input voltage and if  $N_s/N_p$  ratio is greater than 4, then the phase margin decreases with decrease in input voltage. This variation of phase margin with the input AC voltage at different  $N_s/N_p$  ratio is shown in **Fig. 5.2**. The settling time of the LED luminaire is also obtained on Universal AC supply. The settling time is minimum around  $N_s/N_p$  ratio of 0.2 and 4.5 and maximum around  $N_s/N_p$  ratio of 6. The variation in the settling time with  $N_s/N_p$  ratio at  $230V_{rms}$  is shown in **Fig. 5.3**.

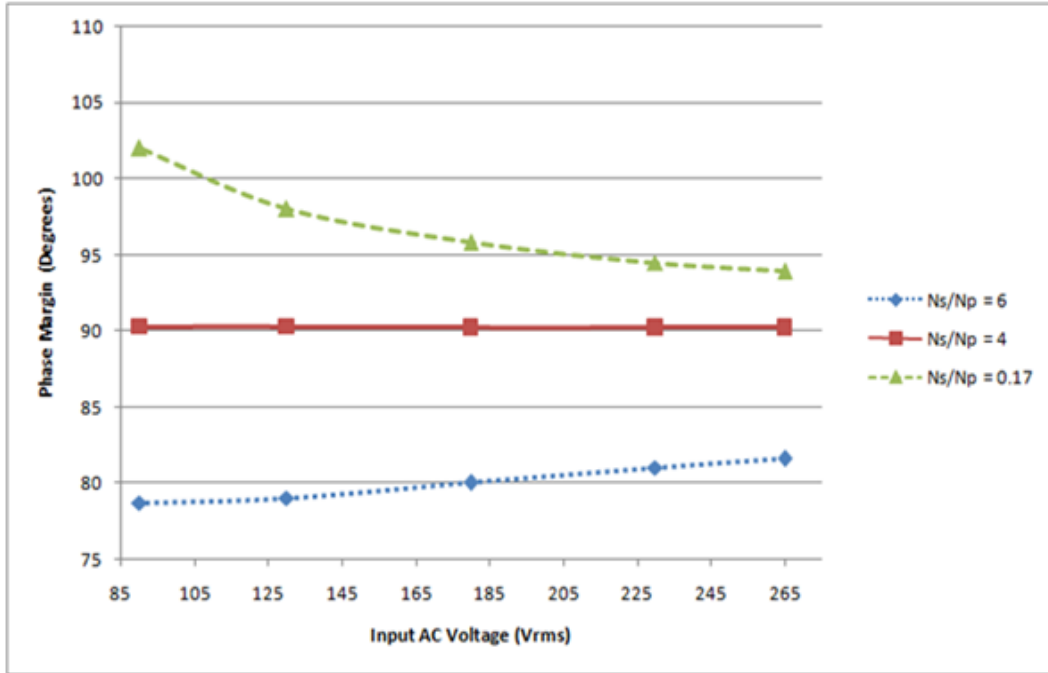


**Fig. 5.2:** Variation of Phase Margin with input AC voltage for different  $N_s/N_p$  ratio

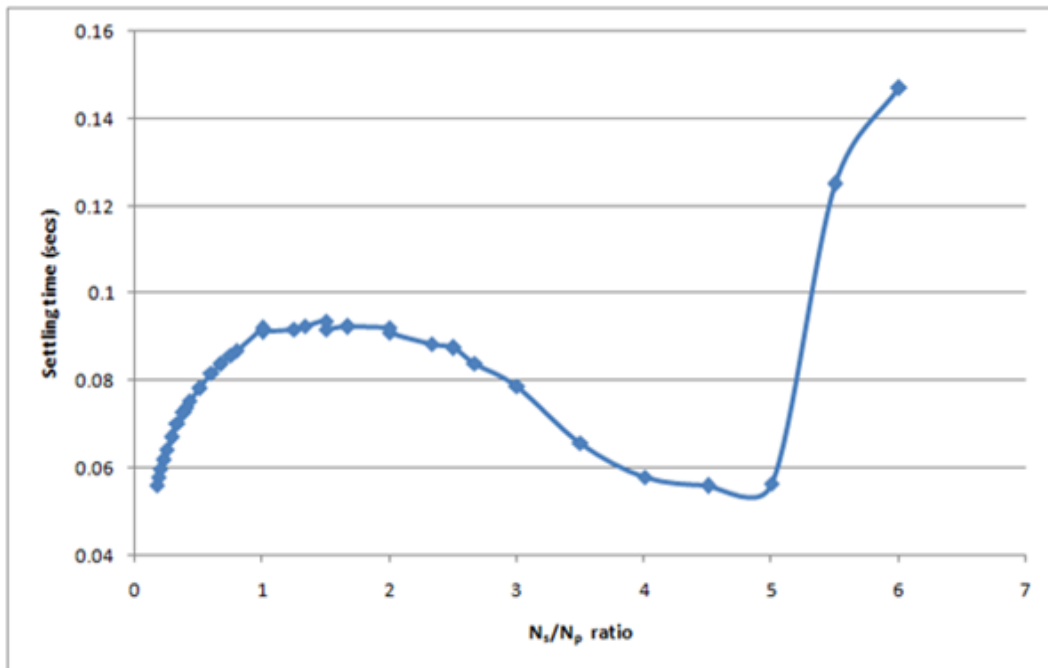


**Fig. 5.3:** Variation of settling time with  $N_s/N_p$  ratio at  $230V_{rms}$

For 72W LED luminaire with  $N_s/N_p$  ratio of 1.5 at 230V, the loop

gain bode plot is shown in **Fig. 5.4** and closed loop system's bode plot and step response are shown in **Figs. 5.5-5.6** respectively.

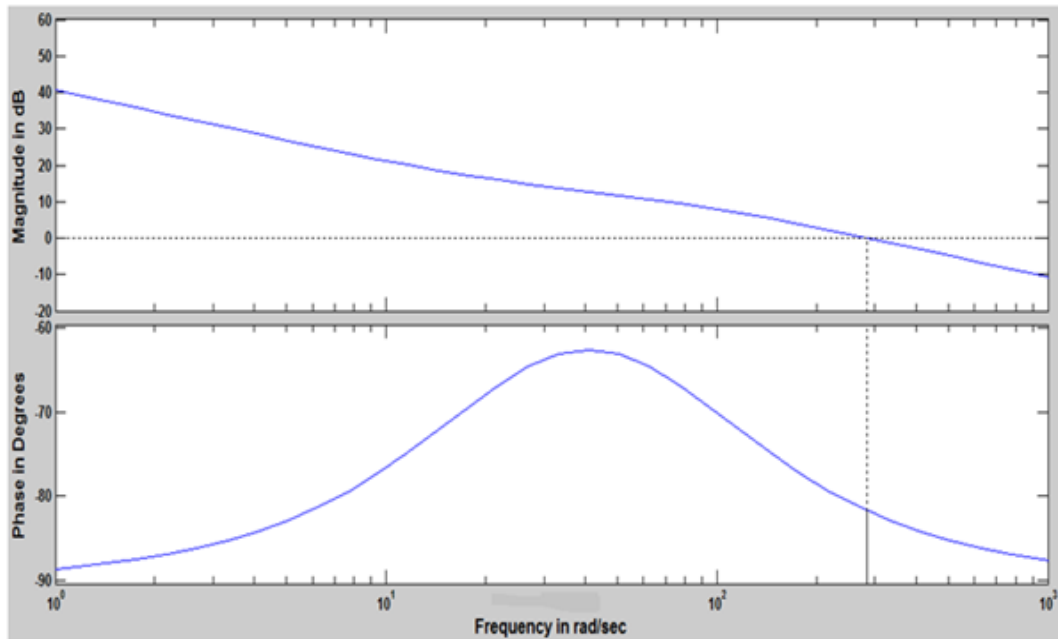


**Fig. 5.4:** Bode plot of loop gain for 72W LED luminaire with  $N_s/N_p$  ratio of 1.5 at  $230V_{rms}$

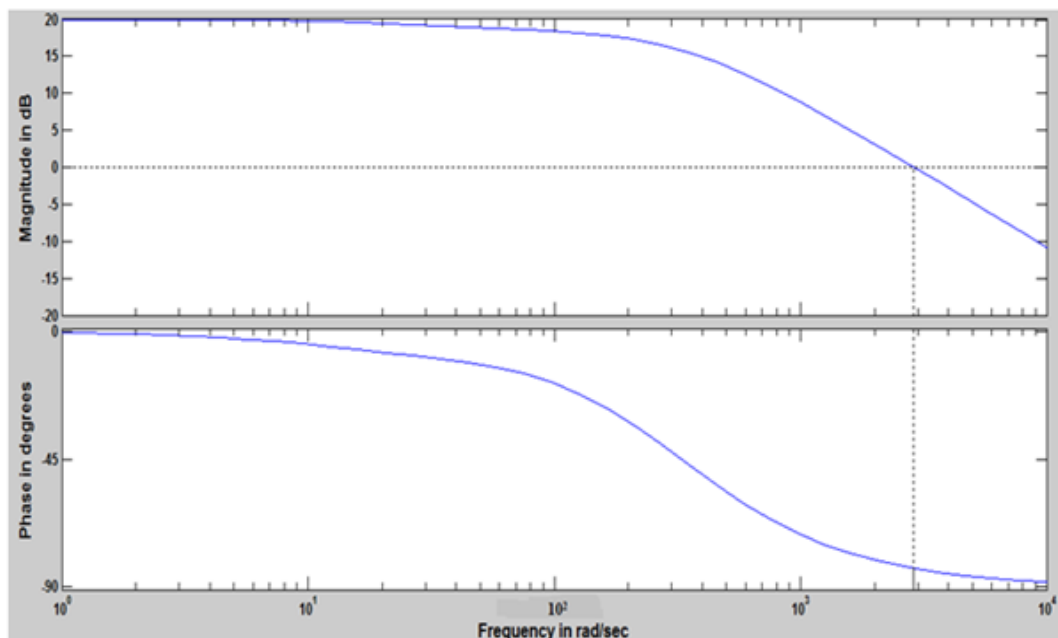


**Fig. 5.5:** Bode plot of closed loop system for 72W LED luminaire with  $N_s/N_p$  ratio of 1.5 at  $230V_{rms}$

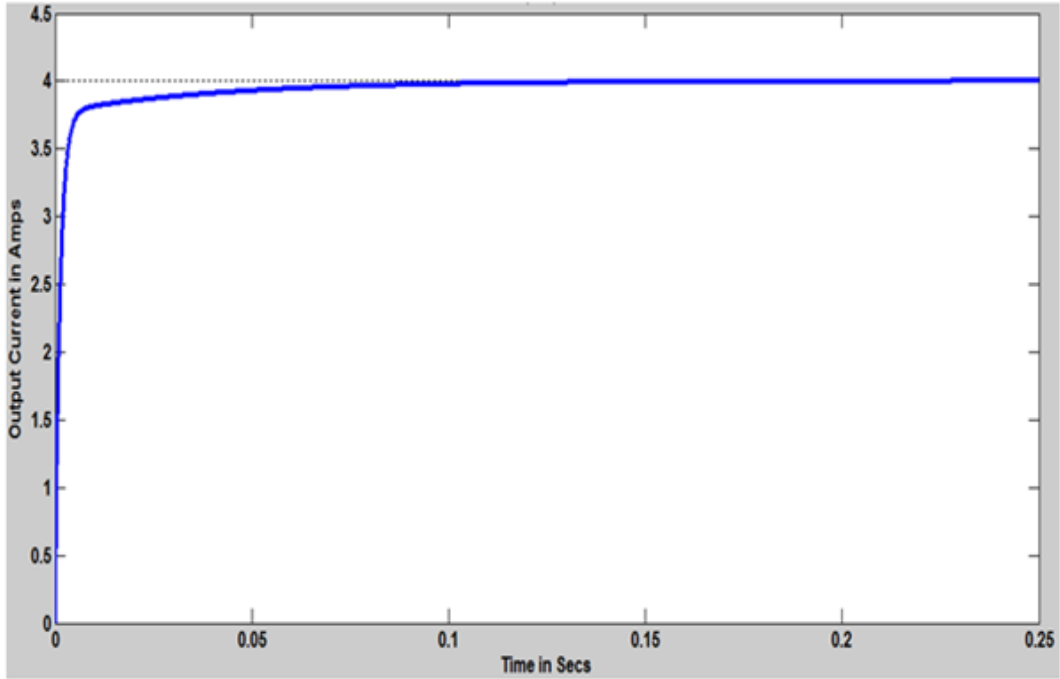


**Fig. 5.6:** Step response of 72W LED luminaire with  $N_s/N_p$  ratio of 1.5 at  $230V_{rms}$

It is observed from bode plots of loop gain shown in **Fig. 5.4** and the closed-loop system shown in **Fig. 5.5**, that there is no peak in bode plot of the closed-loop system near the cut-off frequency as the phase margin is more than 76. The current waveform of the 72W LED luminaire with  $N_s/N_p$  ratio of 1.5 obtained through simulation at  $230V_{rms}$  is shown in **Fig. 5.7** which is similar to the step response obtained in **Fig. 5.6**.



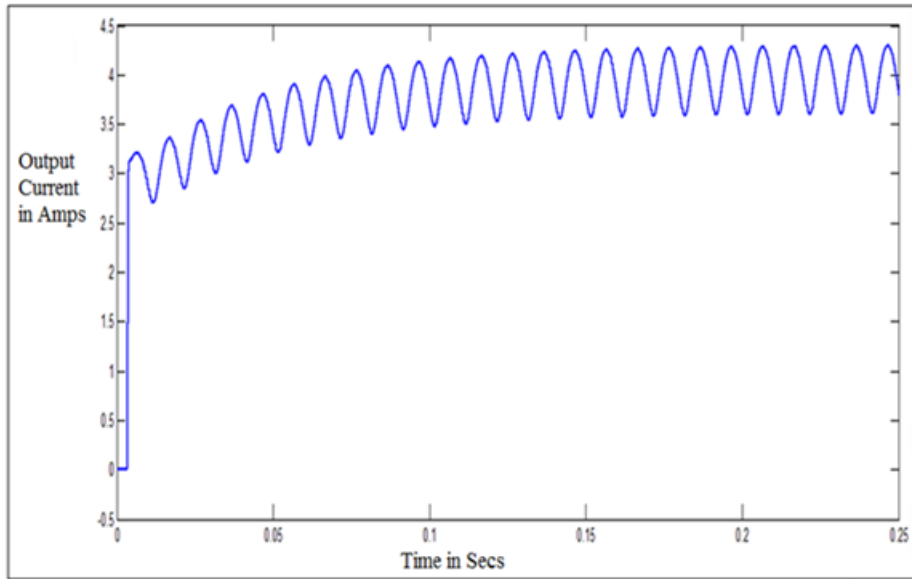


**Fig. 5.7:** Simulated output current waveform for 72W LED luminaire with  $N_s/N_p$  ratio of 1.5 at  $230V_{rms}$

The above results confirm that the operation of the modelled LED luminaire is stable in the output power range of 18W-72W. It is clear that to obtain maximum stability;  $N_s/N_p$  should be kept close to 1. But from the settling time point of view,  $N_s/N_p$  ratio is to be kept around 4.5 or 0.17. However, the electrical performance of the LED luminaire for different  $N_s/N_p$  ratio is also to be considered. The designed LED luminaire delivered best electrical performance for  $N_s/N_p$  ratio of 6, but for  $N_s/N_p$  ratio  $\leq 1$ , the electrical performance of the luminaire do not comply with the recommended standards as mentioned in **Chapter 4** of this work. Therefore, a trade-off between stability, settling time and electrical performance is needed to ascertain the  $N_s/N_p$  ratio of LED luminaires for optimised performance.

## 5.4 Chapter summary

The mathematical model of the designed LED luminaire is formulated to perform stability analysis using the phase margin test. The LED luminaire phase margin is greater than the required phase margin of 76 degrees in the entire output power range of 18W-72W on universal AC supply. Hence, the operation of the modelled LED luminaire is stable and the closed-loop system does not have a peak in the vicinity of the cut-off frequency. The LED luminaire is most stable for  $N_s/N_p$  ratio  $\geq 1$ . The settling time is minimum for  $N_s/N_p$  ratio of 0.2 and 4.5. However, the LED luminaire electrical performance for  $N_s/N_p$  ratio  $\leq 1$  is not satisfactory. So in order to obtain optimised performance from the modelled LED luminaire on universal AC supply in the output power range of 18W-72W, the  $N_s/N_p$  ratio has to be greater than 1 and around 3-4.

## Publications

The publications related to this work are as follows:

### Conference Publications: 1

1. **Vishwanath Gupta**, Biswarup Basak, Kamalika Ghosh & Biswanath Roy. **2017**. Stability analysis of a universal LED driver. **IEEE Calcutta Conference (CALCON), Kolkata, India, 2017, pp. 279-283**, doi: 10.1109/CALCON.2017.8280739.

## **6 Daylight-responsive closed-loop light controllers: Design and Evaluation**

In this chapter, design and performance evaluation of two numbers of daylight-responsive closed-loop light controllers are presented.

The first section deals with a Fuzzy Logic Inference System (FIS) based light controller which is designed and implemented on Arduino Mega micro-controller using C++ programming language instead of simulation in Matlab environment. This is done to eliminate the need for a dedicated computer and additional interfacing accessories for future hardware prototype development. The designed FIS predicts the amount of light output required from artificial lamps and the position of window roller blinds to maintain required illuminance and overall uniformity on the working plane of a model test office room in presence of daylight for all times of the day through out the year. The simulated light controller is tested offline by modelling a test office room using DIALux 4.13 lighting design software. The obtained results from offline testing show that the performance parameters improve after the application of designed FIS based control strategy.

The second section discusses the design and development of a fault-monitoring and motion-sensing light controller for an indoor LED luminaire. The light controller provides wireless control of the light output based on ambient light level and motion sensing and monitors the occurrence of faults in the driver unit and the LED module separately. A hardware prototype of the designed controller is developed and tested in the laboratory. From the obtained results, it is observed that the developed controller successfully detected the fault and satisfactorily controlled the light output from the LED luminaire.

## 6.1 Fuzzy logic based closed-loop light controller

### 6.1.1 Introduction

According to the Energy Statistics report of 2013 by National Statistical Organization (NSO) of India, electrical energy comprised almost 57% of India's overall energy consumption in 2011-2012 and building sector consumes close to 40 percent of that electricity. Lighting accounts for 59% and 28% of total electrical energy consumed by commercial and residential sectors respectively [186]. Electrical energy used for lighting can be decreased with the use of existing technology and the appropriate harvesting of daylight [107–113]. As daylight is dynamic in nature, Fuzzy Logic Inference System (FIS) is advantageous for daylight integrated artificial lighting system to improve quality and quantity of light [114–120, 138]. However, in all the above mentioned works, the FIS is designed in Matlab environment in a computer and the computer must be interfaced with controllers using proper interfacing accessories. In this present work, a closed-loop light controller based on FIS is designed and implemented inside an Arduino-Mega [187] micro-controller instead in the Matlab environment to eliminate the requirement of a computer and interfacing logistics. The proposed light controller can control the artificial lighting and the window roller blinds throughout the day to maintain the required illuminance and overall uniformity.

### 6.1.2 Features and design

The designed light controller is designed for an indoor environment. A model test room having dimensions 5mx4mx3m is simulated in DIALux 4.13 software as shown in **Fig. 6.1**. The room is located in New Delhi having a longitude – 77.2 degrees and latitude – 28.6 degrees. The light loss factor of the room is assumed to be 0.8. The model

room has one south facing window of height 1.2m and width 1m. The window is 1m above the floor and in the centre of the wall. For the calculation of average illuminance and overall uniformity, a calculation surface of length 4m and breadth 3m at a height of 0.76m from the floor with origin at the centre of the room is considered. Two calculation points on the calculation surface one at (2.5m, 1.2m, 0.76m) and the other at (2.5m, 2.8m, 0.76m) are considered for point specific illuminance measurement.

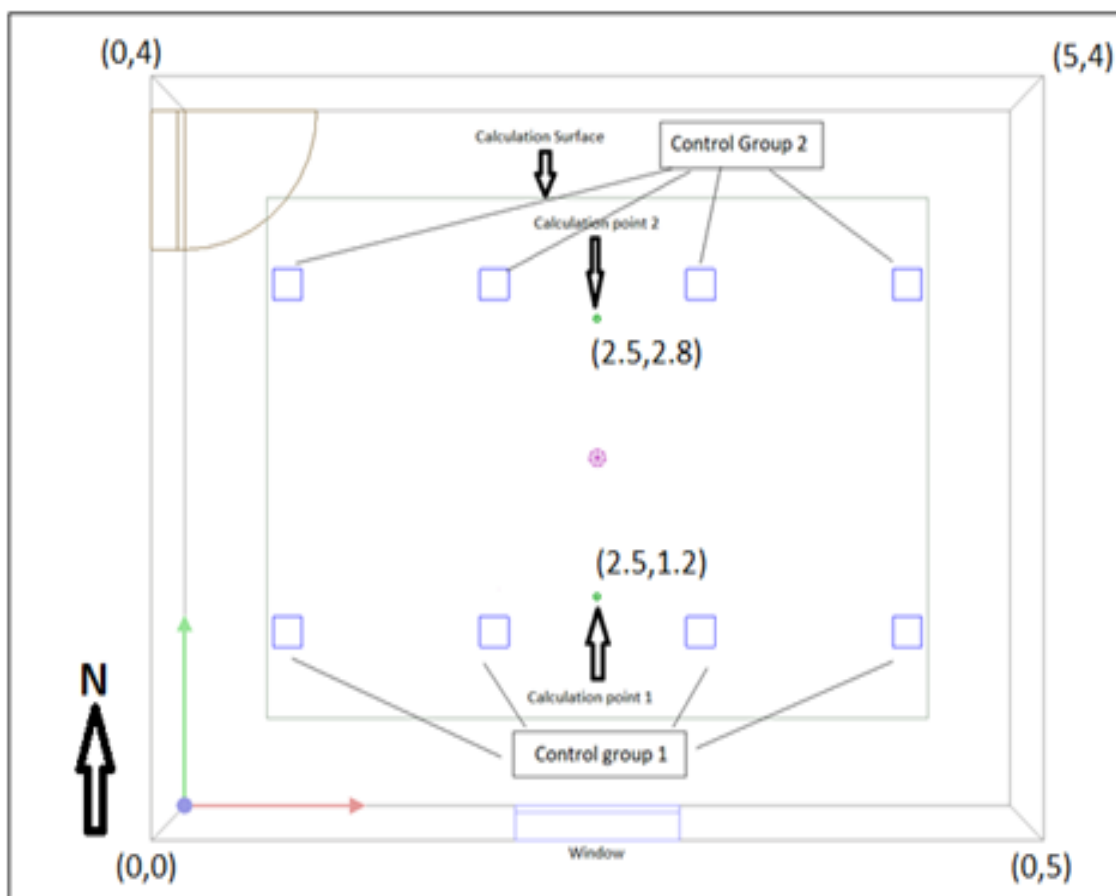


**Fig. 6.1:** Simulated model test room

The light controller is implemented on an Arduino Mega micro-controller. It controls the artificial lighting and the amount of daylight entering the indoor environment to obtain the required amount of illuminance and improve the overall uniformity on the working plane.

The block diagram representation of the light control system is shown in **Fig. 6.2**.

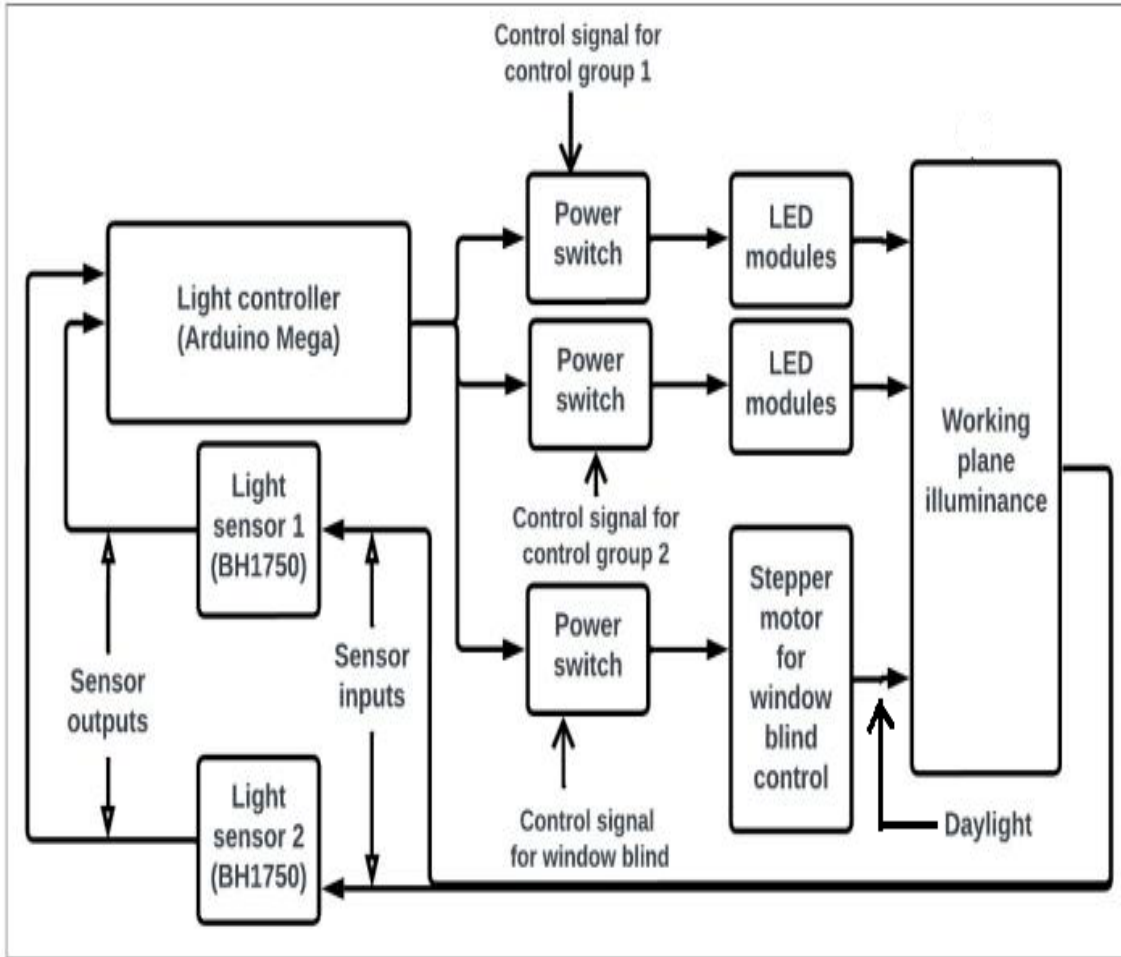


**Fig. 6.2:** Block diagram of the complete light control system

## Features

The closed-loop light controller, with the help of designed FIS, determines the position of the window roller blind and the light output from luminaires (belonging to two control groups) to obtain the required amount of illuminance and improve the overall uniformity on the working plane at all times of the day throughout the year. The designed FIS is not only designed in Matlab-Simulink platform but implemented inside an Arduino Mega micro-controller. This uniqueness

of the light controller obliterates the requirement of a computer and interfacing logistics. Another essential feature of the designed light controller is that it prevents the generated control signal to switch between two values if the amount of ambient light remains constant.

## Design

The heart of the light controller is the designed FIS. The designed FIS predicts the amount of light output required from the luminaires belonging to two control groups and the position of the window roller blind. The FIS consists of 2 inputs (named light1 and light2). These inputs will be the outputs of two BH1750 light sensors [188] placed at any two considered calculation points and 3 outputs (named dimming1, dimming2 and blindPosition) which control the light output from the luminaires of first control group, second control group and the position of roller blind respectively. The fuzzy sets, range of each fuzzy set, membership functions and fuzzy rule base are designed from heuristic knowledge through trial and error process. The fuzzy sets of the inputs and outputs are shown in **Table 6.1**. Fuzzy rule base designed for each of the three outputs are shown in **Tables 6.2-6.4**.

**Table 6.1:** Designed fuzzy sets of the inputs and outputs

Fuzzy signals	Fuzzy set	Shape	Range
light1	verylow1	triangle	0-150-300
	low1	triangle	400-600-800
	medium1	trapezoid	800-1000-1200-1400
	high1	trapezoid	1400-2000-5000-10000
	veryHigh1	trapezoid	8000-10000-12000-12000
light2	verylow2	triangle	0-150-300
	low2	triangle	400-450-500
	medium2	triangle	500-550-600
	high2	triangle	600-700-800
	veryHigh2	trapezoid	800-900-1000-1000
dimming1	optimum1	triangle	20-40-60
	average1	triangle	50-70-90
	full1	triangle	90-100-120
dimming2	lessoptimum2	triangle	40-50-60
	optimum2	triangle	60-70-80
	average2	triangle	80-90-100
	full2	triangle	90-100-110
blindPosition	optimum3	triangle	20-30-40
	belowaverage3	triangle	30-40-50
	average3	triangle	40-50-60

**Table 6.2:** Rule base for control group 1

light1	verylow1 (0-300)	low1 (400-800)	medium1 (800-1400)	high1 (1400-10000)	veryHigh1 (10000 and above)
light2					
verylow2 (0-300)	full1	average1	optimum1	optimum1	optimum1
low2 (400-500)	full1	average1	optimum1	optimum1	optimum1
medium2 (500-600)	full1	average1	optimum1	optimum1	optimum1
high2 (600-800)	full1	average1	optimum1	optimum1	optimum1
veryHigh2 (800 and above)	full1	average1	optimum1	optimum1	optimum1



**Table 6.3:** Rule base for control group 2

	light1	verylow1	low1	medium1	high1	veryHigh1
light2		0-300	400-800	800-1400	1400-10000	10000 and above
verylow2	(0-300)	full2	full2	full2	full2	full2
low2	(400-500)	average2	average2	average2	average2	average2
medium2	(500-600)	optimum2	optimum2	optimum2	optimum2	optimum2
high2	(600-800)	optimum2	optimum2	optimum2	optimum2	optimum2
veryHigh2	(800 and above)	lessoptimum2	lessoptimum2	lessoptimum2	lessoptimum2	lessoptimum2

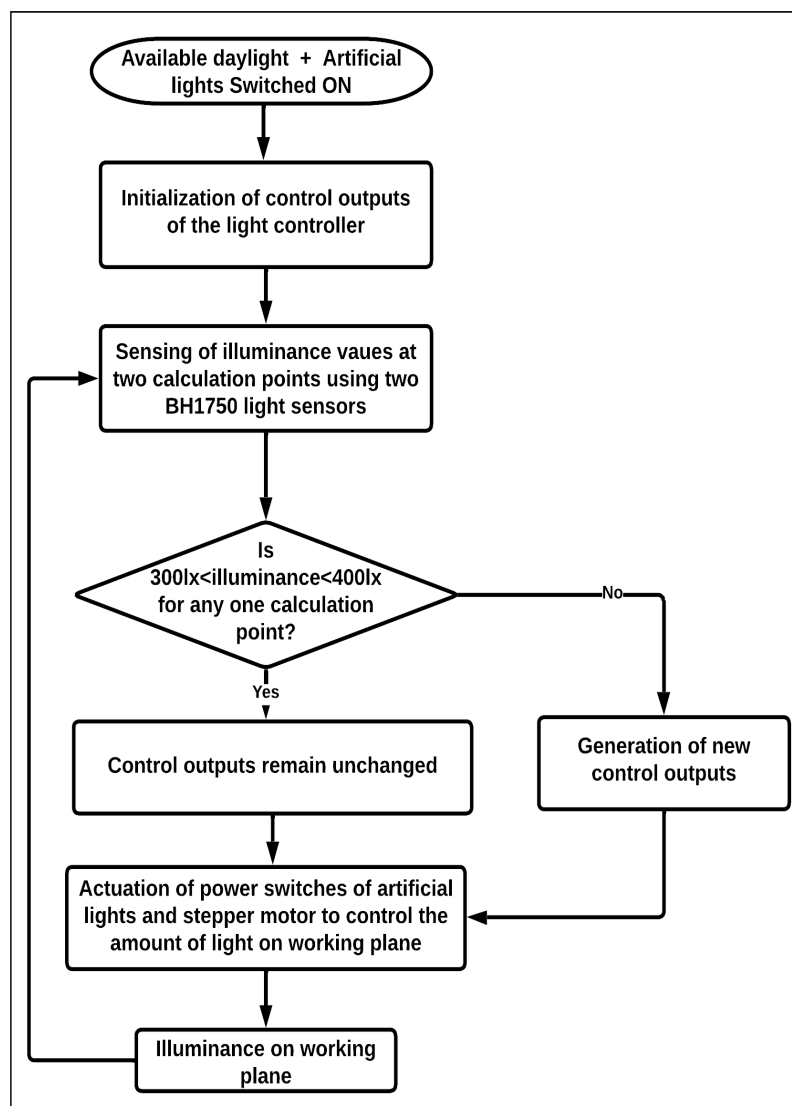
**Table 6.4:** Rule base for control group 3

	light1	verylow1	low1	medium1	high1	veryHigh1
light2		(0-300)	(400-800)	(800-1400)	(1400-10000)	(10000 and above)
verylow2	(0-300)	full3	aboveaverage	aboveaverage	aboveaverage	aboveaverage
low2	(400-500)	full3	aboveaverage3	average3	average3	average3
medium2	(500-600)	full3	average3	average3	average3	optimum3
high2	(600-800)	full3	average3	belowaverage3	belowaverage3	optimum3
veryHigh2	(800 and above)	average3	average3	belowaverage3	belowaverage3	optimum3

### 6.1.3 Principle of operation

The output of the two BH1750 light sensors placed at any two calculation points are given as inputs to the designed closed-loop light controller at regular intervals. The implemented FIS generates three outputs to control the light output of luminaires in the two control group and the position of window roller blind. The operation of the light controller is described in **Fig. 6.3**. Since the controller repeats its action after a regular interval, the illuminance values at the calculation points after the first control iteration, although reduced, are such that for the second iteration, if those values become the input to the designed FIS, the outputs of the light controller will increase the working plane's average illuminance value. Hence, the output of the controller will flip-flop between two values even if the amount of day-

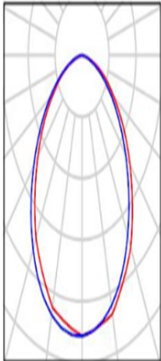
light is unchanged. The speciality of this designed FIS is that it holds the outputs of the previous iteration, if any one of the inputs is in between a particular value (300lx-400lx). This ensures that for second iteration if those values become the input to the designed FIS then the predicted dimming values do not change or flip-flop and therefore, do not increase or decrease the average illuminance even if the amount of daylight is constant.



**Fig. 6.3:** Operational flow diagram of the FIS based light-controller

### 6.1.4 Results and analysis

The proposed closed-loop light controller is tested offline on the model test room using DIALux 4.13 software. The test room is equipped with eight number of dimmable Panasonic PDLM03147 luminaires [189] to obtain the reference level of illuminance of 300lx on the calculation surface without incorporation of daylight and application of dimming. The eight luminaires are divided into two control groups with 4 luminaires each. Each luminaire has a power rating of 14W and luminous flux of 1370 lumens. The luminaire part list is shown in **Fig. 6.4**.

Room 1 / Luminaire parts list			
8 Pieces	Panasonic PDLM03147 Article No.: Luminous flux (Luminaire): 1371 lm Luminous flux (Lamps): 1370 lm Luminaire Wattage: 14.0 W Luminaire classification according to CIE: 100 CIE flux code: 56 86 98 100 100 Fitting: 1 x User defined (Correction Factor 1.000).	See our luminaire catalog for an image of the luminaire.	

**Fig. 6.4:** Luminaire parts list

The result obtained for the test room with only artificial lighting is given in **Table 6.5**.

**Table 6.5:** Obtained results with only artificial lighting

Average illuminance (lx)	Overall uniformity	Illuminance at calculation point 1 (lx)	Illuminance at calculation point 2 (lx)
340	0.85	369	371

If daylight is available, the quality and quantity of light inside the test room will change. To test the proposed light controller, daylight is first incorporated with artificial light that supplies 100% of its rated light output into the simulated test room. Mixed, overcast and clear sky types (incorporating direct sunlight for clear sky type) are used. Four days (two solstices and two equinoxes) and four timings (10AM, 12 Noon, 2PM and 4PM) for each day are considered. The illuminance at calculation points 1 and 2 is obtained for each case and they are then made the input of the light controller, which then generates the control signals, which are basically the amount of dimming required for the luminaires of the two control groups and the position of the window roller blind. The FIS output for all test cases is given in **Table 6.6**.

**Table 6.6:** Outputs predicted by designed FIS

Date	Time	Sky type	Illuminance at calculation point 1 (lx)	Illuminance at calculation point 2 (lx)	Predicted light output for control group 1 (%)	Predicted light output for control group 2 (%)	Predicted position of roller blind (%)	
22 Sept. 2019	10AM	Mixed	1668	588	50	70	50	
		Clear	1140	569	50	70	50	
		Overcast	843	445	70	90	70	
	12NOON	Mixed	1737	572	50	70	50	
		Clear	1333	596	50	70	50	
		Overcast	893	453	70	90	70	
	2PM	Mixed	1538	579	50	70	50	
		Clear	1022	548	50	70	50	
		Overcast	807	440	70	90	70	
	4PM	Mixed	784	454	70	90	70	
		Clear	679	470	70	90	70	
		Overcast	606	408	90	90	70	
	22 Dec. 2019	10AM	Mixed	1558	594	50	70	50
			Clear	1427	679	50	70	50
			Overcast	685	421	90	90	70
12NOON		Mixed	2189	681	50	70	40	
		Clear	21383	786	50	70	40	
		Overcast	737	429	70	90	70	
2PM		Mixed	1360	561	50	70	50	
		Clear	1249	638	50	70	50	
		Overcast	633	417	90	90	70	
4PM		Mixed	519	402	90	90	70	
		Clear	608	462	90	90	70	
		Overcast	483	389	100	100	100	
23rd Mar. 2020		10AM	Mixed	1615	585	50	70	50
			Clear	1086	558	50	70	50
			Overcast	831	443	70	90	70
	12NOON	Mixed	1709	567	50	70	50	
		Clear	1313	593	50	70	50	
		Overcast	897	454	70	90	70	
	2PM	Mixed	1582	581	50	70	50	
		Clear	1060	554	50	70	50	
		Overcast	825	443	70	90	70	
	4PM	Mixed	877	472	70	90	70	
		Clear	714	479	70	90	70	
		Overcast	635	413	90	90	70	
	21st June 2020	10AM	Mixed	1001	476	70	90	70
			Clear	795	471	70	90	70
			Overcast	905	455	70	90	70
12NOON		Mixed	831	433	70	90	70	
		Clear	845	481	70	90	70	
		Overcast	961	463	70	90	70	
2PM		Mixed	1030	484	70	90	70	
		Clear	776	468	70	90	70	
		Overcast	890	453	70	90	70	
4PM		Mixed	909	476	70	90	70	
		Clear	658	449	90	90	70	
		Overcast	712	425	90	90	70	

The comparison of the average illuminance and overall uniformity before and after the application of control are shown in **Figs. 6.5-6.6**. After the application of the designed light controller in the DIALux simulation of the test room, the following are observed from **Figs. 6.5-6.6**:

- 1) the average illuminance level is reduced for each case thereby providing opportunity for energy savings
- 2) the average illuminance level does not fall below the minimum required value of 300lux for each case
- 3) the overall uniformity improves after the application of control for each case

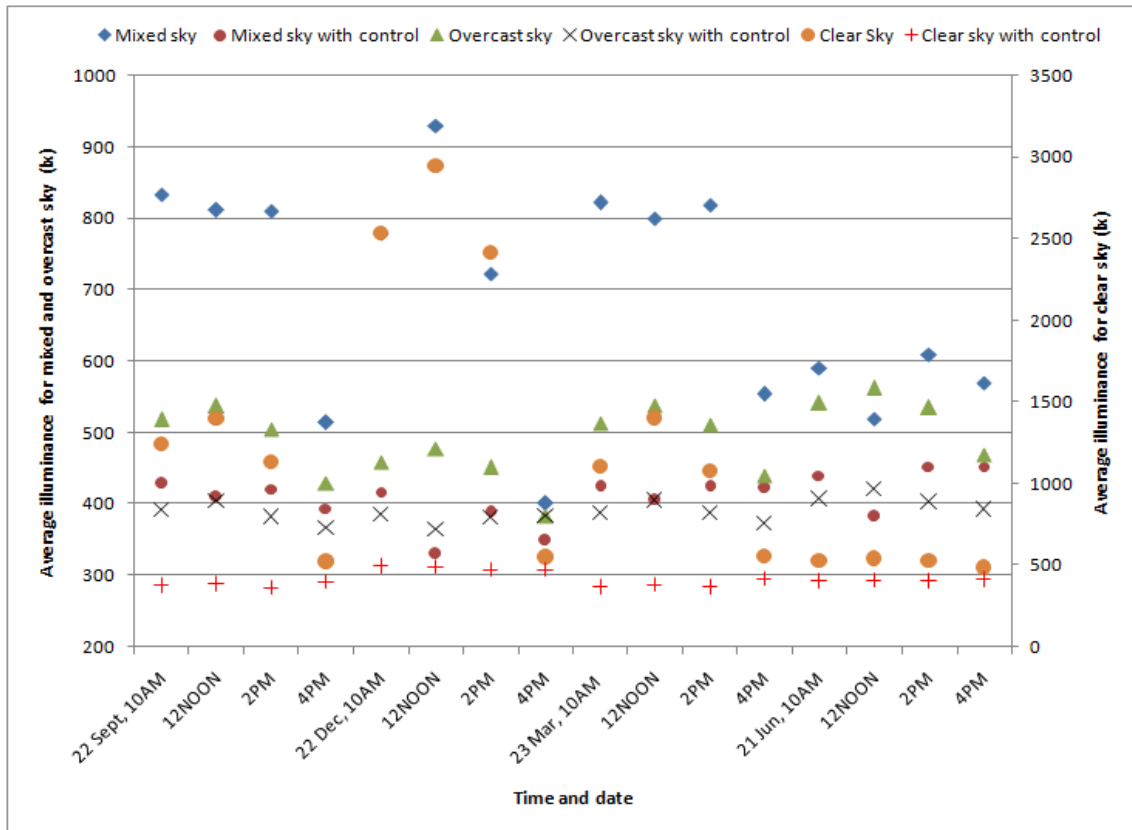


**Fig. 6.5:** Comparison of average illuminance before and after control

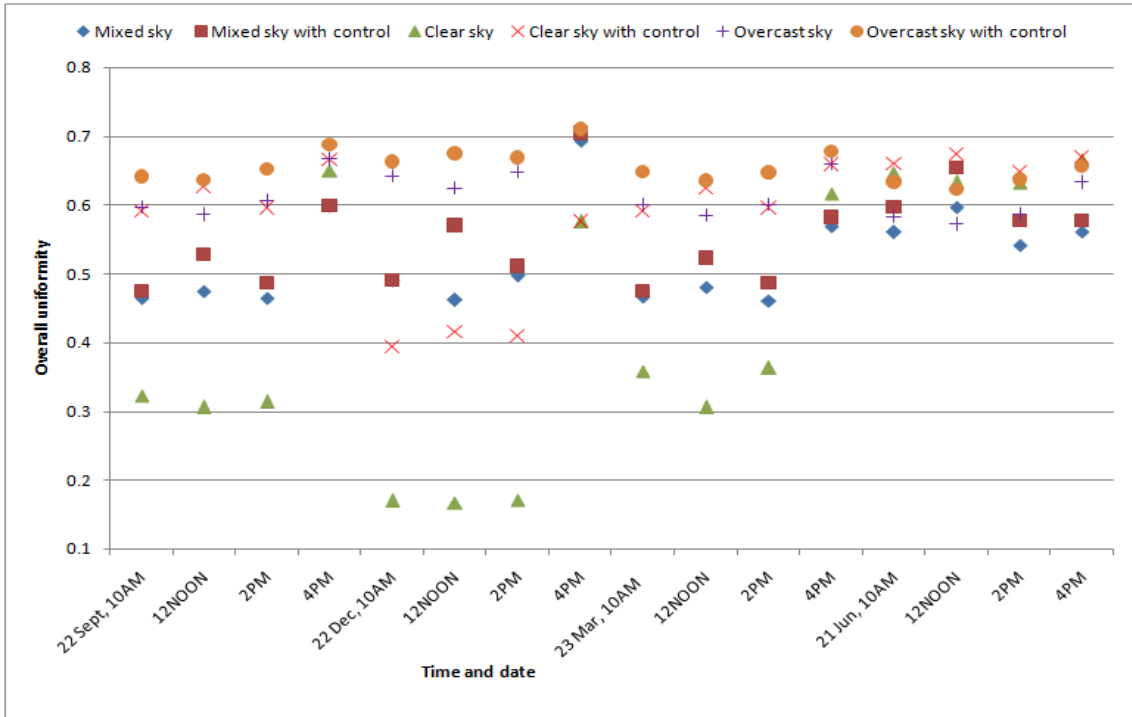


**Fig. 6.6:** Comparison of overall uniformity before and after control

## **6.2 Fault-monitoring and motion-sensing wireless light controller**

### **6.2.1 Introduction**

LED luminaires have the advantages of longer lifetime, low cost, greater design flexibility and high energy efficiency during dimming over other lamps and therefore, are used for saving electrical energy used for lighting [126, 190, 191]. Further electrical energy consumption can be reduced by powering the LEDs only if occupants are present and dimming them when daylight is available for illuminating the indoor environment [109, 110]. At present, wireless lighting control systems are taking over the hard-wired systems because of their greater installation flexibility and lower labour cost for installation [67, 192–195]. Research work was conducted on the wireless control of integrated daylight lighting systems [53, 127–129]. All of the above mentioned works reported satisfactory performance of the developed controller, but none of the above mentioned works and currently available commercial LED luminaires have the capability to detect the location of fault in the luminaire without dismantling the whole luminaire and testing the driver and the LED module individually. However, this strenuous exercise can be excluded by the introduction of a fault detection module in the light controller for the LED luminaire, which will indicate whether the driver or the LED module is faulty and the same can be easily replaced. In this section, the design, development and laboratory testing of a fault-monitoring and motion-sensing wireless light controller for an indoor LED luminaire is presented.



## 6.2.2 Features and design

### Features

The developed light controller has the following features:

- a) capable of detecting and indicating the occurrence of a fault in the LED driver and the LED module separately
- b) capable of controlling the light output based on motion and presence of users
- c) capable of varying artificial light based on available daylight but at the same time keeping the level of illumination on the work plane to the required level
- d) simple and easy installation due to the use of wireless communication

### Design

The proposed light controller consists of one light sensor (BH1750) which can provide the value of illumination on the work plane directly bypassing complex calculation and calibration. It uses I2C protocol for communication with micro-controllers. An inexpensive and low-power PIR sensor is employed to detect motion if the workspace is occupied by users. Arduino Mega is used as the micro-controller for the proposed controller. In this work, two Arduino Mega boards are used. One board is used for obtaining the presence of motion and the available light level on the work plane and generating a control signal to be sent over wireless communication to the second Arduino, which generates a corresponding PWM signal for switching the connected LED lighting system. The second Arduino also obtains the value of voltage and current sensor and indicates the occurrence of fault, if any, in the LED driver or the LED module. One pair of XBee S2C is used to establish wireless communication. XBee S2C works on Zig-

Bee mesh communication protocols in compliance with IEEE 802.15.4 PHY [160]. A voltage sensor module compatible with Arduino is used to detect the fault in LED driver. It can measure up to 25V DC [196]. A ACS712 current sensor module compatible with Arduino is used to detect the fault in LED module. The block diagram of the proposed system with all the components is shown in **Fig. 6.7**.

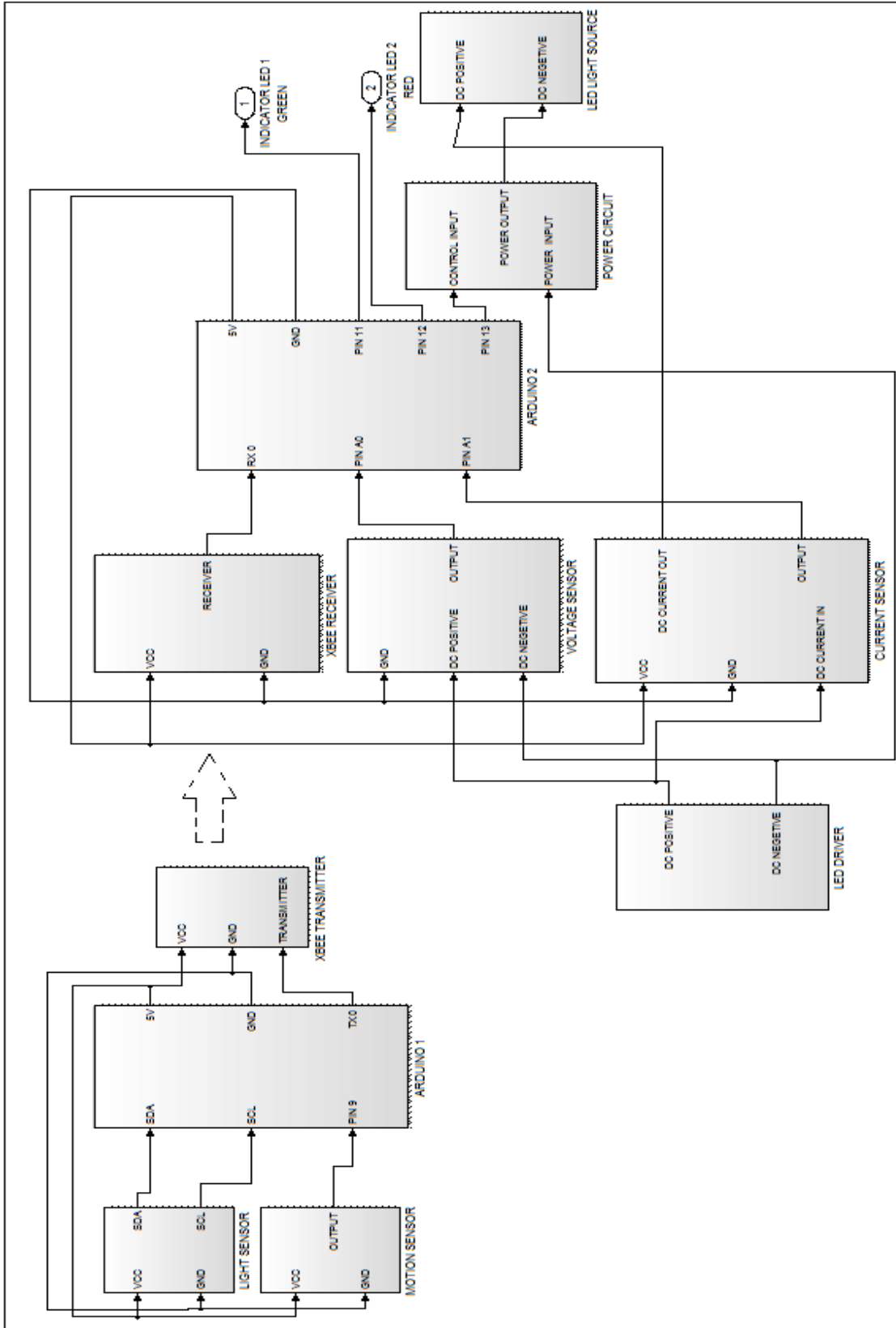
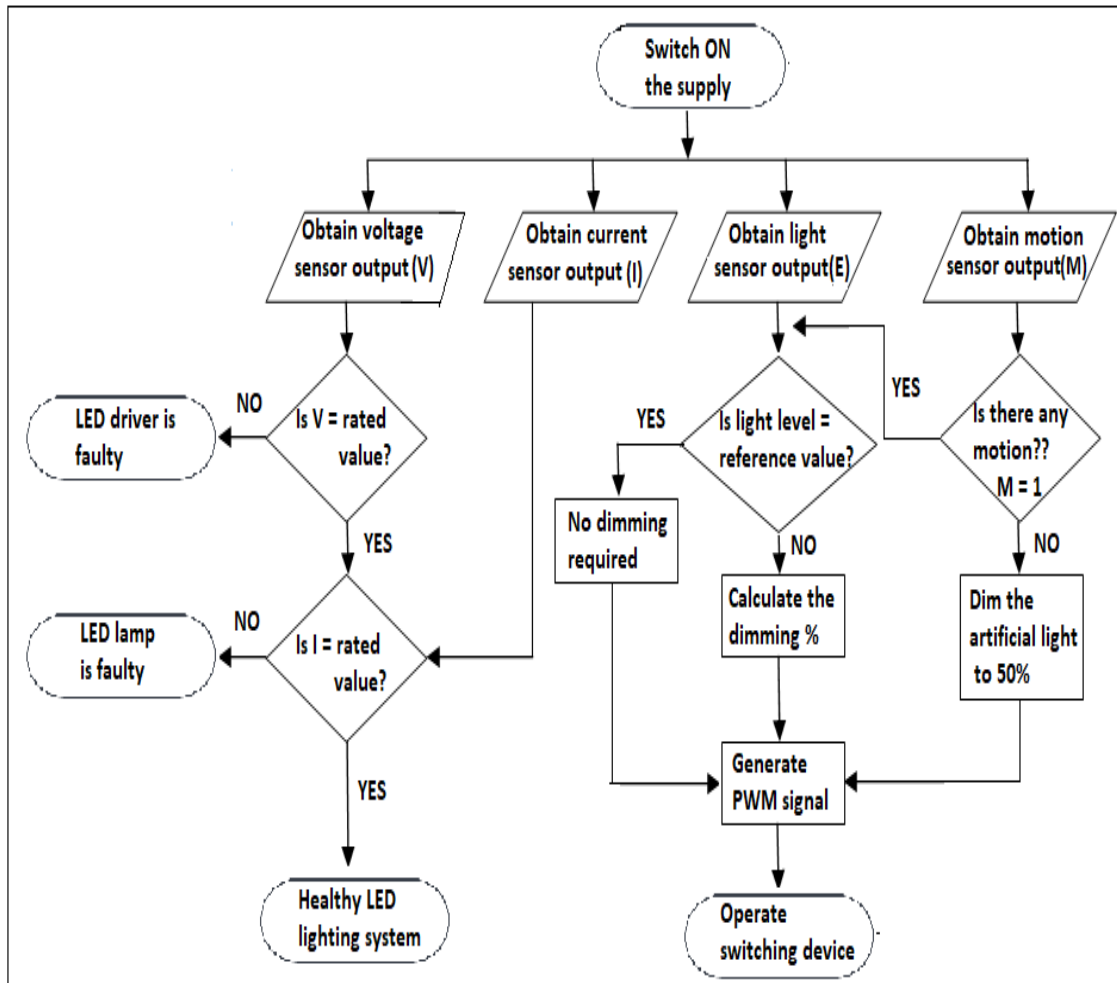


Fig. 6.7: Block diagram of the proposed system

### 6.2.3 Principle of operation

The algorithm for controller operation is given in **Fig. 6.8**. When power is given to the LED luminaire, the outputs of the voltage sensor and current sensor are read as analog inputs by Arduino 2 operating as the micro-controller. The Arduino first detects the voltage sensor output. If this value is not within the operating voltage range of the LED driver, then the LED driver is faulty, which is indicated by switching ON a GREEN indicator LED. If the voltage sensor value is within the rated voltage range, then the Arduino senses the current input of the LED module. If the current value is within the rated range, then the LED module is healthy, otherwise the LED module is faulty, which is indicated by switching ON a RED indicator LED. The Arduino monitors the condition of the LED driver and the LED module every hour. At the same time Arduino 1 reads the output of the motion sensor (should be placed on the ceiling during real-time installation) and light sensor (can be placed on the work-plane, ceiling or wall according to the demand and limitation of particular application). If there is no motion, then it may be assumed that there is no user present, and therefore the light output is fixed at 50% of rated value. If user is present, then the percentage of light output is calculated based on the light sensor output. The reference value of illuminance on the work-plane is to be obtained by the LED lighting system operating in absence of daylight. So, light output from LED module will be reduced if there is daylight available and the light level on the work plane is more than the reference value. Arduino 1 generates a PWM signal that has a pulse width corresponding to the percentage of light output required. This PWM signal is sent to an XBee module, which behaves as a wireless transmitter. This XBee transmits the PWM signal to another XBee module that behaves as a receiver. The XBee receiver then sends the PWM signal to Arduino 2

which generates a proportional control signal for the switching circuit. The switching circuit is made up of a power MOSFET which is used as the switching device. The proposed controller in addition to making the LED lighting system more energy efficient and easy to install detects and indicates the occurrence of faults in the LED driver and LED module separately.



**Fig. 6.8:** Control algorithm of the developed controller

#### 6.2.4 Laboratory testing

A hardware prototype of the proposed controller is developed in laboratory for testing purposes and is shown in **Fig. 6.9**. The controller is

tested on Philips make 10W White LED lighting system. The driver output rating is 40V, 250mA. When the LED module connected to it is dimmed, the current varies from 250mA to 0mA and the voltage varies from 40V to 50V.

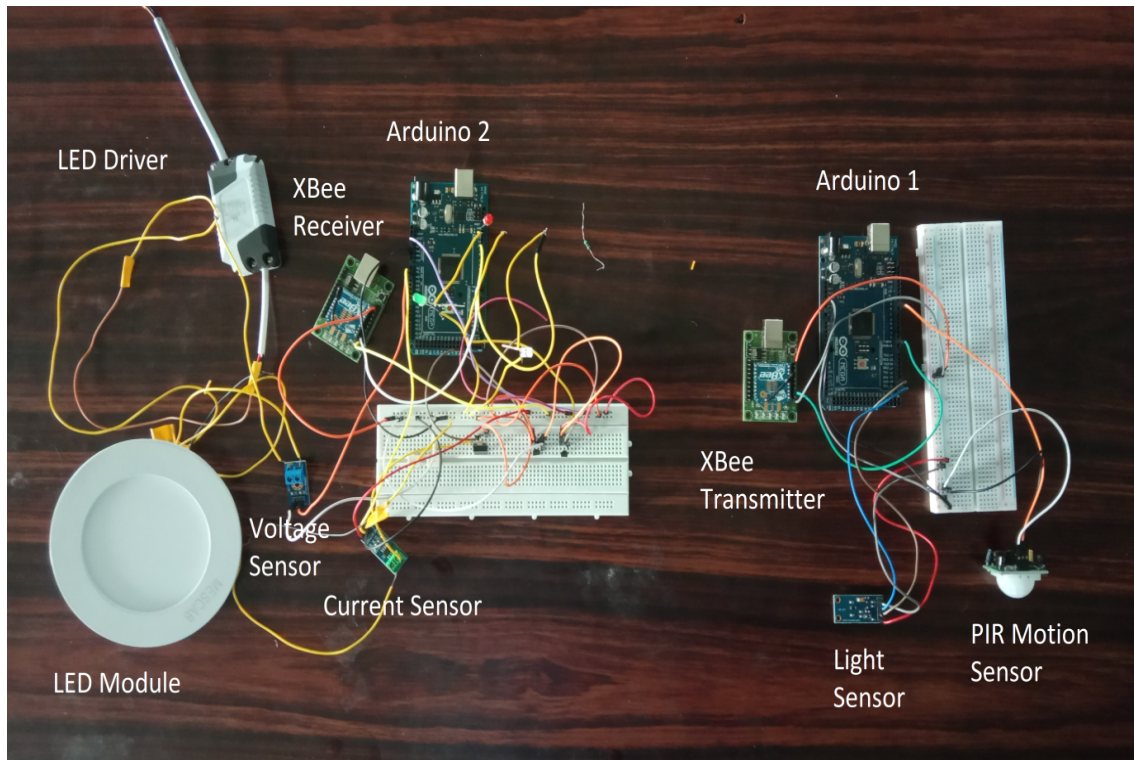


**Fig. 6.9:** Developed hardware setup

### 6.2.5 Results and analysis

During testing, when power supply is given to the LED lighting system, no fault indicator LEDs were ON. Initially there was no motion due to the absence of users, so the light output of the LED module was around 50% of the rated value. When motion was detected, then the LED lighting system is dimmed according to the ambient light level. The light output values from LED module for a particular range of ambient light were assumed for testing purposes only. **Table 6.7** shows the obtained values of control voltage and pulse width of generated PWM signal. The variation of input current and input power of the

LED module with the variation of light output values is shown in **Fig. 6.10**.

**Table 6.7:** Control voltages and pulse width of generated PWM signals

Occupancy	Instantaneous light level (lx)	Prescribed light output (%)	Digital value of Arduino PWM signal	Desired analog value of Arduino PWM signal	Measured control voltage (volts)
Absent	Not Applicable	50	128	2.5	2.4
Present	<300	100	255	5	4.8
	300-400	90	230	4.5	4.3
	400-500	80	204	4	3.8
	500-600	70	179	3.5	3.3
	600-700	60	153	3	2.9
	700-800	50	128	2.5	2.4
	800-900	40	104	2	1.9
	>900	30	77	1.5	1.4

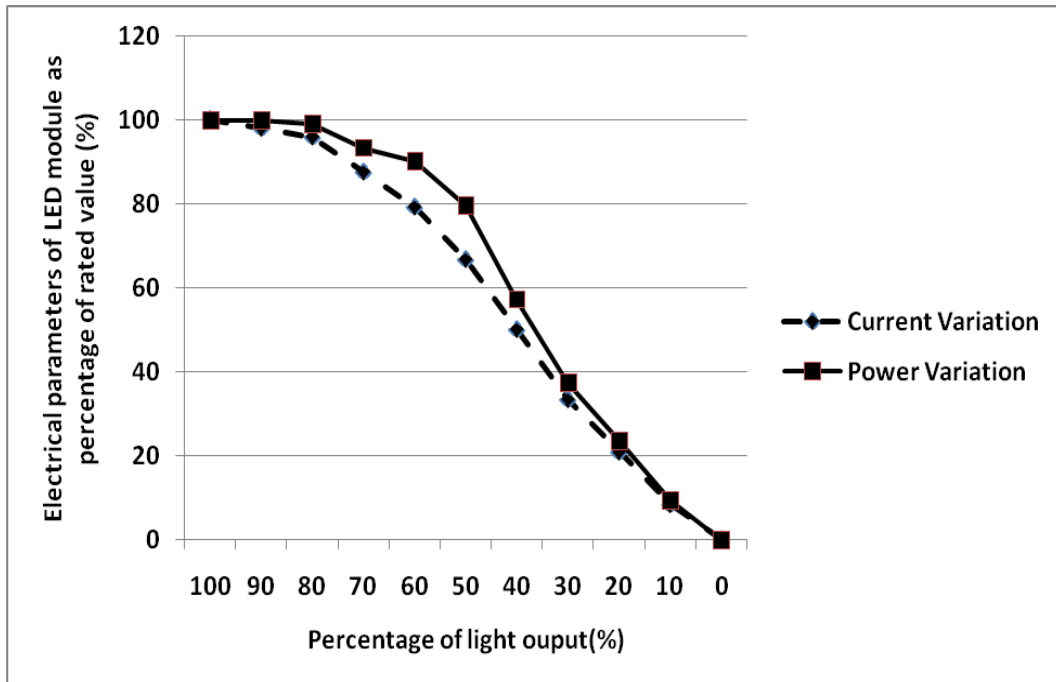


**Fig. 6.10:** Variation of electrical parameters with output light of LED module

Finally, the fault detection and indication capabilities of the developed controller are observed. First, the LED module was made faulty

by open circuiting it with the help of a push button switch. During this operation, the RED indicator LED switched ON. Next the LED driver was made faulty by damaging the electrolytic capacitor and then powering it ON. During this operation, the GREEN indicator LED switched ON.

### **6.3 Chapter summary**

In this work, two sets of daylight-responsive controllers are designed and implemented using the Arduino Mega micro-controller. The FIS based light controller predicts the light output from artificial light sources and the position of window roller blind based on available daylight, whereas the fault-monitoring and motion-sensing wireless light controller controls the light output based on ambient light and user presence, as well as detects the occurrence of fault in the LED driver and LED module separately. The FIS based light controller's performance is evaluated using a model test room simulated in DIALux 4.13 software and that of the fault-monitoring light controller is evaluated by developing a hardware prototype and testing the same in the laboratory. The performance of both the light controllers was found to be satisfactory.



## **Publications**

The publications related to this work are as follows:

### **Conference Publications: 2**

**1. Vishwanath Gupta, Biswarup Basak & Biswanath Roy. 2020.** A Fault-Detecting and Motion-Sensing Wireless Light Controller for LED Lighting System. **2020 IEEE Calcutta Conference (CALCON), Kolkata, India, 2020, pp. 462-466, doi: 10.1109/CALCON49167.2020.9106427.**

**2. Vishwanath Gupta, Biswarup Basak & Biswanath Roy. 2022.** Fuzzy logic based closed-loop light controller for daylight responsive office lighting system. **2nd International Conference on Recent Advances in Modeling and Simulations Techniques in Engineering and Sciences (RAMSTES-22), Jaipur.** Accepted for further processing and publication in Journal of Mines Metals and Fuels (JMMF).



## **7 Design and real time evaluation of a wireless light controller for tunable-white LED luminaire**

In this chapter, a wireless light controller for multiple spectrally tunable-white LED luminaires is designed and developed. The tunable-white luminaires are installed in a test room to test the developed light controller in real time. A mobile app is developed to provide wireless communication support to the light controller. The developed controller, along with the supporting mobile app, can manually or automatically vary the illuminance and CCT as per need. The results of the real-time test show very little variation from the desired values. The light controller also showed satisfactory performance when tested for power failure and wireless communication failure scenarios.

## 7.1 Introduction

Spectrally tunable-white LEDs are one of the most preferred artificial light sources for indoor lighting applications such as health care, education and office work where daylight is unavailable. They not only provide energy savings, but also improve the lives, well-being and health of their end users [133–143]. The operation of tunable-white light sources requires a controller which may be an integral part of the driver unit or a stand-alone unit used in conjunction with the driver and LED module. Commercially, a number of tunable-white LED modules are available along with their dedicated controllers [148, 151, 152, 197]. These commercially available products provide wireless control of CCT and illuminance using mobile applications, but all these products, barring Philips Hue White Ambiance [148] are preferred only for domestic lighting applications as they are stand-alone units with a single controller for single LED lamp. Philips Hue White Ambiance comes with an accessory 'Hue Bridge' that allows 50 units to be connected and controlled through a single mobile app. Academically, many controllers have been proposed for the control of tunable white light sources that can be installed in health care, education and office lighting applications [153–157]. The limitations of the above mentioned works are that the control logic is developed for a single light source. In the research work done by Maity and Roy [52], the controller developed in [155] was modified to control multiple tunable-white LED sources manually and automatically using the IR remote, but it has a limited number of pre-prescribed set points for CCT and illuminance. Also, the experimental results of the multiple luminaire operation were not provided. Moreover, in all the above works, real-time testing of the proposed systems is not done in practical indoor applications. But real-time testing of any system must be done to detect and rectify errors, measure requirements confor-

mance and provides an indication of quality of the developed system [117, 118, 198, 199].

In this present chapter, a wireless light controller that can operate multiple tunable-white LED luminaires in real time is designed and developed.

## **7.2 Wireless light controller**

### **7.2.1 Features**

The distinctive features of the designed wireless light controller are as follows:

- 1) Ability to control the light output from a complete indoor lighting installation, that constitutes multiple tunable-white LED modules consisting of Warm White (WW) and Cool White (CW) LED arrays, using a single micro-controller thereby, saving installation cost, maintenance and labour. It provides independent as well as simultaneous control of CCT (from 2700K-5600K) and illuminance (from 20 lux to 300 lux) using digital control
- 2) Provides option of manual override to the end-user, in addition to automatic CCT and illuminance variation on the work-plane of an indoor environment in accordance with the time of day, to satisfy individual preferences
- 3) Operation of the controller is done with Bluetooth wireless communication via developed dedicated mobile app or through any available Bluetooth serial app.
- 4) Ability to provide continuous unhindered operation of the luminaires during wireless communication failure due to data collisions and transmission errors
- 5) The resetting or restarting of the designed controller in the event of power failure and subsequent power restoration of the lighting application is not necessary as it remains unaffected by power failures

## 7.2.2 Design and development

The light controller's block diagram is shown in **Fig. 7.1**.

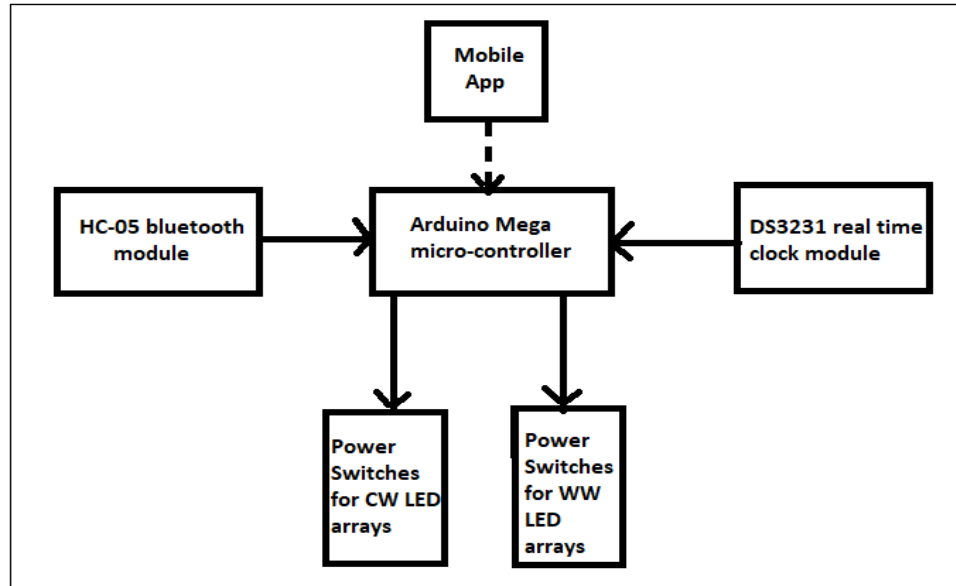


**Fig. 7.1:** Block diagram of the designed light controller

The proposed light controller is implemented using an Arduino Mega 2560 micro-controller module. The Arduino micro-controller executes the logical decisions and generates the required control signal. The generated control signals actuate the power switches that operate the LED luminaires. A Real Time Clock module DS3231 is used to keep track of real time during operation. This ability of keeping track of the real time helps the light controller to set required CCT and illuminance values at that instant of time for a particular day of the year during automatic operation. The light controller is operated by a user through a developed mobile app or any other available Bluetooth serial app. This wireless operation of the developed light controller is accomplished using a Bluetooth module HC-05, which enables the micro-controller to receive from and transmit data to the connected mobile app via wireless communication. The developed hardware prototype of the designed light controller is shown in **Fig. 7.2**

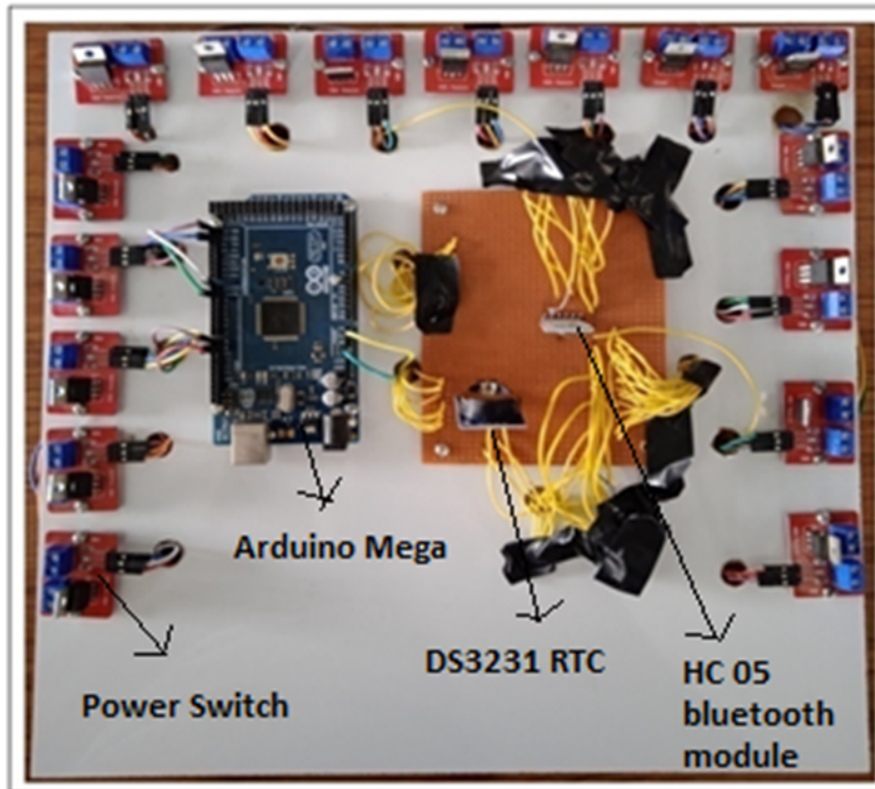


**Fig. 7.2:** Developed hardware prototype of the proposed light controller

### Developed mobile app

The developed mobile app acts as the light controller user interface. The dedicated app for the light controller is built with the help of the online MIT App Inventor software [200] using a simple drag and drop interface along with their block programming system. It allows the user to select the mode of operation and the desired CCT and illuminance values. The unique feature of the mobile app is that data collisions and transmission errors are eliminated by checking for character timeout and polling the data-send function in the block-programming system of the app. It also alerts the user if the Bluetooth communication link with the controller is interrupted. The developed mobile app is shown in **Fig. 7.3**.

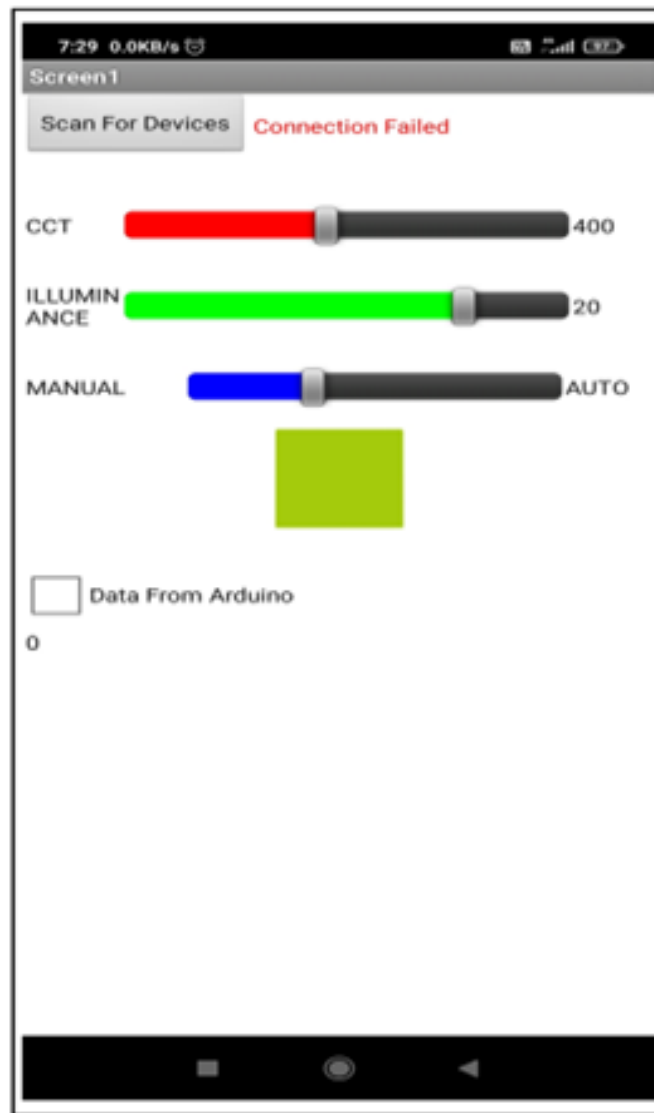


**Fig. 7.3:** Screenshot of the developed mobile app

It is incorporated with the following components:

- a) a push button for scanning the available Bluetooth devices
- b) a label to show whether the Bluetooth device is connected or not
- c) three numbers of sliders (one each for selecting the mode, the desired CCT and the desired illuminance)
- d) a display colour button to verify the change in slider positions
- e) a check box and a label to detect transmission of data from developed controller



The mode selector slider has two options: AUTO and MANUAL. The range of the CCT slider is from 270 to 560 (10:1 scaled version of the required CCT range). The range of illuminance slider is from 0 to 30 (10:1 scaled version of required illuminance range).

### **7.3 Principle of operation**

The algorithm describing the principle of operation of the developed light controller is shown in **Fig. 7.4**.

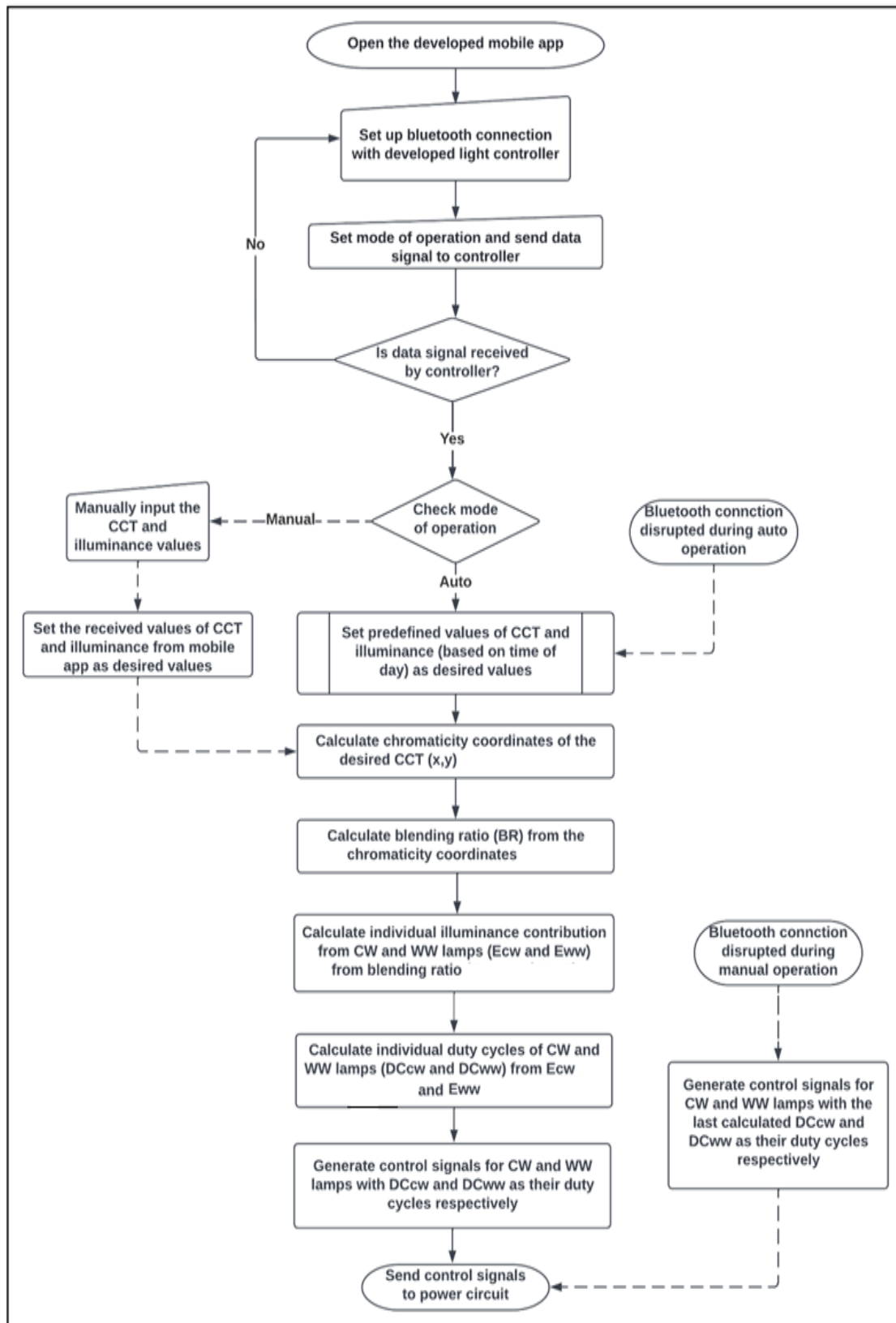


Fig. 7.4: Operating algorithm of the developed controller

At first, the controller and the mobile app are switched ON and the Bluetooth connection between them is set up. Then the operating mode is selected via the mobile app and the CCT and illuminance values are set (in case of manual operation). Simultaneously, the controller examines if there is any serial data transmitted from the app. If there is meaningful serial data available, then it starts its operation. In the first step, it checks the mode of operation (AUTO or MANUAL) provided by the mobile app. If the mode is AUTO then the controller sets the CCT and illuminance values to a predefined set of values according to time and day of the year. If the mode is MANUAL, then the desired CCT and illuminance values are the ones obtained from the user via the app. After the CCT ( $T$ ) and illuminance ( $E_{set}$ ) value are set, chromaticity coordinates of the desired CCT are calculated using equations (7.1) - (7.4). Equations (7.1) and (7.2) are for CCTs in the range of 2222K-4000K and equations (7.3) and (7.4) are for CCTs in the range of 4000K-25000K [201].

$$x = \frac{-0.2661239 \times 10^9}{T^3} - \frac{0.234358 \times 10^6}{T^2} + \frac{0.8776956 \times 10^3}{T} + 0.179991 \quad (7.1)$$

$$y = -0.954947x^3 - 1.37418593x^2 + 2.09137015x - 0.16748867 \quad (7.2)$$

$$x = \frac{-3.0258469 \times 10^9}{T^3} - \frac{2.1070379 \times 10^6}{T^2} + \frac{0.2226347 \times 10^3}{T} + 0.24039 \quad (7.3)$$

$$y = 3.081758x^3 - 5.8733867x^2 + 3.75112997x - 0.37001483 \quad (7.4)$$

Where,  $x, y$  are the chromaticity coordinates and T is the CCT in Kelvin These chromaticity coordinates are then used to calculate the blending ratio (BR) from Grassman's law of colour mixing. The expression for BR is given by (7.5).

$$BR = \frac{(x_c - x)y_w}{(x - x_w)y_c} \quad (7.5)$$

Where,  $x_c, y_c$  and  $x_w, y_w$  are the chromaticity coordinates of CW LEDs and WW LEDs at rated condition.

Subsequently, the blending ratio and the set illuminance value are utilised as given in (7.6) and (7.7) to compute the individual illuminance contribution of WW ( $E_w$ ) and CW ( $E_c$ ).

$$E_c = \frac{E_{set}}{1 + BR} \quad (7.6)$$

$$E_w = E_{set} - E_c \quad (7.7)$$

For the controllers mentioned in previously published research articles [16-21], individual duty cycles of single CW and WW module were calculated from their point-specific individual illuminance contribution at any given point below the light source, as real-time testing was not reported. However, to test the developed controller in real time, individual duty cycles of CW and WW modules are to be calculated from their respective individual average illuminance contribution. The variation of average illuminance for 0-100% duty cycle is obtained for both WW and CW LED modules individually as shown in **Fig. 7.5**. From these experimental data, the expression for individual duty cycles of CW and WW modules is obtained using the curve fitting technique

and is given in (7.8) and (7.9), .

$$DC_{cw} = \frac{E_c - 6.9}{2.3} \quad (7.8)$$

$$DC_{ww} = \frac{E_w - 7.1}{1.96} \quad (7.9)$$

where,  $DC_{cw}$  and  $DC_{ww}$  are the duty cycles of CW and WW lamps respectively.

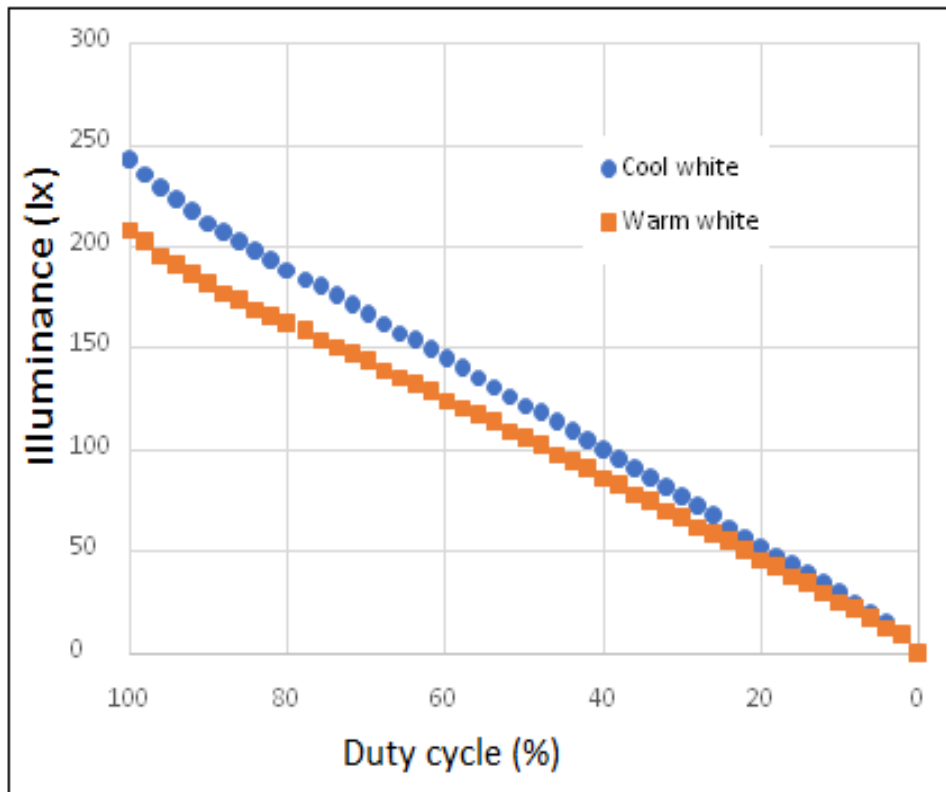


**Fig. 7.5:** Variation of average illuminance on working plane with duty cycle

Finally, the control signals with ascertained duty cycles are fed to the power switches (in this case, MOSFET IRF520), which drives the WW and CW lamps accordingly.

If the Bluetooth wireless communication is interrupted or there is a

power failure during automatic operation, then the predefined CCT and illuminance values for that time of day are set as the desired values. However, if the communication is disrupted or power failure occurs during manual operation then the last calculated values of  $DC_{cw}$  and  $DC_{ww}$  are set as the respective duty cycles.

#### 7.4 Real-time testing

The developed wireless light controller is tested on multiple tunable-white LED luminaire based indoor lighting application installed in a test room.

##### Test room and installed lighting application

The test room used for the real-time testing of the developed controller has dimensions 5mx3mx2.77m with two windows (fully covered with thick cloth curtains to block external light) and a door (closed during time of experiment). The test room has a water-base sky-blue coloured diffused finish ceiling and wall surfaces, whose surface reflectance is 49%. The test room has eight tunable-white LED modules installed inside it. The selected luminaire arrangement is based on the obtained optimised arrangement from PSO optimisation technique [202]. The indoor lighting application can produce CCT in the range of 2700K-5600K and illuminance in the range of 20lx-300lx on the working plane of the test room. The schematic of the room with the installed luminaire arrangement is shown in **Fig. 7.6**. The picture of the room with the installed luminaire arrangement is shown in **Fig. 7.7**. The values in the brackets are the coordinates of the respective luminaires.

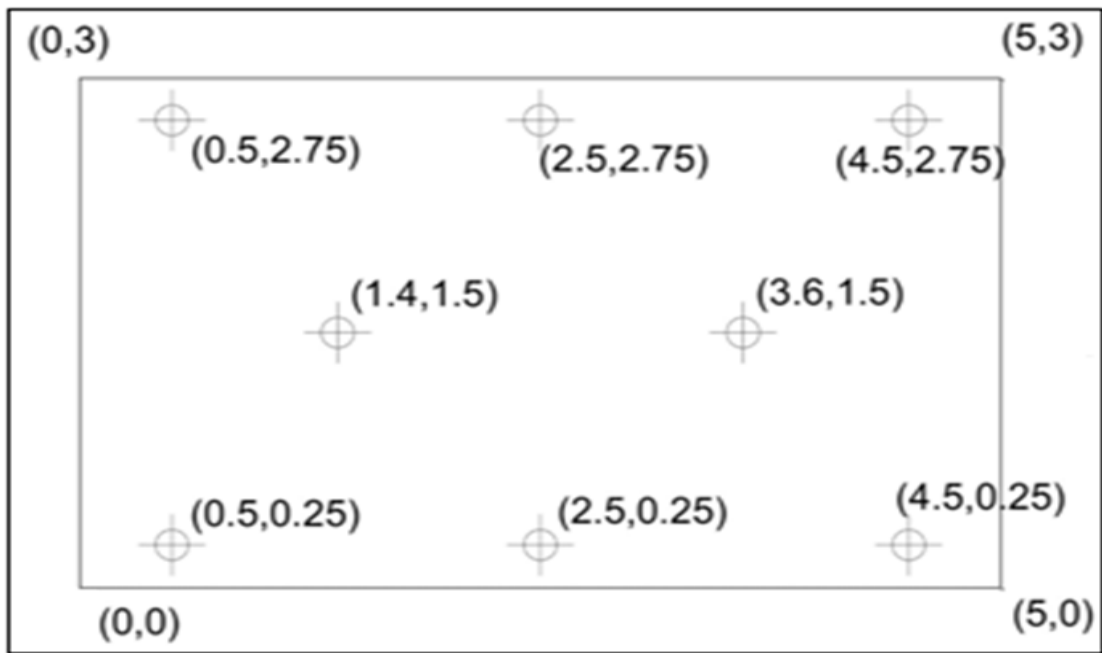


**Fig. 7.6:** Plan view of the installed lighting arrangement in test room

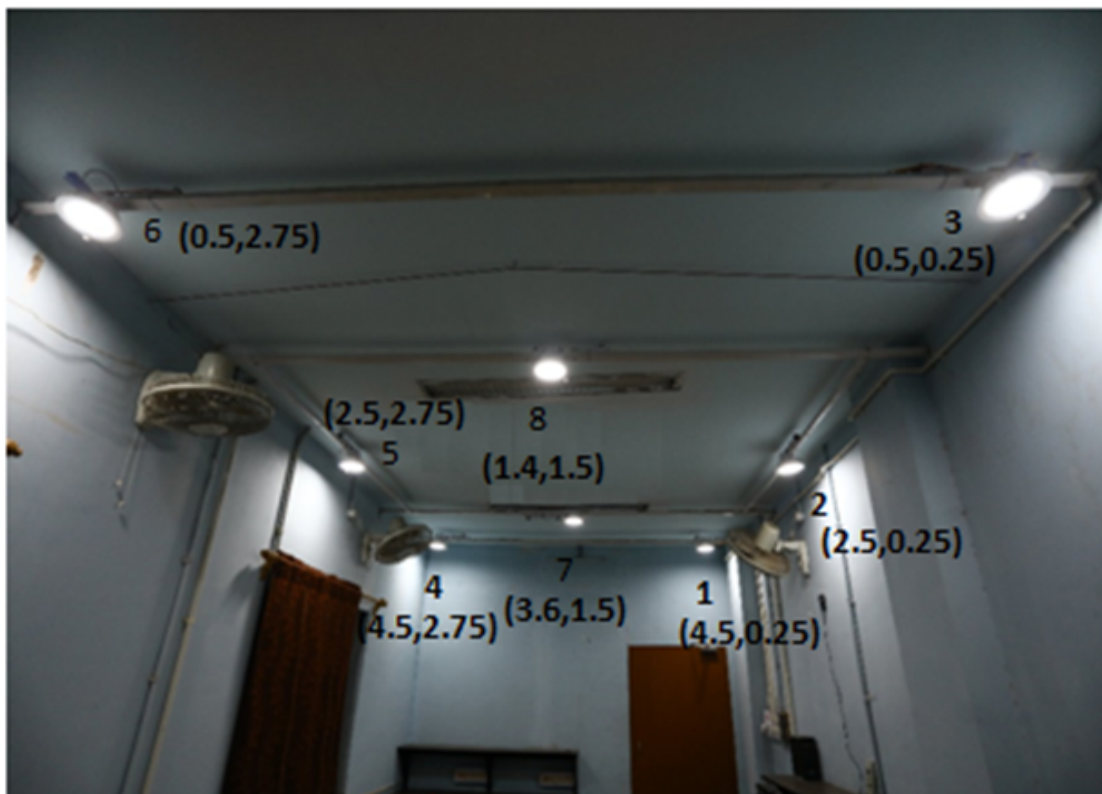


**Fig. 7.7:** Luminaire arrangement in the test room

The installed WLED luminaire consists of a lamp module, a dimmable driver and a Switched Mode Power Supply (SMPS). Each lamp module is made up of evenly distributed separate arrays of WW and CW phosphor-converted blue LED chips and is provided with a white diffuser for thorough mixing of the light. It is operated on Universal AC input (90V-275V) by the dimmable LED driver and SMPS. The technical specifications of the WLED luminaire are provided in **Table 7.1** and its obtained luminous intensity distribution in the form of polar plot is shown in **Fig. 7.8**.

**Table 7.1:** Technical specifications of the installed LED luminaire

Measured parameter		WW LED array	CW LED array
Photometric	CCT (K)	2700	5600
	Luminous flux (lumens)	1000	1100
Electrical	Input Voltage (V)	24	24
	Input Current (mA)	625	625
	Power (W)	15	15

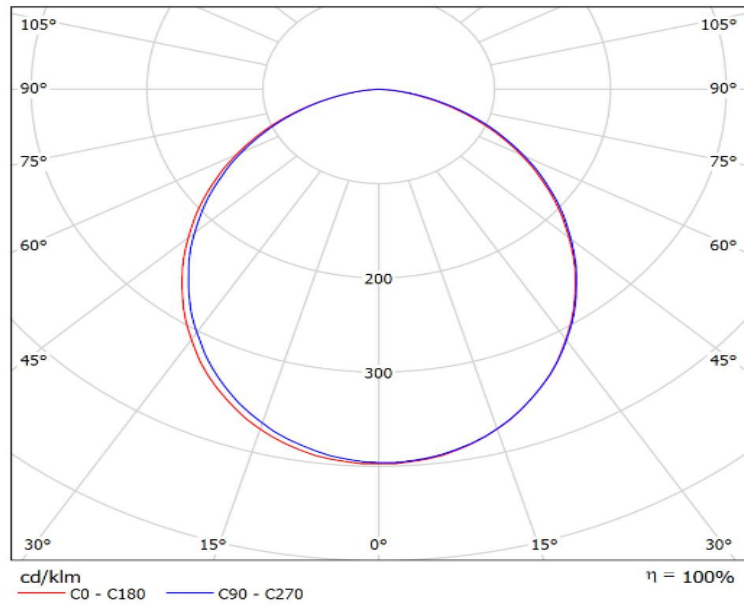


**Fig. 7.8:** Polar diagram of the installed luminaire



The block diagram representation of the installed test lighting system operated with the developed controller is shown in **Fig. 7.9**. The power to the installed lighting system is supplied from programmable AC/DC power source GwINSTEK APS 1102 [179].

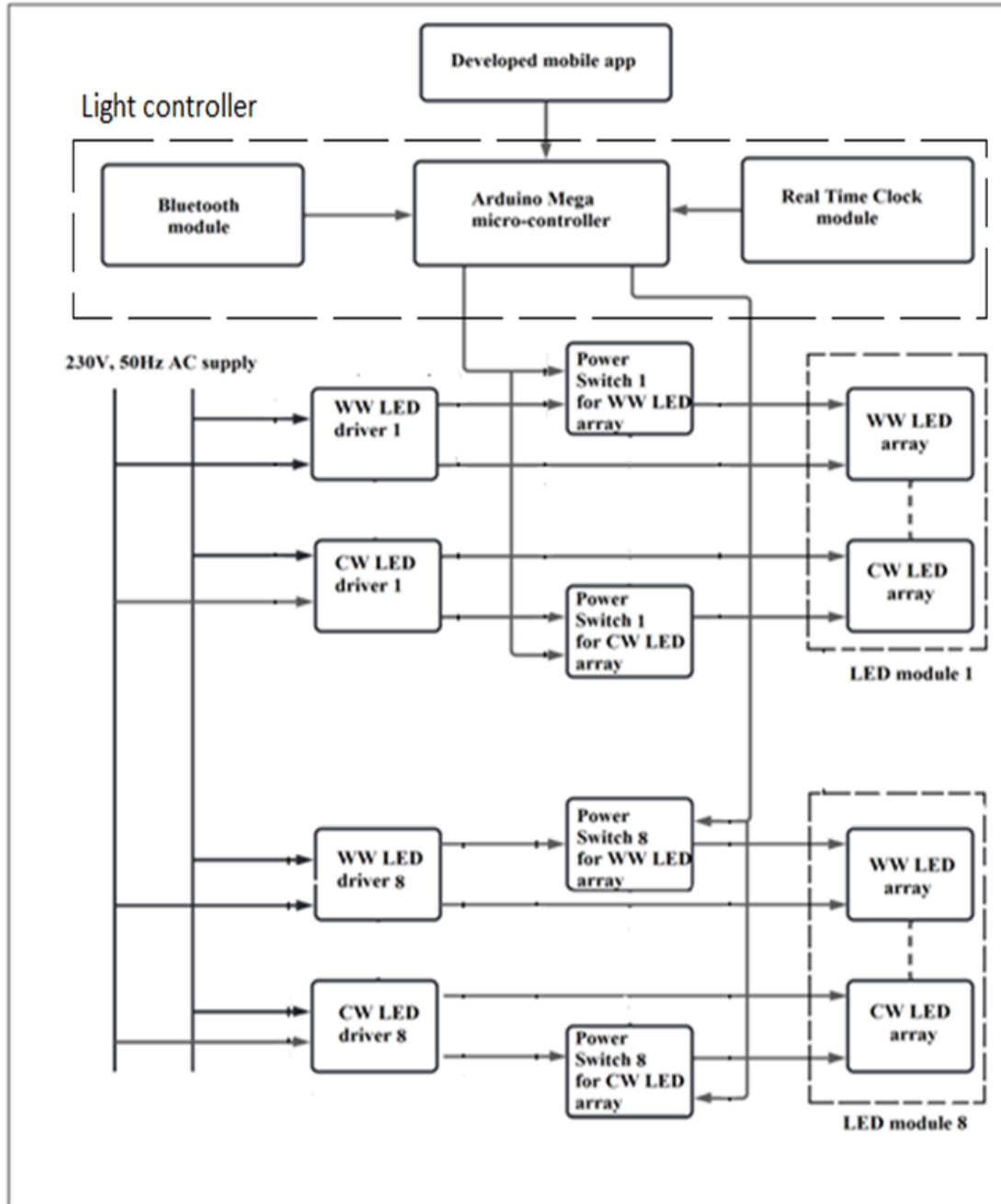


**Fig. 7.9:** Block diagram of the test lighting system operated with developed controller

## Measurement setup

The measurement of CCT and illuminance is carried out on the work-plane, which is 0.8m above the floor. The CCT measurement is done for every one minute interval using Konica Minolta make chromameter CL-200A [175] and the measured data is stored in an excel file using CLS10W version 14.0 software [203]. The illuminance measurement on the working plane is done using Lutron LX-102 digital light meter [204] having provision for analog output. The conversion scale of the above mentioned luxmeters is  $1\text{lx} = 0.1\text{mV}$ . Nine numbers of such light meters and the chromameter are arranged over the working plane to measure point-specific illuminance distribution in order to ascertain the average illuminance and overall uniformity on the work-plane. All the 9 light meters are connected to Agilent make 34970A Data Acquisition System (DAQ) [205] and the analog output of the light meters are recorded during operation of the lighting system for one minute interval. The recorded illuminance data are stored in an excel file from the DAQ using the BenckLink data Logger 3 software. The schematic arrangement of the measurement setup is shown in **Fig. 7.10**. The picture of the real-time measurement setup is shown in **Fig. 7.11**(values in brackets show the coordinates of the luxmeters and chromameter).

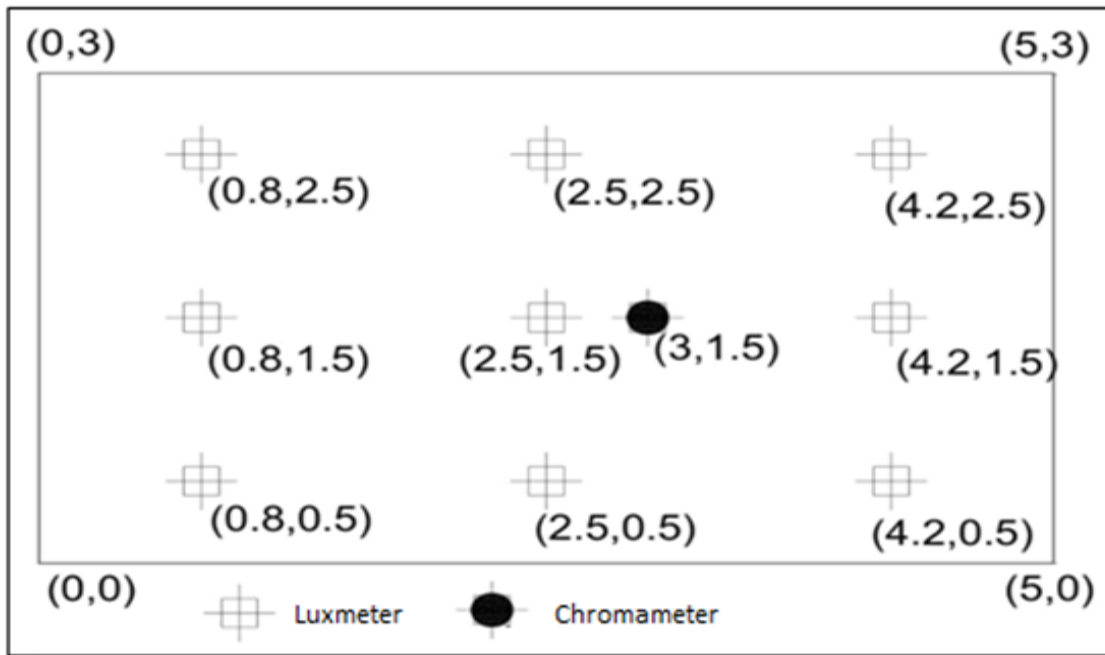


**Fig. 7.10:** Plan view of the measurement setup on the working plane

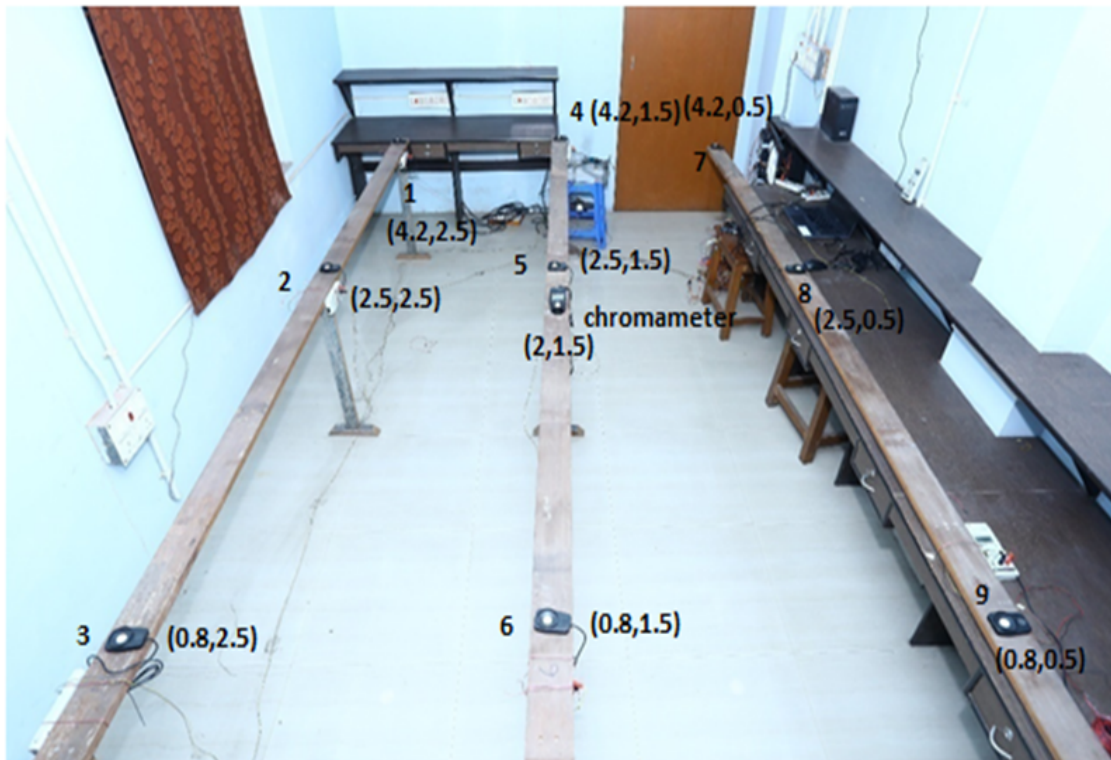


**Fig. 7.11:** Illuminance and CCT measurement setup in the test room

## 7.5 Results and analysis

The developed wireless light controller is tested in real time in AUTO mode and MANUAL mode.

### AUTO mode

The developed wireless controller is tested in AUTO mode by choosing a one hour scaled version of the desired CCT and illuminance pattern [206]. The time-varying profile of the CCT and illuminance pattern is given in **Table 7.2**, is considered.

**Table 7.2:** Desired time varying profile of CCT and illuminance for AUTO mode testing

Time (mins)	0	8	24	29.5	33	37	48	51.5	54	56.5	60
CCT (K)	4700	4600	3000	4600	4700	4500	3000	3500	4000	3300	3000
Illuminance (lx)	280	264	200	248	280	264	200	200	200	200	200

The AUTO mode testing is repeated ten times with same initial conditions to test the repeatability of the developed controller. The obtained results are shown in **Figs. 7.12 - 7.15**. The desired and measured values of CCT and illuminance on the working plane for the 10 different runs are shown in **Fig. 7.12** and **Fig. 7.13** respectively. **Fig. 7.14** shows the variation of measured mean values and desired values of CCT and illuminance with time. **Fig. 7.15** shows the percentage error of measured CCT and illuminance values with respect to desired values. The overall uniformity on the working plane of the test room was also calculated during the 10 test runs. The variation of calculated mean overall uniformity with time is shown in **Fig. 7.16**. During the AUTO mode testing, the wireless communication link between the micro-controller and the mobile app is disrupted purposefully, but the developed controller continued to give desired

performance.

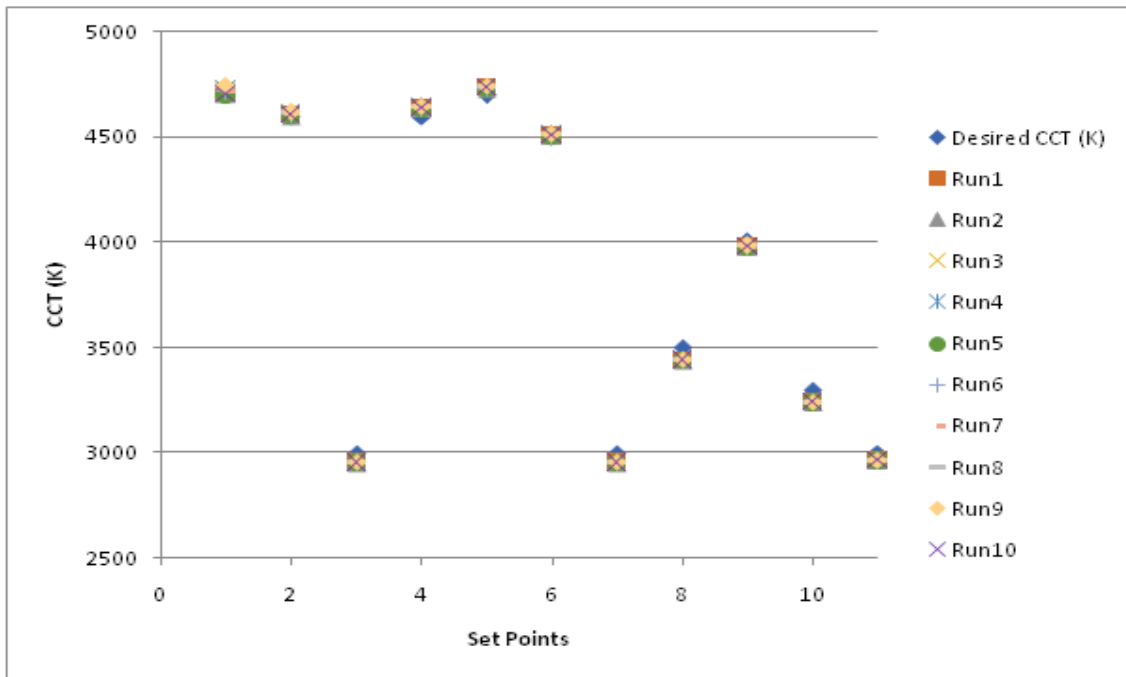


**Fig. 7.12:** Measured CCT in AUTO mode for 10 different runs to check repeatability

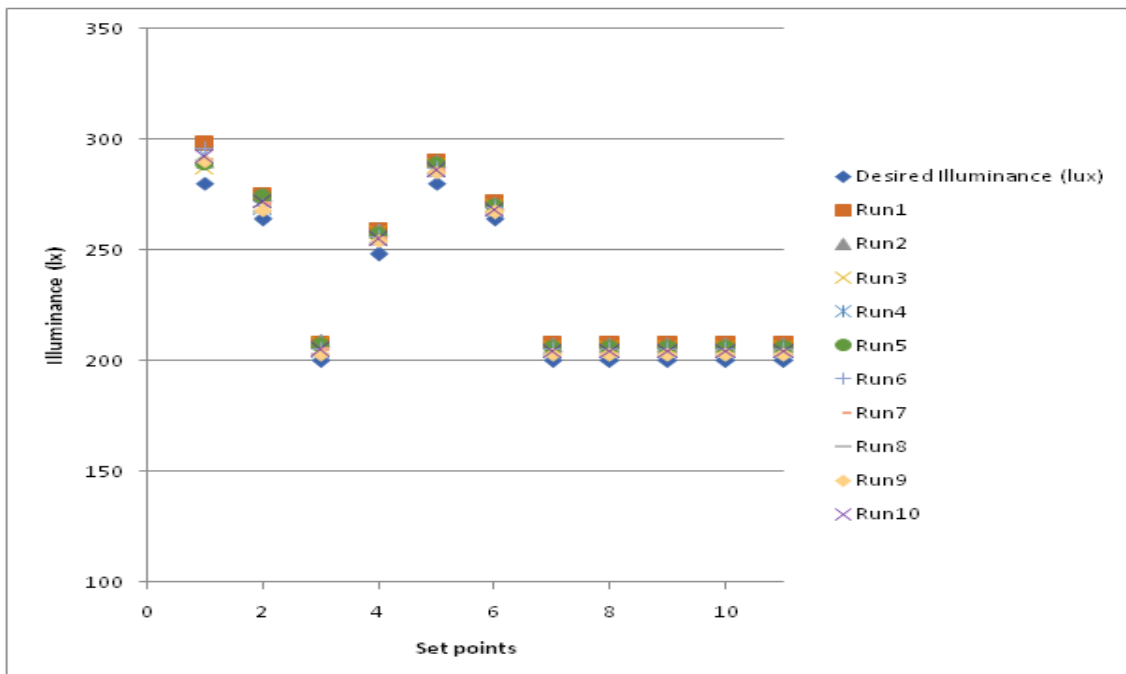


**Fig. 7.13:** Measured illuminance in AUTO mode for 10 different runs to check repeatability

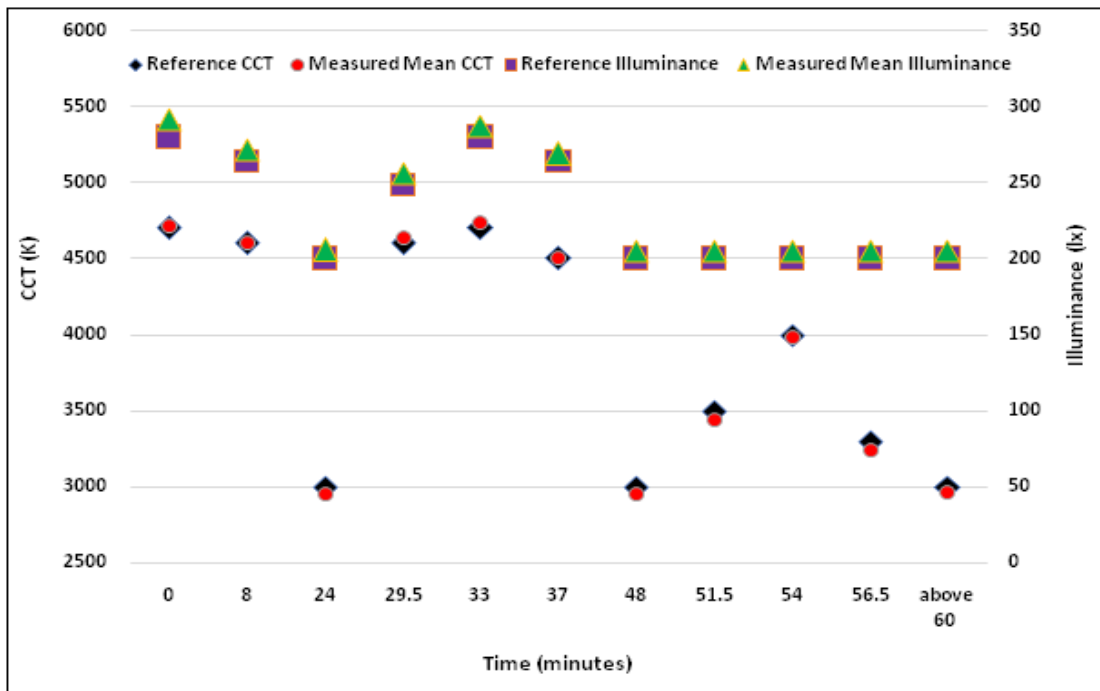


**Fig. 7.14:** Desired vs. measured mean values of CCT and illuminance in AUTO mode

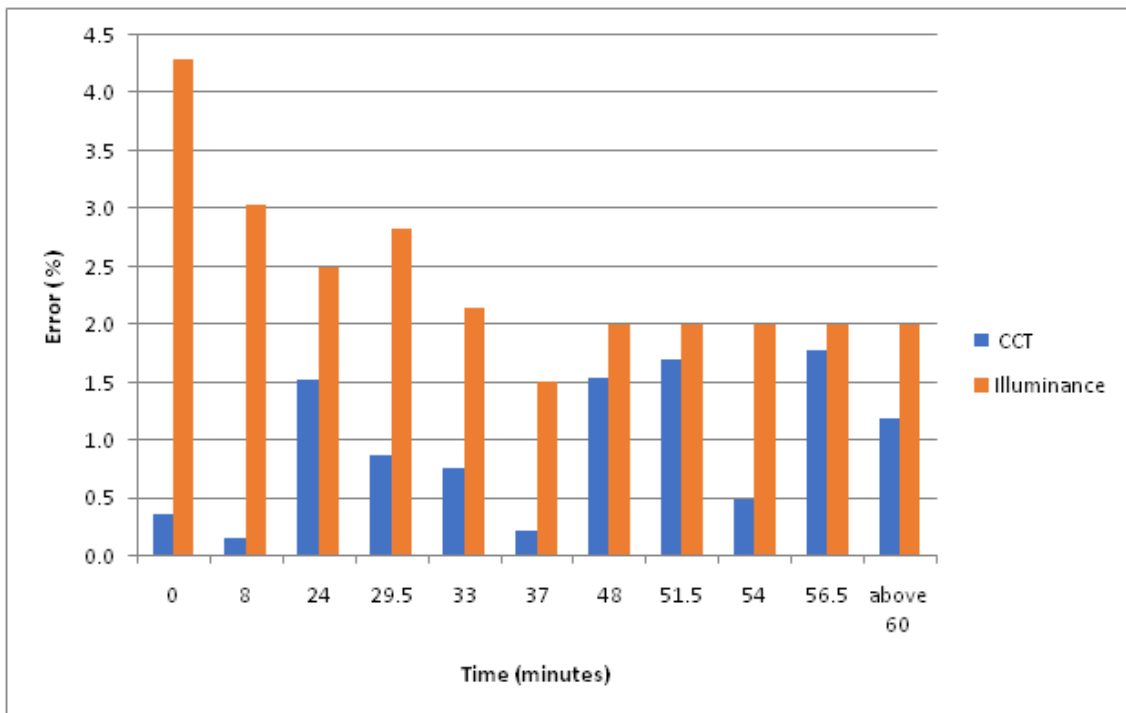


**Fig. 7.15:** Percentage error in CCT and illuminance in AUTO mode

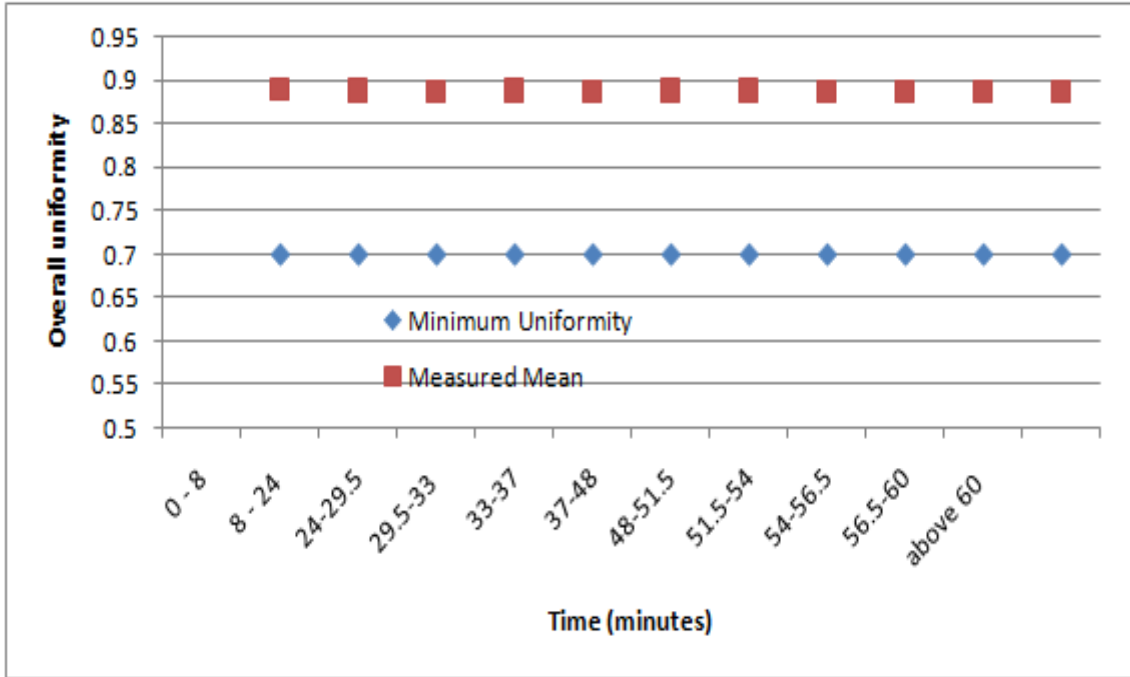


**Fig. 7.16:** Minimum vs. mean calculated uniformity in AUTO mode

From the above experimental results throughout the ten test runs of the developed controller in AUTO mode, following observations are made:

- a) absolute errors of measured CCT values during the 10 different runs remain within the maximum allowable limit of 145K for WW LED (2700K) and 355K for CW LED (5600K) prescribed by CIE Technical Report 158 [207]
- b) percentage errors of CCT and illuminance with respect to desired values were found to be in the range of 0.2%-1.8% in case of CCT and 1.5%-4.3% in case of illuminance.
- c) mean of the calculated values for overall uniformity is 0.89.

### **Power failure scenario**

The developed controller is also experimentally tested for power failure and the subsequent restoration scenario. In the test room, a real-time power failure and subsequent restoration were created during

automatic operation and the results obtained are shown in **Fig. 7.17**. From **Fig. 7.17**, it is observed that there were two power failures at 7 and 54 minutes. The power was restored at 15 minutes and 65 minutes respectively. During power failure, the measured illuminance is around 2lx. However, when the power is restored, the measured illuminance values are 273lx and 202lx (required values are 264lx and 202lx) at 15 minutes and 65 minutes respectively. This feature prevents resetting of the controller after every power failure.

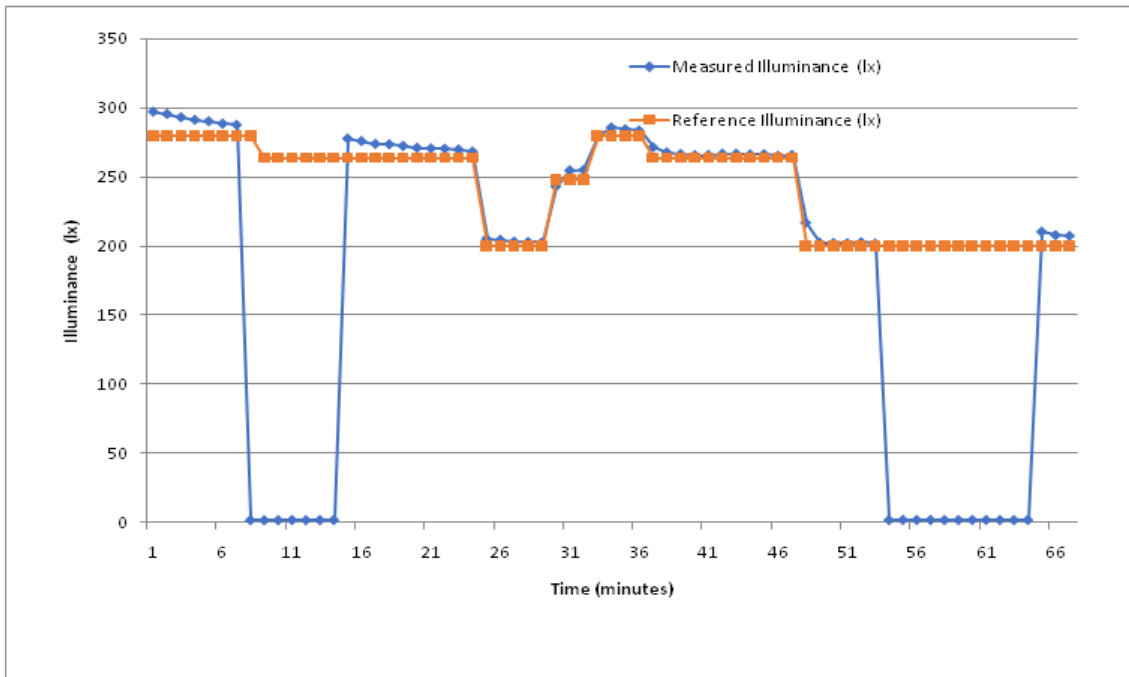


**Fig. 7.17:** Illuminance measurement during power failure and subsequent restoration

### Manual operation

The experimental testing of manual mode operation of the developed controller is carried out in three steps. In the first step, the CCT is varied from 2700K to 5600K keeping the illuminance value constant at 150lx, 200lx, 250lx and 300lx. The obtained results are shown in **Fig. 7.18**. In the second step, the illuminance is varied from 250lx to 20lx keeping the CCT value constant at 3500K, 4200K and 4900K.



The obtained results are shown in **Fig. 7.19**.

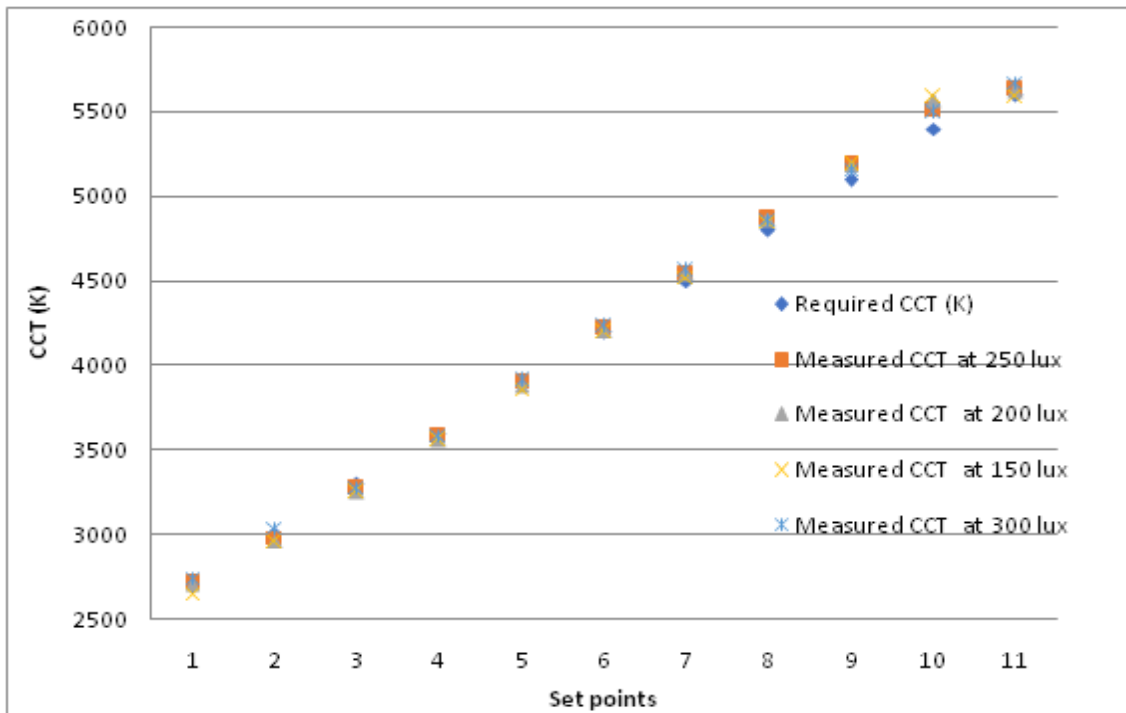


**Fig. 7.18:** Variation of CCT at different constant illuminance values

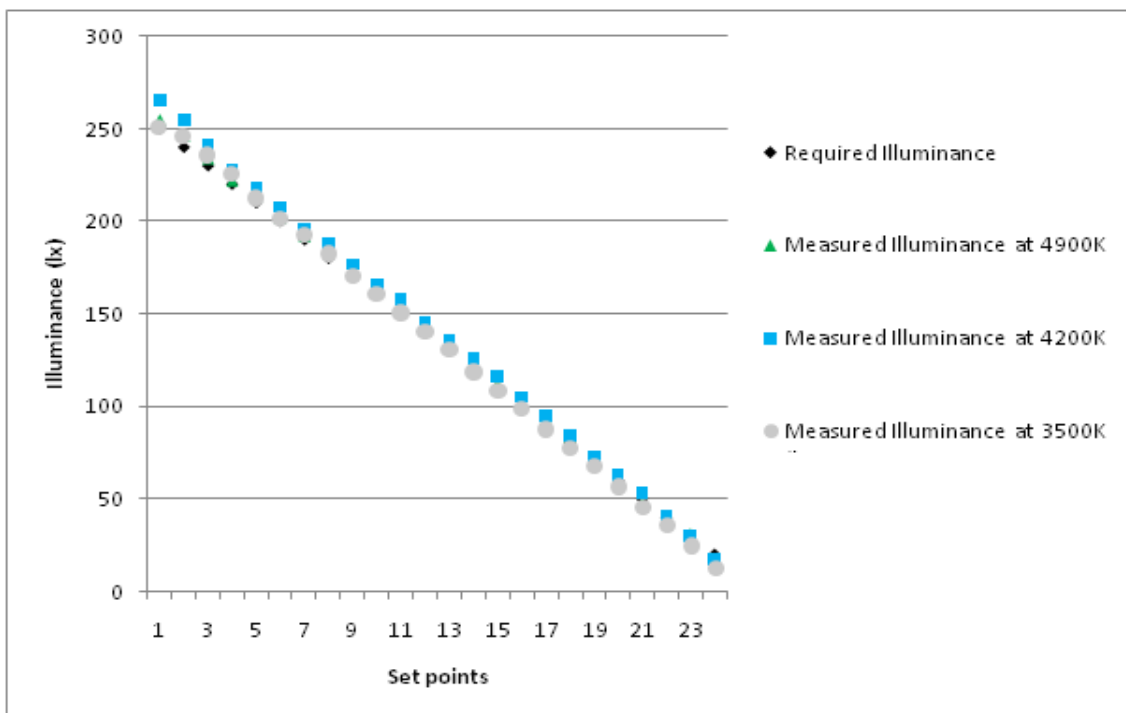


**Fig. 7.19:** Variation of illuminance at different constant CCT values

In the third step, both the CCT and illuminance are varied. 14 sets of illuminance and CCT values are assumed and set manually according to **Table 7.3**. The comparison between set and measured values is shown in **Fig. 7.20** and the percentage error in measured values of CCT and illuminance is shown in **Fig. 7.21**. The overall uniformity on the working plane for the manual set test points is shown in **Fig. 7.22**.

**Table 7.3:** Set points for MANUAL mode testing

Set point	1	2	3	4	5	6	7	8	9	10	11	12	13	14
CCT (K)	2700	2850	3070	3240	3550	3720	3980	4320	4160	5220	4730	5010	4540	5600
Illuminance (lx)	150	160	180	190	170	250	300	270	230	260	210	220	290	240

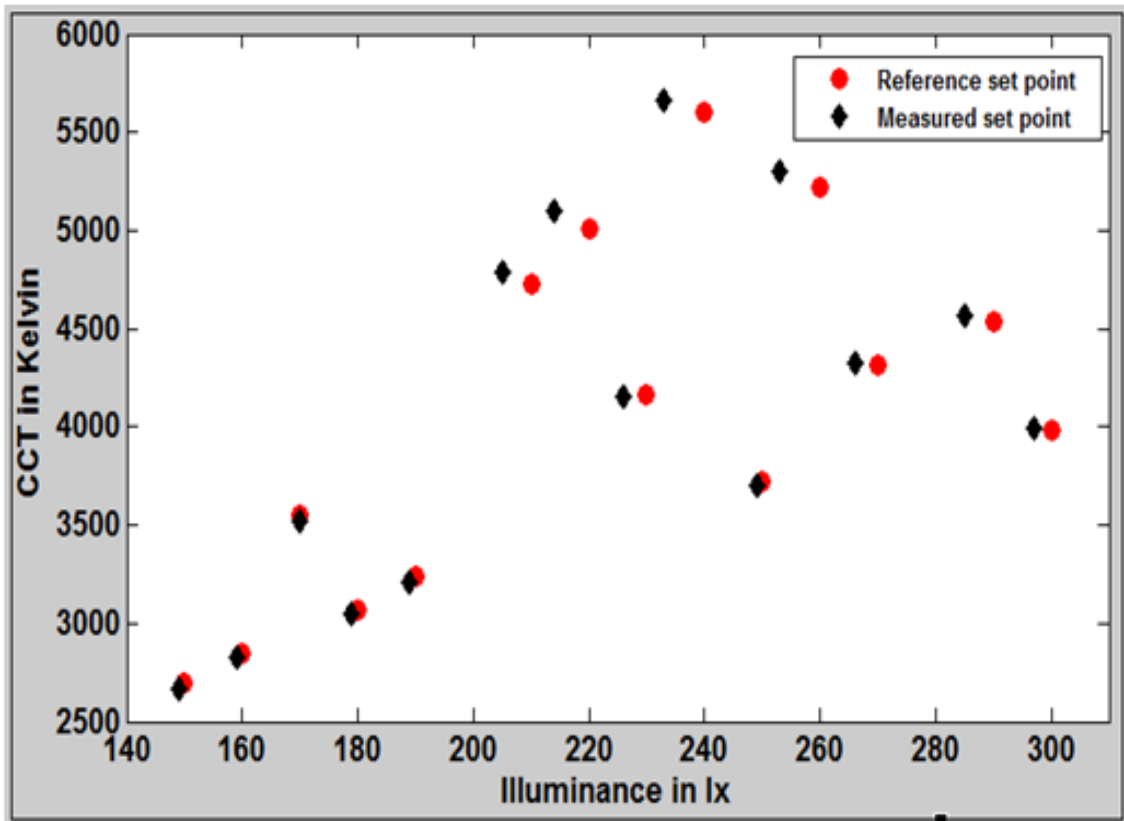


**Fig. 7.20:** Reference vs. measured set points in MANUAL mode

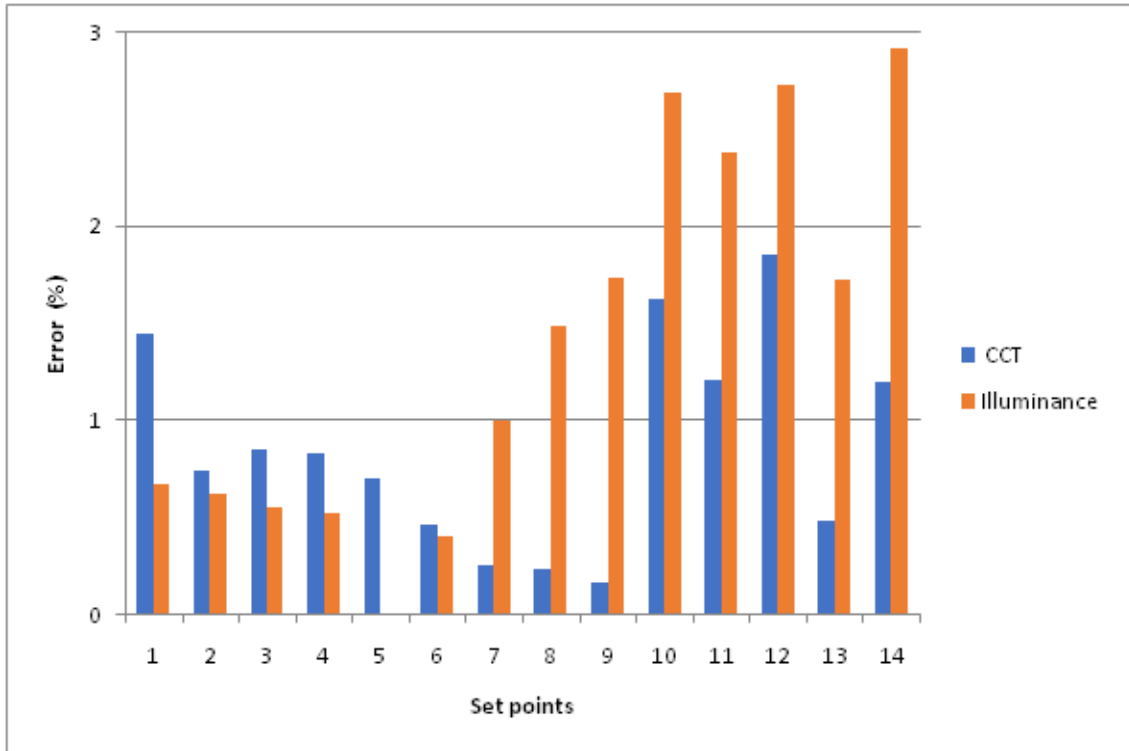


**Fig. 7.21:** Percentage error in CCT and illuminance in MANUAL mode

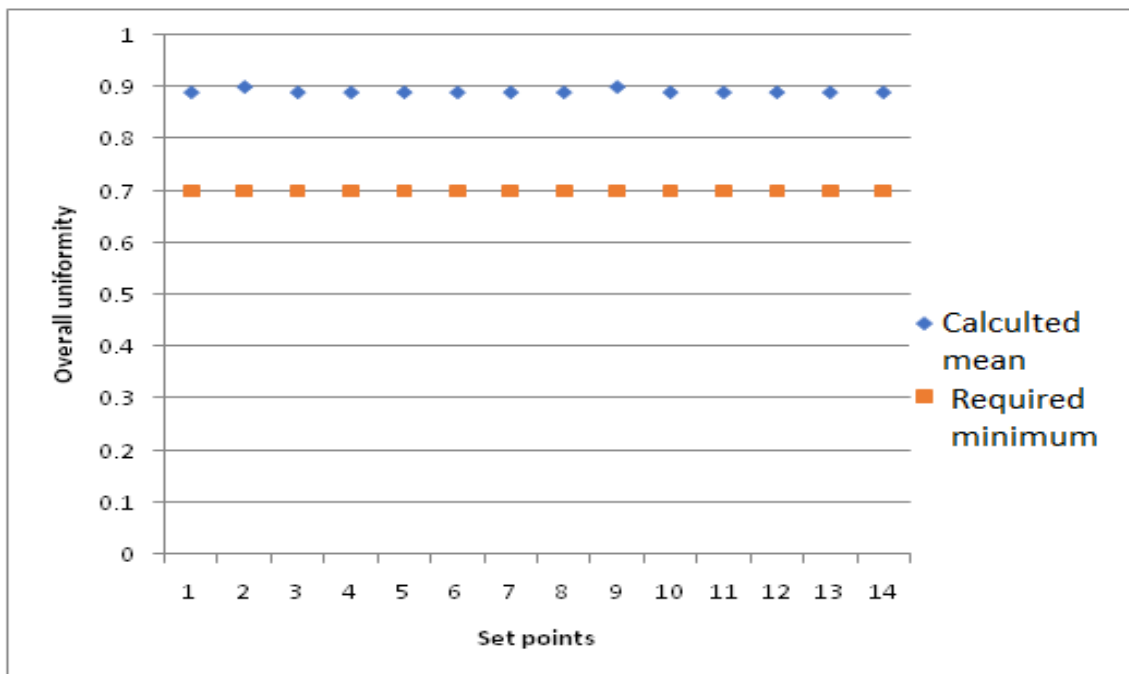


**Fig. 7.22:** Minimum vs. mean calculated uniformity in MANUAL mode

From the above obtained results for MANUAL mode operation, following observations are made:

- a) measured illuminance values do not vary more than 3%
- b) measured CCT values do not vary more than 2% and remain within the maximum allowable limit of 5% for WW LED (2700K) and 6% for CW LED (5600K) prescribed by CIE Technical Report 158 [207]
- c) mean calculated value for overall uniformity is 0.89 which is higher than the minimum required value of 0.7.

## 7.6 Chapter summary

A wireless light controller for spectrally tunable-white LED luminaires operated via a mobile app is developed and tested in real time. Compared to previously developed controllers, the present light controller is updated to manually as well as automatically control multiple luminaires and provide unhindered operation during wireless communication malfunction and power failures with subsequent restoration scenarios. To test the developed controller in real time multiple tunable-white LED based indoor lighting system is installed in a test room, which provides CCT in the range of 2700K-5600K and illuminance in the range of 20 lx-300 lx. The test results for AUTO mode show percentage variation of 0.2%-1.8% in case of CCT and 1.5%-4.3% in case of illuminance. The operation of the light controller also remained unaffected by communication failures and power outages. For the MANUAL mode, the percentage variation of CCT and illuminance is less than 2% and 3% respectively. The above results justify the satisfactory operation and performance of the developed light controller in real time.

## **Publications**

The publications related to this work are as follows:

### **Journal Publications: 1**

**1. Vishwanath Gupta**, Purnima Mandal, Biswarup Basak, & Biswanath Roy. **2023**. A Real-time Wireless Light Controller for Tunable-White LED based Indoor Lighting System. **LEUKOS**. (manuscript communicated on 27th July, 2023)



## 8 Overall conclusions

In the present work, efforts have been made to upgrade the design and improve the performance of prevalent LED luminaire and light controller technologies. The problem statement of the present work has been formulated after conducting a thorough review of the available literature in the field of study and the objective is achieved through the methodical execution of the prescribed procedural steps.

In addition to the study of the technical literature available on LED lighting technologies, commercially available LED luminaires were also studied and tested. The evaluation of electrical and photometric performance of three different commercially available indoor pc-WLED luminaires on AC and DC supply, along with the verification of their compliance with relevant Indian and International standards, is carried out through laboratory experimentation and discussed in **Chapter 3**. The results of laboratory testing showed that the electrical and photometric performance of the LED luminaires depend on the topology of the LED driver circuit and the arrangement of LED chips in the lamp module.

The main objective of the present work is achieved first through the design and performance analysis of a smart fault-adaptive dimmable LED driver and then through the development and performance evaluation of daylight-responsive wireless light controllers.

The concept, design and electrical performance evaluation of a smart fault-adaptive LED luminaire has been introduced in **Chapter 4**. The designed LED luminaire can operate LED modules of unknown output power in the range of 18W-72W with optimised light output under dimming and faulty conditions, thereby ensuring unhindered continuous operation of the lighting system. The LED luminaire model has been simulated and tested on the Matlab-Simulink

platform. From the results obtained through simulation of the LED luminaire at different dimming levels and during fault occurrence, it has been observed that the designed LED driver circuit provides the required voltage and current to connected LED lamp modules on  $90V_{rms}$ - $265V_{rms}$  AC supply. The electrical performance of the LED driver circuit in the output power range of 18W-72W, the input supply range of  $90V_{rms}$  to  $265V_{rms}$  and for dimming range of 100% to 30% and also during the occurrence of a fault is satisfactory and in compliance with IEC-61000-3-2:2014 and IEEE Standard P1789. Input power factor as high as 0.999, %THD as low as 3.33%, efficiency as high as 0.94 and %ripple as low as 4.6% are obtained for the simulated LED driver. The stability analysis of the designed LED luminaire is discussed in **Chapter 5** with the help of phase margin test by formulating the mathematical model of the designed LED luminaire. The phase margin of the LED luminaire system has been found to be more than the required phase margin of 76 degrees in the entire output power range of 18W-72W on Universal AC supply, which confirmed the stable operation of the modelled LED luminaire. The LED luminaire is most stable for  $N_s/N_p$  ratio  $\geq 1$ . The settling time is minimum for  $N_s/N_p$  ratio of 0.2 and 4.5. But, from the LED luminaire electrical performance analysis, it is observed that the electrical performance is better for higher  $N_s/N_p$  ratios than lower  $N_s/N_p$  ratios. Therefore, to obtain optimised performance from the modelled LED luminaire on universal AC supply in the output power range of 18W-72W, the  $N_s/N_p$  ratio has to be greater than 1 and around 3-4.

The second part of the objective has been accomplished through development and performance evaluation of three numbers of daylight-responsive wireless light controllers.

A FIS based light controller has been presented in **Section 6.1** of **Chapter 6**. The light controller is implemented on Arduino Mega



micro-controller using C++ programming language instead of simulation in Matlab environment to make it cost effective by obliterating the need of dedicated computer and additional interfacing accessories for future hardware prototype development. The designed FIS predicts the amount of light output required from artificial lamps and the position of window roller blinds to maintain required illuminance and overall uniformity on the working plane of a model test office room in presence of daylight for all times of the day through out the year. The simulated light controller is tested offline by modelling a test office room using DIALux 4.13 lighting design software under the three available sky-types. The obtained test results at different times of the day for all the three sky-types showed that the illuminance levels on the working plane obtained after control are less than the levels before application of control and do not fall below the minimum required level of 300lx. The overall uniformity also becomes better after the application of control for each of the test case.

A fault-monitoring and motion-sensing light controller for an indoor LED luminaire has been developed and discussed in **Section 6.2** of **Chapter 6**. The light controller provides wireless control of the light output based on ambient light level and motion sensing and monitors the occurrence of faults in the LED driver and the LED module separately. A hardware prototype of the designed controller is fabricated to test it in the laboratory. From the obtained results, it is observed that the developed controller successfully detected the place of the origin of fault (LED driver or LED module) in the luminaire and satisfactorily controlled the light output from the LED luminaire based on ambient light level and human presence.

A wireless light controller for spectral tuning of tunable-white LED luminaires has been introduced in **Chapter 7**. A dedicated mobile app has also been developed for wireless operation of the light con-

troller. The developed controller is tested in real time by making them operate multiple tunable white LED based indoor lighting system installed in a test room. The tunable-white luminaires based lighting system provides CCT in the range of 2700K-5600K and illuminance in the range of 20lx-300lx on the working plane of the test room. The developed light controller has been updated to manually as well as automatically control multiple luminaires and provide unhindered operation during wireless communication malfunctions and power failures with subsequent restoration scenarios. The test results for AUTO mode show percentage variation of 0.2%-1.8% in case of CCT and 1.5%-4.3% in case of illuminance. The operation of the light controller also remained unaffected by communication failures and power outages. For the MANUAL mode, the percentage variation of CCT and illuminance is less than 2% and 3% respectively. The above results justify the satisfactory operation and performance of the developed light controller in real time.

## Prospective applications of the present study

1. The simulated smart fault-adaptive dimmable LED luminaire can be used in road lighting or industrial lighting applications requiring uninterrupted and unhindered operation and instant replacement of a faulty part is not possible.
2. The FIS based light controller is applicable to daylight integrated artificial lighting in indoor spaces to save electrical energy used for lighting.
3. The fault-monitoring and motion-sensing wireless light controller is applicable to lighting applications for art-gallery, museum and commercial offices.
4. The light controller for tunable-white LED luminaires has flexible application. It can be used as a cost-effective and energy-saving alternative compared to artificial lighting without control for indoor spaces where abundant daylight is available. Also, the developed light controller is applicable in indoor lighting for spaces where available daylight is limited or even absent as it can spectrally tune the installed luminaires to vary the CCT on the working plane and provide biological and psychological benefits to the end-users.



## **Future scope**

The present study, in the future, can be extended to:

1. Develop a hardware prototype of the designed smart fault-adaptive dimmable LED driver.
2. Test the FIS based light controller in real time scenario.
3. Make the dynamic light controller closed-loop so that the CCT of light inside an indoor space closely follows the CCT of outside daylight.



## **Annexures**

In this section, some of the data obtained from experimentation and simulation during the course of the work, but not presented in the corresponding chapters, are presented. The calibration of the chromameter used for CCT measurement and computation of MacAdam ellipse step size are also discussed in this section.

## Annexure I

### Additional data of simulated LED driver discussed in *Chapter 4*

The simulated LED driver discussed in detail in *Chapter 4* is also made to operate 27W (3\*3) and 48W(4\*4) LED modules having  $N_S/N_P$  ratio = 1. However, the electrical parameters obtained through simulation do not meet the recommended standards as given in **Table I**.

**Table I:** Obtained data of simulated LED driver operating LED modules having  $N_S/N_P$  ratio = 1

Module Rating (W)	Input Voltage (V)	Current ripple (%)	Input pf	Efficiency (%)	THD (%)
48	265	23.55	0.87	0.85	38.23
	230		0.89	0.87	35.17
	180		0.92	0.89	30.29
	130		0.94	0.90	24.67
	90		0.96	0.91	19.85
27	265	23.33	0.87	0.80	35.50
	230		0.89	0.82	33.13
	180		0.92	0.85	28.53
	130		0.95	0.87	23.10
	90		0.97	0.89	18.00



## Annexure II

### Calibration of chromameter

The Konica Minolta make chromameter CL-200A used for measuring the CCT in *Chapter 7* is first calibrated inside the same test room. The light output from the CW and WW arrays of the tunable white LED luminaires is set for 5 ratios of (CW:WW), viz. 100:0, 75:25, 50:50, 25:75 and 0:100. First, the measurement is done with increasing light output from CW and decreasing light output from WW arrays. The measurement is repeated for the same set of ratios, but this time with decreasing light output from CW arrays and increasing light output from WW arrays. The obtained result is shown in **Fig. I**. It is observed from **Fig. I** that the chromameter under calibration gave almost the same measurement.

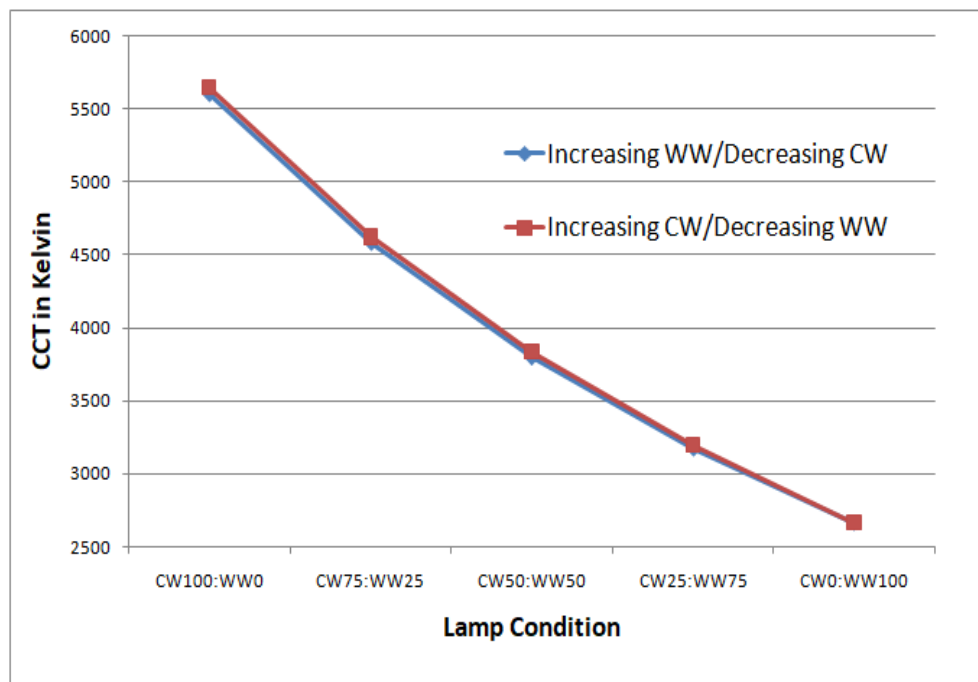


Fig. I: Calibration of chromameter

### Annexure III

#### Efficiency and input power factor calculation of test LED luminaires on AC supply

Efficiency of the test LED luminaires on AC supply is calculated from the measured electrical parameters as shown in **Table II**.

The efficiency is calculated by the following formula:

$$Efficiency = \frac{Measured\ Output\ Power(W)}{Measured\ Input\ Power(W)}$$

The input power factor was calculated by the following formula:

$$Input\ power\ factor = \frac{Measured\ Input\ power(W)}{Input\ voltage(V) \cdot Input\ current(A)}$$

Input pf = Measured Input power (W)/(Input voltage (V)\*Input current (A))

**Table II:** Electrical parameters of the test LED luminaires

Test luminaires	Input voltage (V)	Input current (mA)	Input power factor	Input power (W)	Output voltage (V)	Output current (mA)	Output power (W)	Efficiency
System1	240	95	0.42	9.5	27.6	275.9	7.6	0.80
	230	97	0.42	9.4	27.6	274.7	7.6	0.81
	210	101	0.44	9.3	27.6	272.4	7.5	0.81
	190	107	0.45	9.1	27.6	270.0	7.4	0.82
System2	240	61	0.88	12.9	39.9	246.5	9.8	0.77
	230	64	0.88	12.9	40.0	246.2	9.8	0.76
	210	70	0.89	12.9	39.9	246.6	9.8	0.76
	190	77	0.89	13	39.9	246.6	9.8	0.76
System2	240	54	0.95	12.2	36.2	273.9	9.7	0.80
	230	55	0.95	12.1	36.1	272.7	9.7	0.80
	210	59	0.96	11.9	36.1	270.6	9.6	0.81
	190	64	0.97	11.7	36.1	268.8	9.5	0.82

## Annexure IV

### Colour shift calculation in terms of MacAdam ellipse

For consistency with MacAdam ellipses, the term 'n-step u'v' circle' is defined as a circle in the (u', v') diagram with a radius of n times 0,0011. For a centre point, the n-step u'v' circle corresponding to a n-step MacAdam ellipse is expressed by the following equation:

$$(u - u'_c)^2 + (v - v'_c)^2 = (0.0011 * n)^2$$

There are small differences between the u'v' circles and MacAdam ellipses observed in **Fig. II** but they are considered insignificant in practical applications, especially when considering the experimental uncertainty of MacAdam ellipses derived 70 years ago with only one experimental subject and with only one illuminant for the surrounding field.

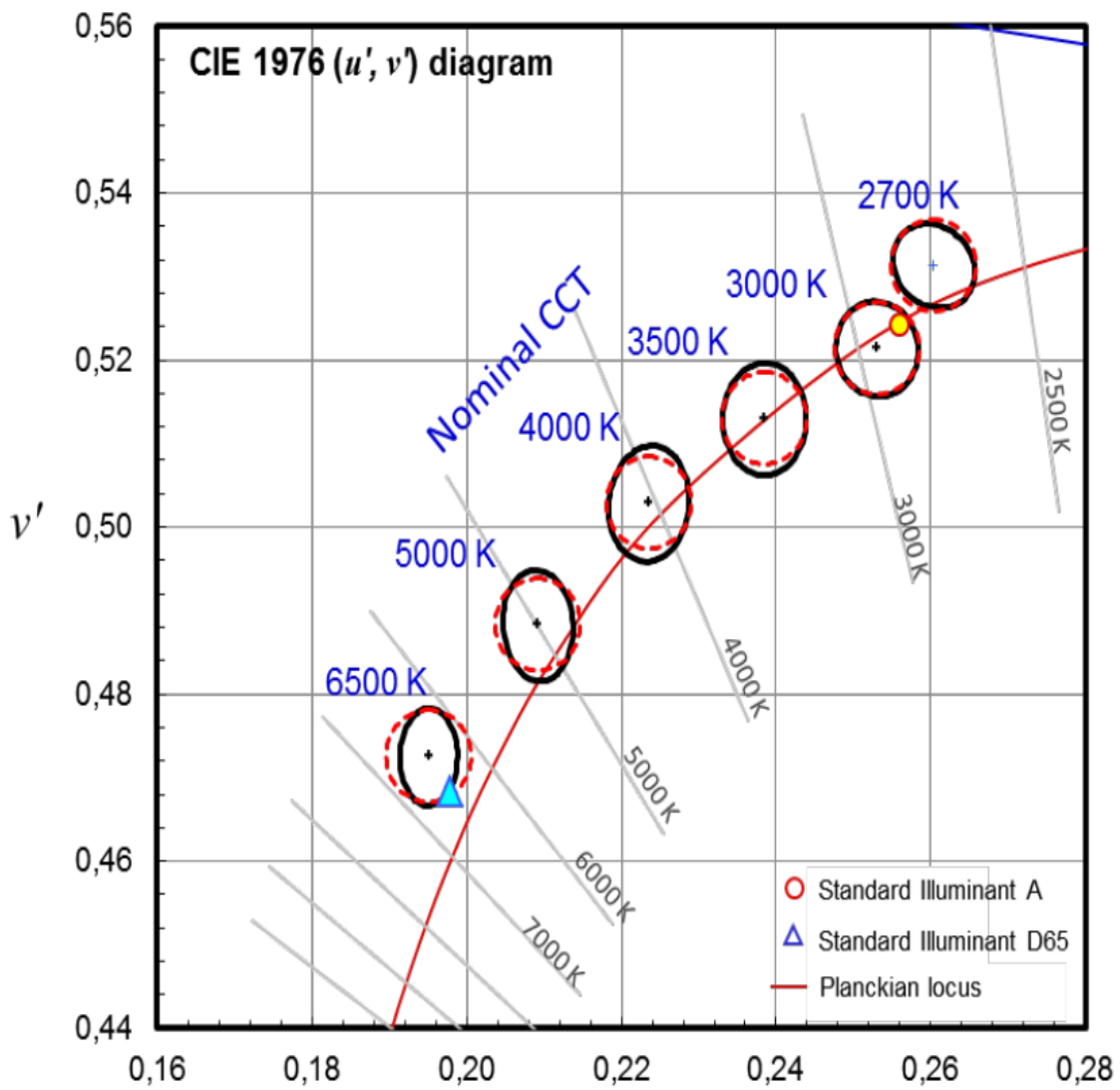


**Fig. II:** Five-step MacAdam ellipses in IEC 60081 (IEC, 1997) and circles (radius 0,0055) in the CIE 1976  $(u', v')$  chromaticity diagram

## Annexure V

### Recommended Standard values of performance parameters of LED luminaire

The recommended standard values of performance parameters of LED luminaire are given in **Table III**.

**Table III:** Recommended Standard parameter values

Parameter	Value	Standard
Input power factor	0.9	IEC 61000-3-2
THD	30%	IEC 61000-3-2
Current ripple	20%	IEEE PAR 1789
Flicker	30%	IEEE PAR 1789
Chromaticity difference in terms of $u'-v'$	0.0013	CIE TN 001:2014



## Bibliography

- [1] International Commission on Illumination, “Ilv: International lighting vocabulary, 2nd edition: Cie s 017/e:2020,” 2020, accessed on 20 December, 2022.
- [2] US Department of Energy, “Energy saver,” 2022, <https://www.energy.gov/energysaver/ledlighting>. Accessed on 02 September, 2022.
- [3] Y. Hiebert, “Light emitting diodes: A brief history,” October 2022, <https://www.ednasia.com/light-emitting-diodes-a-brief-history/>. Accessed on 28 December, 2022.
- [4] J. A. Hoerni, “Method of manufacturing semiconductor devices,” March 1962, uS patent number 3025589. Accessed on 28 December, 2022.
- [5] R. S. A. of Sciences, “The nobel prize in physics 2014,” 2014, press Release, 7th October, 2014. Accessed on 28 December, 2022.
- [6] N. Morris, “Led there be light, nick morris predicts a bright future for leds,” June 2006, [electrooptics.com](http://electrooptics.com). Accessed on 28 December, 2022.
- [7] R. Haitz, “Haitz’s law,” *Nature Photonics*, vol. 1, no. 1, p. 23, 2007.
- [8] J. Hasan and S. S. Ang, “A high-efficiency digitally controlled rgb driver for led pixels,” *IEEE Transactions on Industry Applications*, vol. 47, no. 6, pp. 2422–2429, 2011.
- [9] Y. Hu and M. M. Jovanovic, “A novel led driver with adaptive drive voltage,” in *2008 Twenty-Third Annual IEEE Applied*

*Power Electronics Conference and Exposition*, 2008, pp. 565–571.

- [10] Y. Q. Hu and M. M. Jovanovic, “Led driver with self-adaptive drive voltage,” *IEEE Transactions on Power Electronics*, vol. 23, no. 6, pp. 3116–3125, 2008.
- [11] W. Chen and S. Hui, “A dimmable light-emitting diode (led) driver with mag-amp postregulators for multistring applications,” *Power Electronics, IEEE Transactions on*, vol. 26, pp. 1714 – 1722, 07 2011.
- [12] W. Huang, Y. Yang, and M. R. Luo, “Discomfort glare caused by white leds having different spectral power distributions,” *Lighting Research & Technology*, vol. 50, no. 6, pp. 921–936, 2018.
- [13] W. Tang, J. G. Liu, and C. Shen, “Blue light hazard optimization for high quality white leds,” *IEEE Photonics Journal*, vol. 10, no. 5, pp. 1–10, 2018.
- [14] T.-J. Oh, A. Cho, S.-L. Ki, and I.-C. Hwang, “A low-power and low-cost digitally-controlled boost led driver ic for backlights,” in *2012 IEEE Asian Solid State Circuits Conference (A-SSCC)*, 2012, pp. 237–240.
- [15] C. Deekshitha and L. Shenoy, “Design and simulation of synchronous buck converter for led application,” 05 2017, pp. 142–146.
- [16] J. de Britto, A. E. Demian, L. C. de Freitas, V. J. Farias, E. A. A. Coelho, and J. B. Vieira, “A proposal of led lamp driver for universal input using cuk converter,” in *2008 IEEE Power Electronics Specialists Conference*, 2008, pp. 2640–2644.



- [17] L. Mohamed, N. F. Abdul Hamid, Z. M. Isa, N. Saudin, N. H. Ramly, and N. B. Ahamad, “Cuk converter as a led lamp driver,” in *2012 IEEE International Conference on Power and Energy (PECon)*, 2012, pp. 262–267.
- [18] C.-J. Huang, Y.-C. Chuang, and Y.-L. Ke, “Design of closed-loop buck-boost converter for led driver circuit,” in *2011 IEEE Industrial and Commercial Power Systems Technical Conference*, 2011, pp. 1–6.
- [19] J. Kang, J. Han, and S.-K. Han, “High-efficiency boundary conduction mode tapped-inductor boost led driver,” in *2014 IEEE International Conference on Industrial Technology (ICIT)*, 2014, pp. 261–266.
- [20] M. Rico-Secades, J. Garcia, J. Cardesin, and A. Calleja, “Using tapped-inductor converters as led drivers,” in *Conference Record of the 2006 IEEE Industry Applications Conference Forty-First IAS Annual Meeting*, 2006.
- [21] T.-L. Chern, L.-H. Liu, S.-H. Yeh, Y.-L. Chern, and D.-M. Tsay, “Single-stage flyback converter for led driver with inductor voltage detection power factor correction,” in *2010 5th IEEE Conference on Industrial Electronics and Applications*, 2010, pp. 2082–2087.
- [22] Z. Li, M. Guo, X. Jin, R. Sun, X. Yue, and H. Wang, “A single-stage flyback led driver based on energy distribution without electrolytic capacitor,” in *2019 IEEE PES Asia-Pacific Power and Energy Engineering Conference (APPEEC)*, 2019, pp. 1–5.
- [23] H. Dong, X. Xie, H. Chen, and Z. Jin, “A high power factor led driver based on improved forward-flyback without electrolytic

capacitor,” in *2017 IEEE Applied Power Electronics Conference and Exposition (APEC)*, 2017, pp. 2404–2411.

- [24] M. S. Nazarudin, M. A. A. Rahim, Z. Aspar, A. Yahya, and T. R. Selvaduray, “A flyback smps led driver for lighting application,” in *2015 10th Asian Control Conference (ASCC)*, 2015, pp. 1–5.
- [25] V. Gupta, K. Ghosh, B. Basak, and B. Roy, “Universal control algorithm for automatic current regulated led driver,” *International Journal of Power Electronics*, vol. 12, no. 2, pp. 169–190, 2020.
- [26] S. Lee and H. Do, “A single-switch ac–dc led driver based on a boost-flyback pfc converter with lossless snubber,” *IEEE Transactions on Power Electronics*, vol. 32, no. 2, pp. 1375–1384, 2017.
- [27] A. Jha and B. Singh, “Sepic pfc converter fed led driver,” in *2016 IEEE 1st International Conference on Power Electronics, Intelligent Control and Energy Systems (ICPEICES)*, 2016, pp. 1–6.
- [28] Y. Wang, N. Qi, Y. Guan, C. Cecati, and D. Xu, “A single-stage led driver based on sepic and llc circuits,” *IEEE Transactions on Industrial Electronics*, vol. 64, no. 7, pp. 5766–5776, 2017.
- [29] M. Ali, M. Orabi, M. E. Ahmed, and A. El-Aroudi, “A single stage sepic pfc converter for led street lighting applications,” in *2010 IEEE International Conference on Power and Energy*, 2010, pp. 501–506.
- [30] Y.-W. Bai and Y.-T. Ku, “Automatic room light intensity detection and control using a microprocessor and light sensors,” *IEEE Transactions on Consumer Electronics*, vol. 54, no. 3, pp. 1173–1176, 2008.

- [31] A. Pandharipande, M. Rossi, D. Caicedo, L. Schenato, and A. Cenedese, “Centralized lighting control with luminaire-based occupancy and light sensing,” in *2015 IEEE 13th International Conference on Industrial Informatics (INDIN)*, 2015, pp. 31–36.
- [32] D. Caicedo and A. Pandharipande, “Daylight estimation in a faulty light sensor system for lighting control,” in *Proceedings of the 16th International Conference on Information Fusion*, 2013, pp. 617–622.
- [33] K.-T. Mok, “Modeling and design of current driving circuits for light-emitting diodes,” Ph.D. dissertation, 01 2013.
- [34] F. Bento and A. J. M. Cardoso, “Sensorless current control of large-scale led lighting systems based on simo led drivers,” in *IECON 2019 - 45th Annual Conference of the IEEE Industrial Electronics Society*, vol. 1, 2019, pp. 4280–4285.
- [35] A. M. Patel and M. Ferdowsi, “Advanced current sensing techniques for power electronic converters,” in *2007 IEEE Vehicle Power and Propulsion Conference*, 2007, pp. 524–530.
- [36] J. Chen, T. Sato, K. Yano, H. Shiroyama, M. Owa, and M. Yamada, “An average input current sensing method of llc resonant converters for automatic burst mode control,” *IEEE Transactions on Power Electronics*, vol. 32, no. 4, pp. 3263–3272, 2017.
- [37] C.-N. Wu and Y.-M. Chen, “Inductor current measurement strategy for high-precision output current control,” *IEEE Journal of Emerging and Selected Topics in Power Electronics*, vol. 5, no. 3, pp. 1263–1271, 2017.
- [38] R. Chaki, M. Ghosh, G. K. Panda, P. K. Saha, A. Dey, and A. Banerjee, “An improved dimmable led driving scheme

with low flicker metrics for low voltage application,” *Electric Power Systems Research*, vol. 187, p. 106433, 2020. [Online]. Available: <https://www.sciencedirect.com/science/article/pii/S0378779620302388>

- [39] P. Chen, Y.-H. Chen, J. C. J. S. Marquez, R.-T. Wang, J.-J. Chen, and Y.-S. Hwang, “Low flicker dimmable multichannel led driver with matrix-style dpwm and precise current matching,” *IEEE Transactions on Very Large Scale Integration (VLSI) Systems*, vol. 28, no. 11, pp. 2233–2242, 2020.
- [40] M. K. Barwar, L. K. Sahu, and P. Bhatnagar, “Reliability analysis of flicker-free led driver based on five-level rectifier,” *Optik*, vol. 268, p. 169762, 2022. [Online]. Available: <https://www.sciencedirect.com/science/article/pii/S0030402622010373>
- [41] S. J. Yun, Y. K. Yun, and Y. S. Kim, “A low flicker triac dimmable direct ac led driver for always-on led arrays,” *IEEE Access*, vol. 8, pp. 198 925–198 934, 2020.
- [42] Y. Gao, L. Li, K.-H. Chong, and P. K. T. Mok, “A hybrid led driver with improved efficiency,” *IEEE Journal of Solid-State Circuits*, vol. 55, no. 8, pp. 2129–2139, 2020.
- [43] G. Z. Abdelmessih, J. M. Alonso, N. d. S. Spode, and M. A. D. Costa, “High-efficient electrolytic-capacitor-less offline led driver with reduced power processing,” *IEEE Transactions on Power Electronics*, vol. 37, no. 2, pp. 1804–1815, 2022.
- [44] D. Chatterjee, “Implementation of predictive control algorithm for high power factor high efficiency soft-switched ac-dc led driver using low cost 8-bit digital controller,” in *2021 1st Inter-*

*national Conference on Power Electronics and Energy (ICPEE)*, 2021, pp. 1–6.

- [45] T. Liu, X. Liu, M. He, S. Zhou, X. Meng, and Q. Zhou, “Flicker-free resonant led driver with high power factor and passive current balancing,” *IEEE Access*, vol. 9, pp. 6008–6017, 2021.
- [46] C. Ye, H. W. Chan, D. Lan, P. Das, and S. K. Sahoo, “Efficiency improvement of multichannel led driver with selective dimming,” *IEEE Transactions on Power Electronics*, vol. 35, no. 6, pp. 6280–6291, 2020.
- [47] S.-C. Hsia and J.-J. Ciou, “Single chip design for detection and recovery of series led open/short fault tolerance circuit,” *IET Power Electronics*, vol. 11, no. 15, pp. 2434–2439, 2018.
- [48] K. Laadjal, F. Bento, and A. J. M. Cardoso, “On-line diagnostics of electrolytic capacitors in fault-tolerant led lighting systems,” *Electronics*, vol. 11, no. 9, 2022.
- [49] F. Bento and A. J. Marques Cardoso, “Fault-tolerant led lighting systems featuring minimal loss of luminous flux,” *IEEE Transactions on Industry Applications*, vol. 56, no. 4, pp. 4309–4318, 2020.
- [50] B. Sun, X. Jiang, K.-C. Yung, J. Fan, and M. G. Pecht, “A review of prognostic techniques for high-power white leds,” *IEEE Transactions on Power Electronics*, vol. 32, no. 8, pp. 6338–6362, 2017.
- [51] F. Bento and A. J. Marques Cardoso, “Highly accurate software-based current compensating strategy for fault-tolerant large-scale led lighting systems,” in *2021 IEEE 12th Energy Conversion Congress Exposition - Asia (ECCE-Asia)*, 2021, pp. 2334–2338.

- [52] P. K. Maiti and B. Roy, “Evaluation of a light controller for a led-based dynamic light source,” *Lighting Research & Technology*, vol. 50, no. 4, pp. 571–582, 2018.
- [53] P. K. Maiti, A. D. Singh, and B. Roy, “Design and development of daylight responsive rf light controller,” in *2017 IEEE Calcutta Conference (CALCON)*, 2017, pp. 309–313.
- [54] P. Maiti and B. Roy, “Evaluation of a daylight-responsive, iterative, closed-loop light control scheme,” *Lighting Research & Technology*, vol. 52, no. 2, pp. 257–273, 2020.
- [55] M. J. Murdoch, “Dynamic color control in multiprimary tunable led lighting systems,” *Journal of the Society for Information Display*, vol. 27, no. 9, pp. 570–580, 2019.
- [56] R. Malik, K. Ray, and S. Mazumdar, “A low-cost, wide-range, cct-tunable, variable-illuminance led lighting system,” *LEUKOS*, vol. 16, no. 2, pp. 157–176, 2020.
- [57] B. Das and S. Mazumdar, “Low cost, high color rendition, cct variable lighting system based on w-g-b led,” *Optik*, vol. 231, p. 166321, 2021. [Online]. Available: <https://www.sciencedirect.com/science/article/pii/S0030402621000607>
- [58] IESNA, “Iesna lighting handbook: References and applications,” 2000, 9th ed. New York (NY): Illuminating Engineering Society of North America.
- [59] T. Q. Khan, *LED Lighting: Technology and Perception*. Wiley, 2014.
- [60] Donald A. Neamen, *Semiconductor Physics and Devices*, 4th ed. McGraw Hill, 2012.

- [61] Crystal, “What are the different types of led chips?” 2022, <https://www.lepro.com/learning/led-chip/>. Accessed on 28 December, 2022.
- [62] S. Hui and Y. Qin, “A general photo-electro-thermal theory for light emitting diode (led) systems,” *Power Electronics, IEEE Transactions on*, vol. 24, pp. 1967 – 1976, 09 2009.
- [63] D. Gacio, J. Alonso, A. Calleja, J. García, and M. Rico-Secades, “A universal-input single-stage high-power-factor power supply for hb-leds based on integrated buck–flyback converter,” *IEEE Transactions on Industrial Electronics*, vol. 58, no. 2, pp. 589–599, 2011.
- [64] D. Park, Z. Liu, and H. Lee, “A 40 v 10 w 93%-efficiency current-accuracy-enhanced dimmable led driver with adaptive timing difference compensation for solid-state lighting applications,” *IEEE Journal of Solid-State Circuits*, vol. 49, no. 8, pp. 1848–1860, 2014.
- [65] B. Singh, A. Shrivastava, A. Chandra, and K. Al-Haddad, “A single stage optocoupler-less buck-boost pfc driver for led lamp at universal ac mains,” in *2013 IEEE Industry Applications Society Annual Meeting*, 2013, pp. 1–6.
- [66] J. Baek and S. Chae, “Single-stage buck-derived led driver with improved efficiency and power factor using current path control switches,” *IEEE Transactions on Industrial Electronics*, vol. 64, no. 10, pp. 7852–7861, 2017.
- [67] J. Kim, J. Moon, and G. Moon, “Analysis and design of a single-switch forward-flyback two-channel led driver with resonant-blocking capacitor,” *IEEE Transactions on Power Electronics*, vol. 31, no. 3, pp. 2314–2323, 2016.

- [68] Q. Luo, J. Huang, Q. He, K. Ma, and L. Zhou, “Analysis and design of a single-stage isolated ac–dc led driver with a voltage doubler rectifier,” *IEEE Transactions on Industrial Electronics*, vol. 64, no. 7, pp. 5807–5817, 2017.
- [69] B. Poorali and E. Adib, “Analysis of the integrated sepic-flyback converter as a single-stage single-switch power-factor-correction led driver,” *IEEE Transactions on Industrial Electronics*, vol. 63, no. 6, pp. 3562–3570, 2016.
- [70] Y. Wang, J. Huang, W. Wang, and D. Xu, “A single-stage single-switch led driver based on class-e converter,” *IEEE Transactions on Industry Applications*, vol. 52, no. 3, pp. 2618–2626, 2016.
- [71] C. Wong, K. Loo, Y. Lai, M. Chow, and C. Tse, “An alternative approach to led driver design based on high-voltage driving,” *IEEE Transactions on Power Electronics*, vol. 31, no. 3, pp. 2465–2475, 2016.
- [72] H.-J. Chiu, Y.-K. Lo, J.-T. Chen, S.-J. Cheng, C.-Y. Lin, and S.-C. Mou, “A high-efficiency dimmable led driver for low-power lighting applications,” *IEEE Transactions on Industrial Electronics*, vol. 57, no. 2, pp. 735–743, 2010.
- [73] S. Moon, G. Koo, and G. Moon, “Dimming-feedback control method for triac dimmable led drivers,” *IEEE Transactions on Industrial Electronics*, vol. 62, no. 2, pp. 960–965, 2015.
- [74] L. Lohaus, A. Rossius, S. Dietrich, R. Wunderlich, and S. Heinen, “A dimmable led driver with resistive dac feedback control for adaptive voltage regulation,” *IEEE Transactions on Industry Applications*, vol. 51, no. 4, pp. 3254–3262, 2015.
- [75] Brooke Sault, “Wiring leds correctly: Series parallel circuits explained!” 2021, <https://www.ledsupply.com/blog/wiring-leds->



correctly-series-parallel-circuits-explained/. Accessed on 20 December, 2022.

- [76] Y. Hassan, M. Orabi, M. Ismeil, and A. Alshreef, “Study the effect of series and parallel leds connections on the output current ripple for led driver of solar street lighting,” in *2017 Nineteenth International Middle East Power Systems Conference (MEPCON)*, 2017, pp. 1492–1499.
- [77] OSRAM, “Comparison of simple led circuits for low power leds,” 2020, <https://www.osram.com/appsn/AppNotes/Web/AppNotes.aspx?show=led>. Accessed on 15 September, 2022.
- [78] R. Pinto, M. Cosetin, T. Marchesan, M. da Silva, G. Denardin, J. Fraytag, A. Campos, and R. do Prado, “Design procedure for a compact lamp using high-intensity leds,” in *2009 35th Annual Conference of IEEE Industrial Electronics*, 2009, pp. 3506–3511.
- [79] M. Doshi and R. Zane, “Control of solid-state lamps using a multiphase pulsewidth modulation technique,” *IEEE Transactions on Power Electronics*, vol. 25, no. 7, pp. 1894–1904, 2010.
- [80] C.-Y. Hsieh, Y.-S. Wei, K.-H. Chen, and T.-C. Lin, “Efficient led driver with an adaptive reference tracking technique,” in *2009 16th IEEE International Conference on Electronics, Circuits and Systems - (ICECS 2009)*, 2009, pp. 291–294.
- [81] N. Ning, W. Chen, D. Yu, C. Feng, and C. B. Wang, “Self-adaptive load technology for multiple-string led drivers,” *Electronics Letters*, vol. 49, pp. 1170–1171, 2013.
- [82] S. Fu, M. Chen, X. Lee, and T. Yoshihara, “A high efficiency multi-channel led driver based on converter-free technique and load adaptive method,” in *2014 International SoC Design Conference (ISOCC)*, 2014, pp. 42–43.

- [83] P.-J. Liu, S.-R. Hsu, C.-W. Chang, C.-Y. Liao, and L.-H. Chien, “Dimmable white led driver with adaptive voltage feedback control,” in *2015 IEEE 2nd International Future Energy Electronics Conference (IFEEEC)*, 2015, pp. 1–4.
- [84] C. Chiu, C. Shen, and G. Hsieh, “Universal lighting control of unknown connected light emitting diode arrays via a t–s fuzzy model-based approach,” *IET Power Electronics*, vol. 8, no. 2, pp. 151–164, 2015.
- [85] J. He, X. Ruan, and L. Zhan, “Adaptive voltage control for bidirectional converter in flicker-free electrolytic capacitor-less ac–dc led driver,” *IEEE Transactions on Industrial Electronics*, vol. 64, no. 1, pp. 320–324, 2017.
- [86] T. Gucin, B. Fincan, and M. Biberoglu, “A series resonant converter-based multichannel led driver with inherent current balancing and dimming capability,” *IEEE Transactions on Power Electronics*, vol. 34, no. 3, pp. 2693–2703, 2019.
- [87] W. Yu, J. Lai, H. Ma, and C. Zheng, “High-efficiency dc–dc converter with twin bus for dimmable led lighting,” *IEEE Transactions on Power Electronics*, vol. 26, no. 8, pp. 2095–2100, 2011.
- [88] A. S. Jwania, “Control circuit for led lamps in automobile applications,” Jun 2012.
- [89] IEC, “Electromagnetic compatibility (emc) - part 3-2: Limits - limits for harmonic current emissions (equipment input current 16 a per phase),” 2018, geneva,IEC.Accessed on 22 December, 2022.
- [90] CIE, “Chromaticity difference specification for light sources tn 001:2014,” 2014, accessed on 20 December, 2022.

- [91] IEEE P1789, “Recommending practices for modulating current in high brightness leds for mitigating health risks to viewers,” 2010, modified: November 3, 2015. Accessed on 22 December, 2022.
- [92] S. Musumeci, “Passive and active topologies investigation for led driver circuits,” in *Light-Emitting Diodes and Photodetectors*, M. Casalino and J. Thirumalai, Eds. Rijeka: IntechOpen, 2021, ch. 3. [Online]. Available: <https://doi.org/10.5772/intechopen.97098>
- [93] Y. Wang, J. M. Alonso, and X. Ruan, “A review of led drivers and related technologies,” *IEEE Transactions on Industrial Electronics*, vol. 64, no. 7, pp. 5754–5765, 2017.
- [94] X. Ruan, B. Wang, K. Yao, and S. Wang, “Optimum injected current harmonics to minimize peak-to-average ratio of led current for electrolytic capacitor-less ac–dc drivers,” *IEEE Transactions on Power Electronics*, vol. 26, no. 7, pp. 1820–1825, 2011.
- [95] Q. Luo, S. Zhi, C. Zou, B. Zhao, and L. Luowei, “Analysis and design of a multi-channel constant current light-emitting diode driver based on high-frequency ac bus,” *Power Electronics, IET*, vol. 6, pp. 1803–1811, 11 2013.
- [96] M. Arias, D. G. Lamar, J. Sebastián, D. Balocco, and A. Dillo, “High-efficiency led driver without electrolytic capacitor for street lighting,” in *2012 Twenty-Seventh Annual IEEE Applied Power Electronics Conference and Exposition (APEC)*, 2012, pp. 1224–1231.
- [97] H.-J. Chiu and S.-J. Cheng, “Led backlight driving system for large-scale lcd panels,” *IEEE Transactions on Industrial Electronics*, vol. 54, no. 5, pp. 2751–2760, 2007.

- [98] H.-J. Chiu, T.-H. Song, S.-J. Cheng, C.-H. Li, and Y.-K. Lo, “Design and implementation of a single-stage high-frequency hid lamp electronic ballast,” *IEEE Transactions on Industrial Electronics*, vol. 55, no. 2, pp. 674–683, 2008.
- [99] S. Moon, G.-B. Koo, and G.-W. Moon, “A new control method of interleaved single-stage flyback ac–dc converter for outdoor led lighting systems,” *IEEE Transactions on Power Electronics*, vol. 28, no. 8, pp. 4051–4062, 2013.
- [100] L. Jia, Y. Liu, and D. Fang, “High power factor single stage flyback converter for dimmable led driver,” *2015 IEEE Energy Conversion Congress and Exposition (ECCE)*, pp. 3231–3238, 2015.
- [101] M.-G. Kim, “Proportional-integral (pi) compensator design of duty-cycle-controlled buck led driver,” *IEEE Transactions on Power Electronics*, vol. 30, no. 7, pp. 3852–3859, 2015.
- [102] D. Jiang, H. Zhang, and G. Hua, “High reliability driving solution for solid state lighting,” in *2016 13th China International Forum on Solid State Lighting (SSLChina)*, 2016, pp. 57–59.
- [103] S. G. Colaco, “Adaptive predictive lighting controllers for daylight artificial light integrated schemes,” 2011.
- [104] V. Crisp, “Preliminary study of automatic daylight control of artificial lighting,” *Lighting Research & Technology*, vol. 9, no. 1, pp. 31–41, 1977.
- [105] L. Doulos, A. Tsangrassoulis, and F. Topalis, “Quantifying energy savings in daylight responsive systems: The role of dimming electronic ballasts,” *Energy and Buildings*, vol. 40, pp. 36–50, 12 2008.

- [106] D. Li and C. Lok, “An investigation of daylighting performance and energy saving in a daylit corridor,” *Energy and Buildings*, vol. 35, 05 2003.
- [107] N. Gentile, E. S. Lee, W. Osterhaus, S. Altomonte, C. Naves David Amorim, G. Ciampi, V. Garcia-Hansen, M. Maskarenj, M. Scorpio, and S. Sibilio, “Evaluation of integrated daylighting and electric lighting design projects: Lessons learned from international case studies,” *Energy and Buildings*, vol. 268, p. 112191, 2022.
- [108] X. Yu and Y. Su, “Daylight availability assessment and its potential energy saving estimation –a literature review,” *Renewable and Sustainable Energy Reviews*, vol. 52, pp. 494–503, 2015.
- [109] H. Han and J. T. Kim, “Application of high-density daylight for indoor illumination,” *Energy*, vol. 35, no. 6, pp. 2654–2666, 2010.
- [110] A. Ge, P. Qiu, J. Cai, W. Wang, and J. Wang, “Hybrid daylight/light-emitting diode illumination system for indoor lighting,” *Appl. Opt.*, vol. 53, no. 9, pp. 1869–1873, 2014.
- [111] T. S. Kumar, C. Kurian, and S. Shetty, “A data-driven approach for the control of a daylight+artificial light integrated scheme,” *Lighting Research & Technology*, vol. 52, no. 2, pp. 292–313, 2020.
- [112] K. R. Wagiman, M. N. Abdullah, M. Y. Hassan, N. H. Mohammad Radzi, A. H. Abu Bakar, and T. C. Kwang, “Lighting system control techniques in commercial buildings: Current trends and future directions,” *Journal of Building Engineering*, vol. 31, p. 101342, 2020.

- [113] D. Plorer, S. Hammes, M. Hauer, V. van Karsbergen, and R. Pfluger, “Control strategies for daylight and artificial lighting in office buildings” a bibliometrically assisted review,” *Energies*, vol. 14, no. 13, 2021.
- [114] Q.-U. Ain, S. Iqbal, and H. Mukhtar, “Improving quality of experience using fuzzy controller for smart homes,” *IEEE Access*, vol. 10, pp. 11 892–11 908, 2022.
- [115] J. Liu, W. Zhang, X. Chu, and Y. Liu, “Fuzzy logic controller for energy savings in a smart led lighting system considering lighting comfort and daylight,” *Energy and Buildings*, vol. 127, pp. 95–104, 2016.
- [116] M. T. Lah, B. Zupancic, J. Peternelj, and A. Krainer, “Daylight illuminance control with fuzzy logic,” *Solar Energy*, vol. 80, pp. 307–321, 2006.
- [117] S. Colaco, C. Kurian, V. George, and A. Colaco, “Integrated design and real-time implementation of an adaptive, predictive light controller,” *Lighting Research Technology*, vol. 44, no. 4, pp. 459–476, 2012.
- [118] S. G. Varghese, C. P. Kurian, V. I. George, and T. S. S. Kumar, “Daylight-artificial light integrated scheme based on digital camera and wireless networked sensing-actuation system,” *IEEE Transactions on Consumer Electronics*, vol. 65, no. 3, pp. 284–292, 2019.
- [119] A. C. KunduracÄ and Z. T. Kazanasmaz, “Fuzzy logic model for the categorization of manual lighting control behaviour patterns based on daylight illuminance and interior layout,” *Indoor and Built Environment*, vol. 28, no. 5, pp. 584–598, 2019.

- [120] S. R. Perumal and F. Baharum, “Design and simulation of a circadian lighting control system using fuzzy logic controller for led lighting technology,” *Journal of Daylighting*, vol. 9, no. 1, pp. 64–82, 2022.
- [121] C. Kurian, S. Kuriachan, J. Bhat, and R. Aithal, “An adaptive neuro-fuzzy model for the prediction and control of light in integrated lighting schemes,” *Lighting Research & Technology*, vol. 37, no. 4, pp. 343–351, 2005.
- [122] C. Kurian, R. Aithal, J. Bhat, and V. George, “Robust control and optimisation of energy consumption in daylight–artificial light integrated schemes,” *Lighting Research Technology - LIGHTING RES TECHNOL*, vol. 40, pp. 7–24, 03 2008.
- [123] W. Driel and X. Fan, *Solid State Lighting Reliability*, 01 2013.
- [124] B. Sun, X. Fan, W. van Driel, and G. Zhang, *Reliability Prediction of Integrated LED Lamps with Electrolytic Capacitor-Less LED Drivers*, 1st ed., ser. Solid State Lighting Technology and Application Series. Springer Science+Business Media, 2018, pp. 455–486.
- [125] B. Sun, X. Fan, C. Qian, and G. Zhang, “Pof-simulation-assisted reliability prediction for electrolytic capacitor in led drivers,” *IEEE Transactions on Industrial Electronics*, vol. 63, no. 11, pp. 6726–6735, 2016.
- [126] A. Pandharipande and D. Caicedo, “Daylight integrated illumination control of led systems based on enhanced presence sensing,” *Energy and Buildings*, vol. 43, no. 4, pp. 944–950, 2011.
- [127] L. Thet, A. Kumar, N. Xavier, and S. Panda, “A smart lighting system using wireless sensor actuator network,” in *2017 Intelligent Systems Conference (IntelliSys)*, 2017, pp. 217–220.

- [128] T. de Rubeis, M. Muttillio, L. Pantoli, I. Nardi, I. Leone, V. Stornelli, and D. Ambrosini, “A first approach to universal daylight and occupancy control system for any lamps: Simulated case in an academic classroom,” *Energy and Buildings*, vol. 152, pp. 24–39, 2017.
- [129] A. Peruffo, A. Pandharipande, D. Caicedo, and L. Schenato, “Lighting control with distributed wireless sensing and actuation for daylight and occupancy adaptation,” *Energy and Buildings*, vol. 97, pp. 13–20, 2015.
- [130] C. Ding and T. Zhang, “Research on health monitoring of led lighting system,” in *2016 Prognostics and System Health Management Conference (PHM-Chengdu)*, 2016, pp. 1–5.
- [131] T. Sutharssan, S. Stoyanov, C. Bailey, and Y. Rosunally, “Prognostics and health monitoring of high power led,” *Micromachines*, vol. 3, no. 1, pp. 78–100, 2012.
- [132] A. Freddi, G. Ippoliti, M. Marcantonio, D. Marchei, A. Monteriu, and M. Pirro, “A fault diagnosis and prognosis led lighting system for increasing reliability in energy efficient buildings,” in *IET Conference on Control and Automation 2013: Uniting Problems and Solutions*, 2013, pp. 1–6.
- [133] M. Frackson and C. Suvagau, “White tunable led lighting: A literature analysis report conservation and energy management engineering,” 08 2017.
- [134] M. Figueiro, “An overview of the effects of light on human circadian rhythms: Implications for new light sources and lighting systems design,” *Journal of Light Visual Environment*, vol. 37, pp. 51–61, 01 2013.



- [135] R. J. Lucas, D. M. Peirson, Stuart N. and Berson, T. M. Brown, H. M. Cooper, C. A. Czeisler, M. G. Figueiro, P. D. Gamlin, S. W. Lockley, J. B. O’Hagan, L. L. Price, I. Provencio, D. J. Skene, and G. C. Brainard, “Measuring and using light in the melanopsin age,” *Trends in Neurosciences*, vol. 37, no. 1, pp. 1–9, 2014.
- [136] J. H. Oh, S. Yang, and Y. Do, “Healthy, natural, efficient and tunable lighting: Four-package white leds for optimizing the circadian effect, color quality and vision performance,” *Light: Science Applications*, vol. 3, 02 2014.
- [137] L. Bellia, A. Pedace, and G. Barbato, “Lighting in educational environments: An example of a complete analysis of the effects of daylight and electric light on occupants,” *Building and Environment*, vol. 68, 06 2013.
- [138] S. Berman, M. Navvab, M. Martin, J. Sheedy, and W. Tithof, “A comparison of traditional and high colour temperature lighting on the near acuity of elementary school children,” *Lighting Research Technology*, vol. 38, pp. 41–52, 03 2006.
- [139] M. Mott, D. Robinson, A. Walden, J. Burnette, and A. Rutherford, “Illuminating the effects of dynamic lighting on student learning,” *SAGE Open*, vol. 2, 06 2012.
- [140] M. Figueiro and M. Rea, “Office lighting and personal light exposures in two seasons: Impact on sleep and mood,” *Lighting Research and Technology*, vol. 48, no. 3, pp. 352–364, 12 2016.
- [141] W. van Bommel, “Non-visual biological effect of lighting and the practical meaning for lighting for work,” *Applied ergonomics*, vol. 37, pp. 461–6, 08 2006.

- [142] H. Juslén and A. Tenner, “Mechanisms involved in enhancing human performance by changing the lighting in the industrial workplace,” *International Journal of Industrial Ergonomics*, vol. 35, pp. 843–855, 09 2005.
- [143] M. Wei, K. Houser, B. Orland, D. Lang, N. Ram, M. Sliwinski, and M. Bose, “Field study of office worker responses to fluorescent lighting of different cct and lumen output,” *Journal of Environmental Psychology*, vol. 39, 09 2014.
- [144] Philips, “Philips color kinetics: iw fuse powercore,” 2017, <http://www.colorkinetics.com/ls/intelliwhite/iwfusepc/>. Accessed on 28 December, 2022.
- [145] —, “Philips floatplane suspended led,” 2017, <http://www.lightingproducts.philips.ca/our-brands/ledalite/floatplane-suspended-led.html>. Accessed on 28 December, 2022.
- [146] —, “Philips boldplay suspended,” 2017, <http://www.ledalite.com/products/boldplay/suspended>. Accessed on 28 December, 2022.
- [147] Acuitybrands, “Tunable white,” 2017, <http://www.acuitybrands.com/products/lighting/featured-technology/mainstream-dynamic/tunable-white>. Accessed on 28 December, 2022.
- [148] Philips Hue, “Starter kit: 4 e26 smart bulbs (60 w),” 2018, <https://www.philips-hue.com/en-ca/p/hue-white-ambiance-starter-kit-e26/046677471996>. Accessed on 22 February, 2022.
- [149] TP-Link, “Smart bulbs — lb120,” 2017, [http://www.tp-link.com/us/products/details/cat-5609\\_LB120.html](http://www.tp-link.com/us/products/details/cat-5609_LB120.html). Accessed on 28 December, 2022.

- [150] Sengled, “Sengled element plus,” 2017, <https://www.sengled.com/products/element-plus>. Accessed on 28 December, 2022.
- [151] Ilumi, “A19 led smart light bulbs,” 2022, <https://ilumi.co/collections/a19-led-smartbulb>. Accessed on 22 February, 2022.
- [152] Kasa Smart, “Kasa smart light bulb, multicolor,” 2021, <https://www.kasasmart.com/us/products/smart-lighting>. Accessed on 22 February, 2022.
- [153] J. Gilman, M. Miller, and M. Grimaila, “A simplified control system for a daylight-matched led lamp,” *Lighting Research and Technology*, vol. 45, pp. 614–629, 10 2013.
- [154] Qiao, et.al., “Design of smart light source based on bi-color led with single duty cycle for correlated color temperature adjustment,” *Optical and Quantum Electronics*, vol. 53, no. 610, pp. 614–629, 10 2021.
- [155] P. K. Maiti and B. Roy, “Development of dynamic light controller for variable cct white led light source,” *LEUKOS*, vol. 11, no. 4, pp. 209–222, 2015.
- [156] A. T. L. Lee, H. Chen, S.-C. Tan, and S. Y. Hui, “Precise dimming and color control of led systems based on color mixing,” *IEEE Transactions on Power Electronics*, vol. 31, no. 1, pp. 65–80, 2016.
- [157] H.-T. Chen, S.-C. Tan, and S. Y. Hui, “Nonlinear dimming and correlated color temperature control of bicolor white led systems,” *IEEE Transactions on Power Electronics*, vol. 30, no. 12, pp. 6934–6947, 2015.
- [158] Craig Dilouie, “Introduction to wireless lighting controls,” 2017, lighting Control Association.

<https://lightingcontrolsassociation.org/2018/03/23/introduction-to-wireless-lighting-controls/>. Accessed on 28 December, 2022.

- [159] G. Andia Vera, S. D. Nawale, S. Tedjini, and Y. Duroc, “Passive uhf rfid backscattering for indoor lighting control,” in *2014 Annual IEEE India Conference (INDICON)*, 2014, pp. 1–4.
- [160] Components101, “Xbee s2c-rf module,” 2021, <https://components101.com/wireless/xbee-s2c-module-pinout-datasheet>. Accessed on 5 December, 2022.
- [161] C. Guo, X. Zou, C. Ma, and R. Zhang, “Development of wireless light control system based on zigbee,” *Communications and Network*, vol. 05, pp. 29–33, 01 2013.
- [162] Z. Ke and C. Xiao, “Research of intelligent street light system based on zigbee,” in *2016 International Conference on Industrial Informatics - Computing Technology, Intelligent Technology, Industrial Information Integration (ICIICII)*, 2016, pp. 255–258.
- [163] H. Khawari, M. Baghaei-Nejad, S. R. Alawi, and M. Jafari, “Intelligent lighting control system based on zigbee communication technique,” 2013.
- [164] V. Gupta, B. Basak, and B. Roy, “A fault-detecting and motion-sensing wireless light controller for led lighting system,” in *2020 IEEE Calcutta Conference (CALCON)*, 2020, pp. 462–466.
- [165] H. Kim, W. Yang, Y. S. Cho, and D. Park, “Design of led lighting system using bluetooth wireless communication,” *Journal of the Korean Institute of Illuminating and Electrical Installation Engineers*, vol. 29, pp. 1–7, 02 2015.
- [166] Y. Peng, K. Xia, and J. Wang, “Lighting control system based on

smart phone and bluetooth,” *Applied Mechanics and Materials*, vol. 602-605, pp. 1260–1263, 08 2014.

- [167] A. E. Amoran, A. S. Oluwole, E. O. Fagorola, and R. Diarah, “Home automated system using bluetooth and an android application,” *Scientific African*, vol. 11, p. e00711, 2021. [Online]. Available: <https://www.sciencedirect.com/science/article/pii/S2468227621000156>
- [168] C. Feng, X. Wang, Z. Li, W. Lin, H. Ji, and S. Shen, “Smart lighting system based on bluetooth,” *Journal of Physics: Conference Series*, vol. 1976, no. 1, p. 012028, jul 2021. [Online]. Available: <https://dx.doi.org/10.1088/1742-6596/1976/1/012028>
- [169] B. Hussain, C. Qiu, and C. P. Yue, “Smart lighting control and services using visible light communication and bluetooth,” in *2019 IEEE 8th Global Conference on Consumer Electronics (GCCE)*, 2019, pp. 1–2.
- [170] Y. Shuangshuang, L. Jianqi, O. Xiaoqing, Z. Qingshan, and L. Jianying, “Design of intelligent lighting controller based on bluetooth,” in *2019 IEEE International Conference on Service Operations and Logistics, and Informatics (SOLI)*, 2019, pp. 1–4.
- [171] US Department of Energy, “Energy saver,” 2022, <https://www.energy.gov/energysaver/led-lighting>.
- [172] OSRAM, “Led standards regulations,” 2022, <https://www.osram.com/os/products/illumination-applications/tools-and-service/led-standards-regulations.jsp>. Accessed on 05 December, 2022.
- [173] Bureau of Indian Standards, “Method of measurement of lumen maintenance of solid state light (led) sources,” 2012, accessed on 20 December, 2022.

- [174] GwInstek, “Gpr-h series linear d.c. power supply,” 2021, <https://www.gwinstek.com/en-IN/products/detail/GPR-H>. Accessed on 20 December, 2022.
- [175] Konica Minolta, “Cl-200a chroma meter,” 2022, <https://sensing.konicaminolta.us/us/products/cl-200a-chroma-meter>. Accessed on 20 December, 2022.
- [176] JETI Technische Instrumente GmbH, “Operating instructions; spectroradiometer specbos1200,” 2006, <https://www.yumpu.com/en/document/read/8414102/spectroradiometer-specbos-1201-1301-1401-lichtconsultnl>. Accessed on 21 December, 2022.
- [177] Keysight, “6812b ac power source / power analyzer, 750 va, 300 v, 6.5 a,” 2022, <https://www.keysight.com/in/en/product/6812B/performance-ac-power-source-750-va-300-v-65-a.html>. Accessed on 20 December, 2022.
- [178] Tektronix, “Bench oscilloscopes for design, debug and education,” 2022, <https://www.tek.com/en/products/oscilloscopes/benchtopy-oscilloscopes>. Accessed on 20 December, 2022.
- [179] GwInstek, “Aps-1102,” 2021, <https://www.gwinstek.com/en-global/products/detail/APS-1102>. Accessed on 20 December, 2022.
- [180] Vishay semiconductors, “Temt6000,” 2004, <https://html.alldatasheet.com/html-pdf/117488/VISHAY/TEMT6000/217/1/TEMT6000.html>. Accessed on 20 December, 2022.
- [181] Tektronix, “Gds-2202e gwinstek,” 2022, <https://www.tme.com/in/en/details/gds-2202e/digital-oscilloscopes/gw-instek>. Accessed on 20 December, 2022.

- [182] J. Byun, I. Hong, B. Lee, and S. Park, “Intelligent household led lighting system considering energy efficiency and user satisfaction,” *IEEE Transactions on Consumer Electronics*, vol. 59, no. 1, pp. 70–76, 2013.
- [183] Lumileds, “Lumileds ds061 luxeon rebel es product datasheet,” <http://www.lumileds.com/uploads/17/DS61-pdf>. Accessed 25 November 2016.
- [184] V. Gupta, K. Ghosh, and B. Roy, “Design topology based comparative study on electric and photometric parameters of commercially available led lamp systems,” in *2017 2nd International Conference for Convergence in Technology (I2CT)*, 2017, pp. 116–123.
- [185] R. Erickson and D. Maksimovich, *Fundamentals of Power Electronics*. Kluwer Academic Publishers, 2000.
- [186] Centre for Science and Environment, “Energy and buildings,” 2014, <https://cdn.cseindia.org/userfiles/Energy-and-%20buildings.pdf>. Accessed on 23 May, 2022.
- [187] Arduino.cc, “Arduino mega 2560 rev3,” 2021, <https://store.arduino.cc/products/arduino-mega-2560-rev3>. Accessed on 21 December, 2022.
- [188] ROHM semiconductor, “Digital 16bit serial output type ambient light sensor ic,” 2011, <https://www.mouser.com/datasheet/2/348/bh1750fvi-e-186247.pdf>. Accessed on 5 May, 2022.
- [189] Panasonic, “Pdlm03147,” 2021, <https://panasonic.net/electric-works/lighting/products/specpdf/pdlm03147.pdf>. Accessed on 5 May, 2022.

- [190] C. Branas, F. J. Azcondo, and J. M. Alonso, “Solid-state lighting: A system review,” *IEEE Industrial Electronics Magazine*, vol. 7, no. 4, pp. 6–14, 2013.
- [191] S. Ozenc, M. Uzunoglu, and O. Guler, “Experimental evaluation of the impacts of considering inherent response characteristics for lighting technologies in building energy modeling,” *Energy and Buildings*, vol. 77, pp. 432–439, 2014.
- [192] Y. Wang and Z. Wang, “Design of intelligent residential lighting control system based on zigbee wireless sensor network and fuzzy controller,” in *2010 International Conference on Machine Vision and Human-machine Interface*, 2010, pp. 561–564.
- [193] Anixter Inc., “Wired vs. wireless lighting control,” 2022, <https://www.anixter.com/en-au/resources/literature/techbriefs>. Accessed on 5 December, 2022.
- [194] J. Attachie, G. Owusu, and S. Ohene Adu, “Enhancement of wireless lighting control system,” *Journal of Electrical and Computer Engineering*, vol. 2021, pp. 1–7, 10 2021.
- [195] C. Dandelski, B.-l. Wenning, D. V. Perez, D. Pesch, and J.-p. M. Linartz, “Scalability of dense wireless lighting control networks,” *IEEE Communications Magazine*, vol. 53, no. 1, pp. 157–165, 2015.
- [196] Electronics hub, “Interfacing voltage sensor with arduino – measure up to 25v using arduino,” 2022, <https://create.arduino.cc/projecthub/ingo-lohs/ac-current-sensor-182aff>. Accessed on 5 December, 2022.
- [197] Signify, “Floatplane suspended,” 2018, <https://www.signify.com/en-us/products/indoor-luminaires/architectural-linear/suspended/floatplane-suspended>. Accessed on 22 February, 2022.



- [198] Perry HC, “Real time system testing - mit 16.070,” 2001, <http://web.mit.edu/16.070/www/year2001/tl30.pdf>. Accessed on 25 February, 2022.
- [199] I. Chew, V. Kalavally, C. P. Tan, and J. Parkkinen, “A spectrally tunable smart led lighting system with closed-loop control,” *IEEE Sensors Journal*, vol. 16, no. 11, pp. 4452–4459, 2016.
- [200] Massachusetts Institute of Technology, “Mit app inventor,” 2022, <https://appinventor.mit.edu/>. Accessed on 22 February, 2022.
- [201] H.-J. Choi and B.-S. Kang, “Color temperature conversion apparatus for variably changing color temperature of input image and method thereof,” April 2006.
- [202] P. Mandal, D. Dey, and B. Roy, “Optimization of luminaire layout to achieve a visually comfortable and energy efficient indoor general lighting scheme by particle swarm optimization,” *LEUKOS*, vol. 17, no. 1, pp. 91–106, 2021.
- [203] Konica Minolta, “Data management software cl-s10w,” 2019, <https://www.konicaminolta.com/instruments/download/software/light/cl-s10w/index.html>. Accessed on 20 December, 2022.
- [204] Lutron, “Lutron lx-102 light meter, analog output,” 2016, <https://www.multilab.in/lutron/lightmeters/lx102-lightmeter-lutron.html>. Accessed on 20 December, 2022.
- [205] Keysight Technologies, “34970a data acquisition / data logger switch unit,” 2023, <https://www.keysight.com/in/en/product/34970A/34970a-data-acquisition-control-mainframe-modules.html>. Accessed on 20 December, 2022.

<https://www.keysight.com/in/en/product/34970A/34970a-data-acquisition-control-mainframe-modules.html>. Accessed on 20 December, 2022.

- [207] Y. de Kort and K. Smolders, "Effects of dynamic lighting on office workers: First results of a field study with monthly alternating settings," *Lighting Research & Technology*, vol. 42, no. 3, pp. 345–360, 2010.
- [208] CIE, "Ocular lighting effects on human physiology and behaviour cie 158:2004," 2004, accessed on 20 December, 2022.

Vishwanath Gupta  
12/04/23